ACS NANO

www.acsnano.org

REVIEW

Research Progress of Flexible Electronic Devices Based on Electrospun Nanofibers

Shige Wang, Peng Fan, Wenbo Liu, Bin Hu, Jiaxuan Guo, Zizhao Wang, Shengke Zhu, Yipu Zhao, Jinchen Fan, Guisheng Li,* and Lizhi Xu*

Cite This: *ACS Nano* 2024, 18, 31737–31772

Read Online

ACCESS | Metrics & More | Article Recommendations

ABSTRACT: Electrospun nanofibers have become an important component in fabricating flexible electronic devices because of their permeability, flexibility, stretchability, and conformability to three-dimensional curved surfaces. This review delves into the advancements in adaptable and flexible electronic devices using electrospun nanofibers as the substrates and explores their diverse and innovative applications. The primary development of key substrates for flexible devices is summarized. After briefly discussing the principle of electrospinning, process parameters that affect electrospinning, and two major electrospinning techniques (i.e., single-fluid electrospinning and multifluid electrospinning), the review shines a spotlight on the recent breakthroughs in multifunctional and stretchable electronic devices that are based on electrospun substrates. These advancements include flexible sensors, flexible energy harvesting and storage devices, flexible accessories for electronic devices, and flexible environmental monitoring devices. In particular, the review outlines the challenges and potential solutions of developing electrospun nanofibers for flexible electronic devices, including overcoming the incompatibility of multiple interfaces, developing 3D microstructure sensor arrays with gradient geometry for various imperceptible on-skin devices, etc. This review may provide a comprehensive understanding of the rational design of application-oriented flexible electronic devices based on electrospun nanofibers.

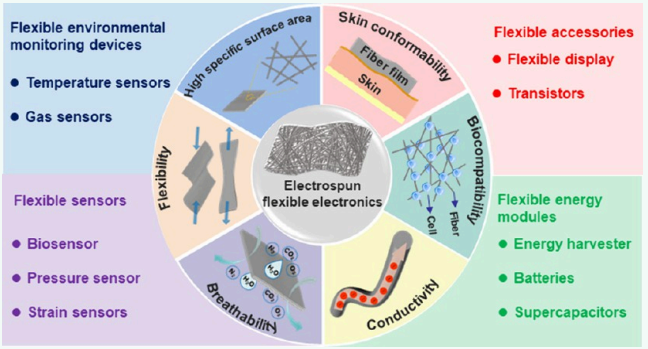

KEYWORDS: *electrospun nanofibers, stretchable electronics, electrospinning technique, flexible substrate, flexible sensors, energy modules, wearable sensors, e-skin, biomedical devices, environmental monitoring devices*

1. INTRODUCTION

Flexible electronics refers to a class of electronic devices and circuits that are designed to be bendable, stretchable, and conformable to diverse surfaces.[1,2] Manufacturing flexible electronics requires the design of flexible substrates, the identification of inherently soft materials, and the advancement of technologies to facilitate the formation of conductive networks on these flexible substrates.[3,4] Unlike traditional rigid electronics made from materials like glass or silicon wafer substrates, flexible electronics utilize flexible substrates and unconventional fabrication techniques to achieve mechanical flexibility without compromising the electrical performance.[5,6] Moreover, the combination of conductive materials and flexible substrates can synergistically enhance electronics' mechanical and electrical characteristics.[7,8] As a result, they are extensively utilized in the creation of flexible displays,[9] sensors,[10] artificial skins,[11] batteries,[12] capacitors,[13] implantable bioelectronics,[1] *etc.*

Over the last two decades, flexible electronics based on various conventional thin film substrates, including polyimide (PI), polyethylene naphthalate, and elastomers (e.g., polystyrene-ethylene-butylene-styrene, polydimethylsiloxane (PDMS), and Ecoflex), have witnessed significant advancements.[14−16] Nevertheless, typical flexible thin-film electronics often exhibit limited air and moisture permeability, affecting wearing comfort, particularly during long-term body monitoring.[17] Studies have indicated that prolonged skin and tissue attachment can cause thermophysiological discomforts like dampness, clamminess, and skin inflammation.[18,19] In more

Received: September 18, 2024
Revised: October 9, 2024
Accepted: October 11, 2024
Published: November 5, 2024

https://doi.org/10.1021/acsnano.4c13106
ACS Nano 2024, 18, 31737−31772

Scheme 1. Illustration Showcasing a Variety of Electrospun Nanofiber-Based Flexible Electronics for Multiple Applications[a]

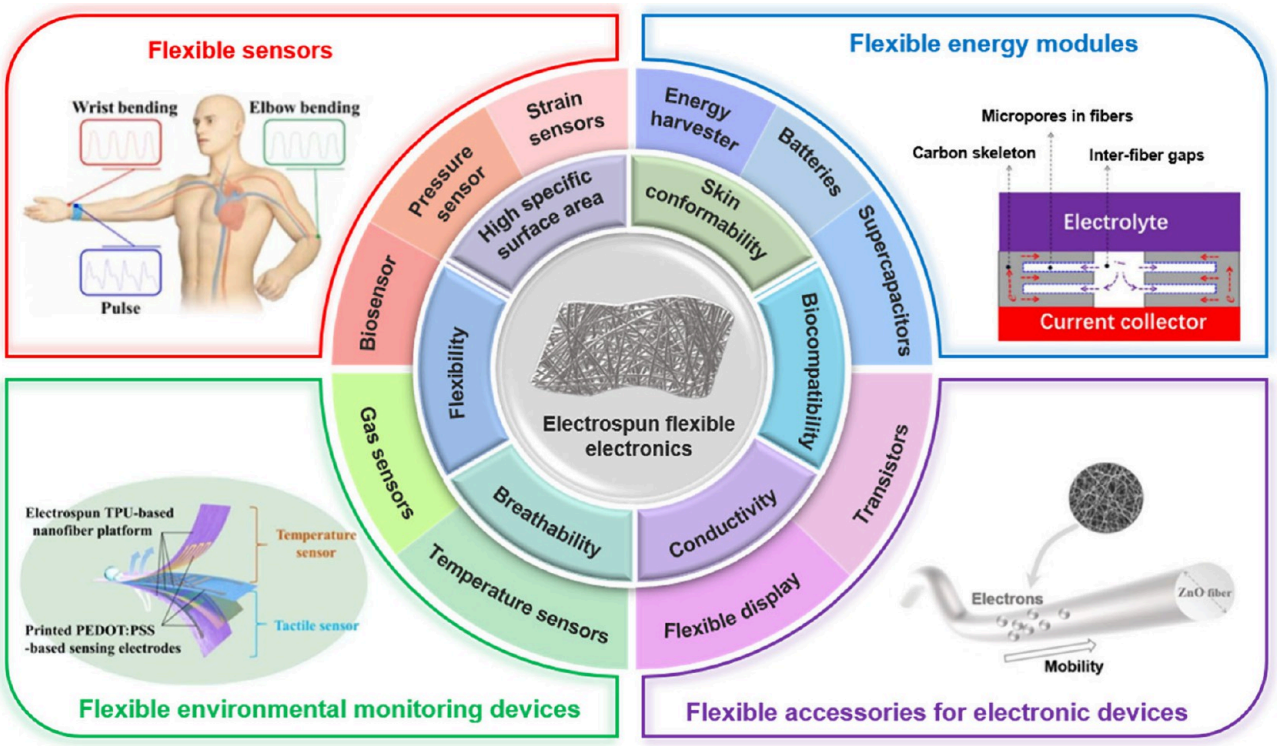

[a]Reprinted with permission from ref 38. Copyright 2023 Wiley-VCH. Reprinted with permission from ref 39. Copyright 2023 Elsevier. Reprinted with permission from ref 40. Copyright 2024 Elsevier. Reprinted with permission from ref 41. Copyright 2023 Elsevier.

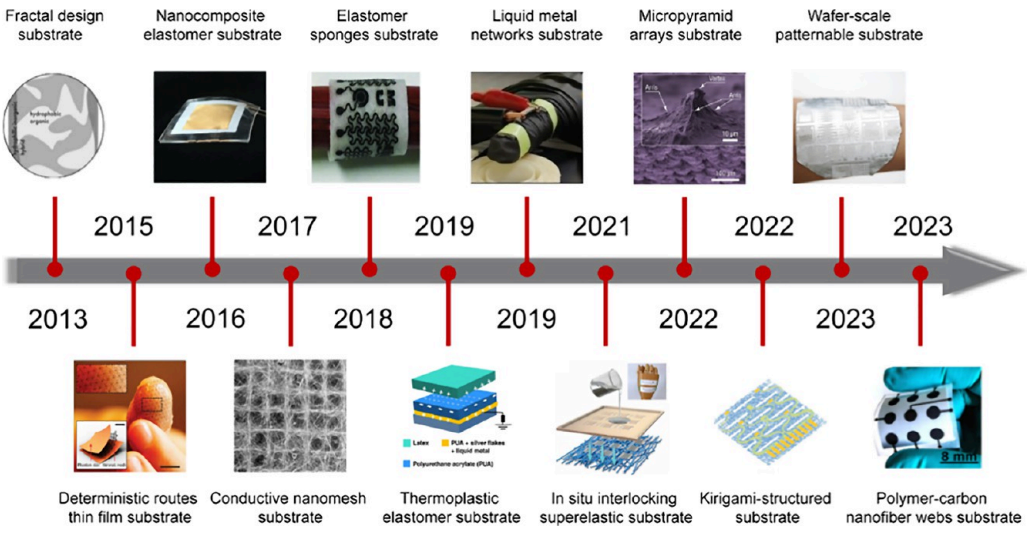

Figure 1. Several typical flexible devices.[20,42,45−54] Reprinted from ref 20 with permission. Copyright 2023 The American Association for the Advancement of Science. Reprinted with permission under a Creative Commons [CC BY] License from ref 42. Copyright 2015 The Authors; published by Springer Nature. Reprinted from ref 45 with permission. Copyright 2013 Wiley-VCH. Reprinted from ref 46 with permission. Copyright 2016 American Chemical Society. Reprinted from ref 47 with permission. Copyright 2017 Wiley-VCH. Reprinted from ref 48 with permission. Copyright 2018 Wiley-VCH. Reprinted with permission under a Creative Commons [CC BY] License from ref 49. Copyright 2019 The Authors; published by Springer Nature. Reprinted from ref 50 with permission. Copyright 2019 Wiley-VCH. Reprinted from ref 51 with permission. Copyright 2022 Wiley-VCH. Reprinted from ref 52 with permission. Copyright 2024 Elsevier. Reprinted with permission under a Creative Commons [CC BY] License from ref 53. Copyright 2022 The Authors; published by Springer Nature. Reprinted from ref 54 with permission under a Creative Commons CC-BY 4.0 License. Copyright 2023 The Author(s); published by American Chemical Society.

severe cases, *in vivo* implantation can potentially lead to malignancies due to inadequate permeability of the device.[20]

Presently, there has been increasing advocacy for supersoft, permeable, and stretchable electronics with long-term, continuous, and reliable performance. These flexible electronic devices can be manufactured on porous elastomeric substrates that provide excellent flexibility and high moisture, air, and liquid permeability.[21,22] Electrospun nanofibers offer excep-

https://doi.org/10.1021/acsnano.4c13106
ACS Nano 2024, 18, 31737−31772

tional breathability, skin conformability, flexibility, and tunable mechanical properties, enabling the creation of soft and conformable electronic devices. This flexibility allows the devices to be integrated seamlessly into various shapes and surfaces, enhancing their adaptability and usability.[23,24] To achieve the ideal 3D interface between flexible electronics and skin, three conditions should be satisfied: (i) excellent conformal capability of flexible electronics for large-area skin integration, (ii) high-performance electronics enabling high-quality electrophysiological signal acquisition, and (iii) good biocompatibility and breathability as the foundation for long-term wearability.[25−27]

Electrospun nanofibers have an exceptionally high surface-area-to-volume ratio, which is advantageous for promoting efficient charge transport and enhancing the sensitivity and response time of the devices.[28] The porous structure of electrospun nanofibers not only facilitates the incorporation of functional materials (e.g., conductive polymers, nanoparticles, and biomolecules) but also effectively mimics the diverse extracellular matrix.[29,30] Furthermore, the scalable and cost-effective fabrication process of electrospinning makes it suitable for large-scale production of flexible electronic components, enhancing the versatility and application potential. By doping with different components, enhanced mechanical and electrical properties can be achieved, thereby expanding their application scopes in flexible modules.[31] As a consequence, although many applications are still in the experimental or early development stages, electronics based on electrospun nanofibers present vast opportunities across a broad spectrum of application domains including, but not limited to, personalized biosensors,[32,33] tension electrodes,[34] capacitive sensors,[35] friction sensors,[36] piezoelectric sensors,[37] and nanogenerators.[25]

This review highlights the advancements in adaptable and flexible electronic devices that leverage electrospun nanofibers and delves into potential avenues for diverse and innovative applications. The types of raw ingredients used to prepare nanofibers using the electrostatic spinning technique are presented. Then, this review offers in-depth insights into flexible sensors (biosensors, pressure sensors, and other sensors), flexible energy sensors (energy harvester, batteries, and supercapacitors), and other flexible devices (flexible display and transistors), primarily using electrospun nanofibers as the substrate. The objective is to elucidate the details and functions of these devices, offering a comprehensive understanding of the capabilities and inspiring innovative ideas of electrospun nanofibers in the field (Scheme 1). Finally, the review presents an outlook on future challenges encountered by electrospun flexible electronics and offers viable solutions to address these issues.

2. DEVELOPMENT OF STRETCHABLE ELECTRONICS

The primary development of several typical flexible devices is listed in Figure 1. In the initial stage, ductile metals (e.g., gold, silver, copper, and platinum) were used to create coplanar thin films that function directly as conductive electrodes. These films were combined with intricately designed stretchable patterns, including filamentary serpentines, self-similar fractals, and horseshoes.[42] The fractal design concepts for stretchable electronics enabled the effective accommodation of mechanical deformations of hard electronics.[43] In a pioneer study, Rogers and colleagues reported that thin films of rigid electronic materials, when patterned into deterministic fractal designs and bonded to elastomers, exhibited tunable mechanical properties with significant implications for stretchable device design. Specifically, they demonstrated the effectiveness of fractal constructs such as Peano, Greek cross, and Vicsek patterns in creating space-filling structures of electronic materials. These structures were utilized in precision monitors and actuators, electrophysiological sensors, and antennas. These devices, designed for conformal skin mounting, possess attributes including being invisible under magnetic resonance imaging. This suggests that fractal design concepts are essential strategies for integrating hard and soft materials.[43] Nevertheless, a significant challenge that persists involves the risk of catastrophic failures in these electrodes, which can occur due to unforeseen circumstances, including accidental overstretching beyond fracture limits, defect-driven cracks, and edge-initiated delamination.[44]

After that, researchers explored many strategies to incorporate stretchability and/or conformability into thin-film substrates, aiming to achieve seamless integration with the skin for acquiring high-fidelity physiological and biochemical signals.[54−56] In a typical scheme, Lee et al. reported a straightforward strategy that utilized nanocomposite elastomer substrate in integrating one-dimensional metallic nanowires (NWs) to serve as electrodes in skin-mountable electronic devices. This nanocomposite elastomer comprised a layer of tightly interconnected Cu NWs embedded within a diluted PI matrix. The Cu NWs functioned as electrical conductors, while the PI served as the elastomeric substrate. This method significantly improved the mechanical properties of ultrathin, flexible electronics, reducing the risk of fracture and delamination and thus prolonging their operational lifespan.[44] However, planar substrates have consistently been a significant limitation in enhancing the weight, softness, and permeability of on-skin electronics. Additionally, a systematic investigation into the long-term psychological and physiological effects of these devices is necessary. Recently, certain room-temperature liquid metal was used to fabricate flexible conductors using elastic channels and elastomeric matrix et al. as the substrates.[49,50] These advancements have resulted in stretchable conductors that exhibit excellent conductivity, stretchability, and, in certain instances, self-healing capability. However, these elastic substrates are not permeable.

A primary solution to these issues is the design of substrate-free or porous elastomer sponge-based on-skin electronics.[57] Unlike traditional thin-film planar electronics, such substrate-free or porous elastomer sponge-based on-skin electronics are highly flexible, gas-permeable, ultrathin, and inflammation-free. As a demonstration, Someya and co-workers reported the design of substrate-free on-skin electronics for extended attachment to human skin.[19] In their study, an intertwined, mesh-like Poly(vinyl alcohol) (PVA) nanofibrous sheet (fiber diameter: 300 to 500 nm) was created. Then, a thick Au layer (thickness: 70−100 nm) was deposited on the top of the mesh-like PVA nanofibrous sheet and patterned using a shadow mask. By applying water to nanomesh conductors placed on the skin, the PVA nanofibers quickly dissolved, enabling the nanomesh conductors to firmly attach to the skin. This wearable sensor (electronics) provided outstanding breathability, allowing sweat glands to remain unobstructed, and preserved its flexibility, ensuring comfort for the user, even when worn for long durations on irregular skin surfaces. Moreover, the impedance at the skin contact was sufficiently low to allow for high-precision electromyogram recordings,

https://doi.org/10.1021/acsnano.4c13106
ACS Nano 2024, 18, 31737−31772

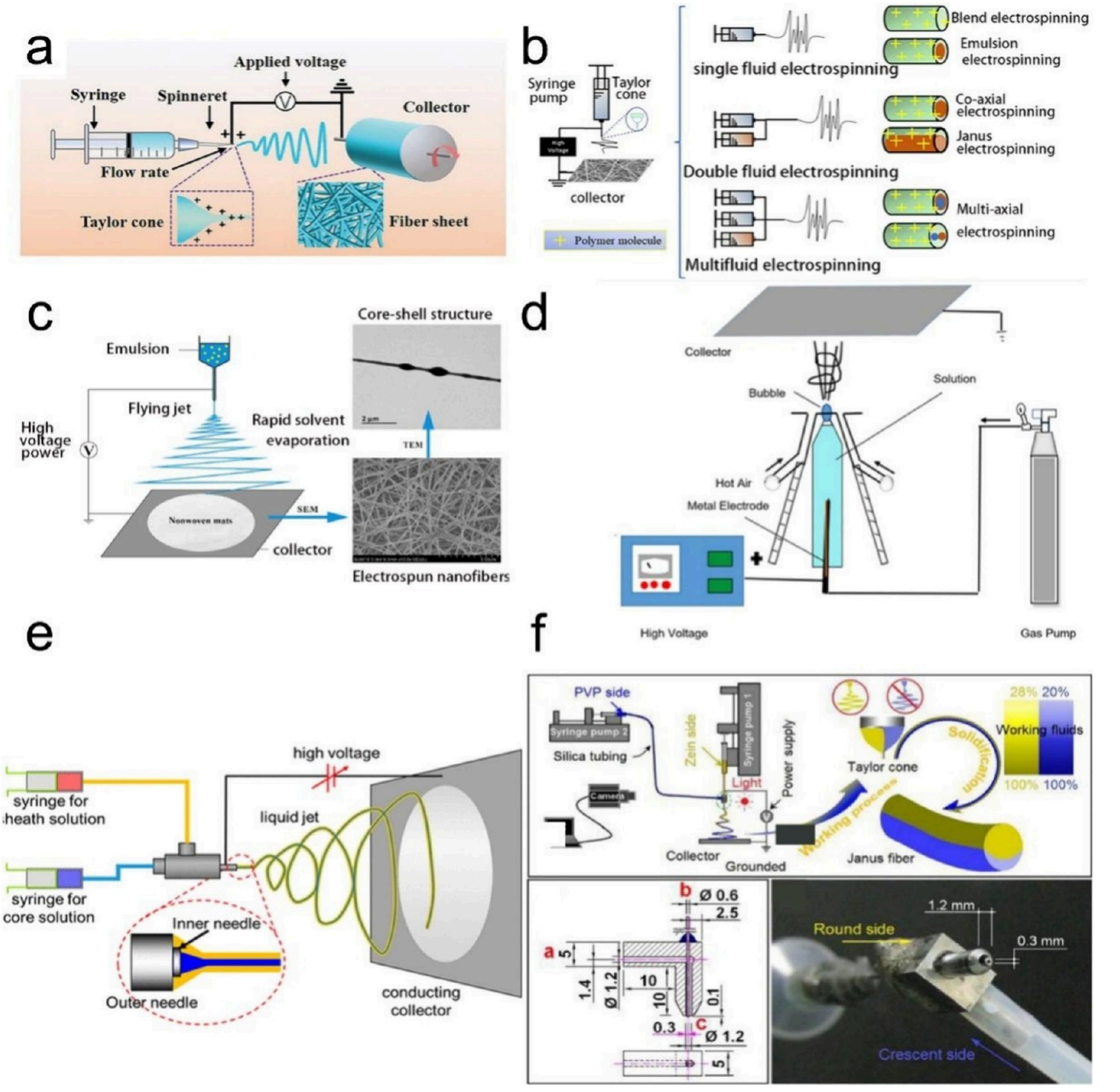

Figure 2. (a) Schematic diagram illustrating the basic experimental setup for electrospinning. Reprinted with permission under a Creative Commons [CC BY] License from ref 70. Copyright 2023 The Authors. Published by Wiley-VCH. (b) Classification of needle-based electrospinning setups based on fluid quantity. Reprinted from ref 105 with permission. Copyright 2022 Wiley-VCH. (c) Schematic of emulsion electrospun. Reprinted from ref 107 with permission. Copyright 2018 Elsevier. (d) A typical facility for needleless electrospinning. Reprinted from ref 105 with permission. Copyright 2022 Wiley-VCH. (e) Diagram of the fundamental setup for coaxial electrospun or modified coaxial electrospun. Reprinted from ref 115 with permission. Copyright 2017 American Chemical Society. (f) The schematic of side-by-side electrospun, design details of the side-by-side spinneret, and image of a side-by-side spinneret. Reprinted from ref 119 with permission. Copyright 2020 Elsevier.

delivering signal quality on par with traditional gel electrodes. In another study, a versatile and efficient method for fabricating multifunctional on-skin electronics utilizing porous, highly gas-permeable sponges was introduced.[48] This approach features laser-patterned porous graphene as the sensing components, paired with sugar-templated silicone elastomer sponges as the substrates. Examples of the prototype devices include electrophysiological, hydration, and temperature sensors, as well as joule-heating elements, all delivering signal quality comparable to traditional, rigid, nonbreathable devices. Additionally, the devices demonstrate exceptional water-vapor permeability (~18 mg cm^{-2} h^{-1}), about 18 times higher than nonporous silicone elastomers, and exhibit rapid water-wicking performance postpolydopamine treatment, reaching 1 cm in 30 s, similar to cotton. These characteristics enable effective perspiration transport and evaporation, reducing discomfort and inflammation risks, thus enhancing their long-term usability.

Another challenge for supersoft and permeable thin-film planar electronics is the difficulty of patterning high-resolution

https://doi.org/10.1021/acsnano.4c13106
ACS Nano 2024, 18, 31737−31772

microelectrodes on these substrates. For example, the patternable feature sizes achieved so far typically range from 100 μm to millimeters, which falls significantly short of the requirements for advanced bioelectronics (typically demand sizes down to a few micrometers). Moreover, the required electrode density of advanced bioelectronics is over 100 electrodes/cm^2, a level far beyond the capabilities of conventional planar electronics.[58−60] Zeng and Yu introduced a method for wafer-scale patterning aimed at the high-resolution creation of ultrasoft, stretchable, and breathable liquid metal microelectrodes (μLMEs).[20] This method demonstrated a 2-μm patterning capability, achieving an ultrahigh density of approximately 75,500 electrodes/cm^2 on a 100 mm diameter elastic fiber mat. The wafer-scale fabrication method for wafer-patterned, permeable, and stretchable μLMEs involved several key steps. Initially, a silicon wafer was coated with a sacrificial layer, followed by the deposition of a stretchable polymer substrate. Liquid metal, typically gallium-based alloys, was then patterned onto the polymer substrate using photolithography and microcontact printing techniques. The liquid metal patterns were encapsulated with another layer of stretchable polymer to form a sandwich structure. Finally, the sacrificial layer was dissolved to release the μLMEs from the wafer, resulting in highly stretchable, permeable, and biocompatible microelectrodes suitable for chronic implantation in bioelectronics applications. Despite many excellent results achieved over the past decade, the incompatibility of different machining processes still makes it highly challenging to create an ideal 3D interface that conforms to the skin.

The necessity of electrospun nanofibers as flexible electronic device substrates lies in their exceptional flexibility, permeability, sensitivity, and biocompatibility, which can significantly enhance the user comfort and minimize the risk of adverse skin reactions and allowing for prolonged wear without irritation in health monitoring, prosthetics, and interactive systems.[41,61] For flexible sensors, they can be directly written, printed, patterned, or sputtering-electrodeposited onto the electrospun substrate.[62−65] For flexible energy and other modules, the electrospun nanofibers primarily act as a binder, substrate, or channel material to afford the device assembly.[66−68] Their capacity for integration with other advanced materials further augments their functionality and application scopes.[69]

3. ELECTROSPINNING TECHNIQUE AND ELECTROSPUN NANOFIBERS

3.1. Principles of Electrospinning. Electrospinning applies a high-voltage power to generate sufficient electrostatic force and overcome the polymer solution surface tension. When the surface tension is overcome, the fluid's hemispherical surface at the nozzle's tip stretches to form a conical shape called a "Taylor cone". As the strength of the electric field increases, the "Taylor cone" will deform until the jet is extruded from its apex. Throughout this process, the solvent will evaporate as the jet moves toward the collector. Once the solvent fully evaporates, the stretching of the jet ceases, resulting in the deposition of minuscule diameter fibers onto the earthed collector in the shape of nonwoven structures (Figure 2a).[70] The typical electrospinning process involves the selection of appropriate polymer precursor solutions, the selection of dopants, and the optimization of electrospinning conditions. By regulating the electrospinning parameters, electrospun nanofibers can be produced with diverse morphologies and properties. The capacity to customize the morphological characteristics of nanofibers to meet varying requirements endorses their application versatility.[71]

3.2. Influence Factors of Electrospinning. By manipulating polymer and solvent type, polymer molecular weight, concentration, conductivity, and surface tension, electrospinning allows the creation of fibrous products with varying fiber morphology, diameter, pore size, and spatial organization. Besides, circumstance temperature and humidity, along with processing parameters such as voltage, solution feeding rate, and collection distance, also influence fiber morphologies.[72−75] The morphology of nanofibers plays a crucial role in determining their performance and applicability in flexible electronics. Variations in fiber diameter, porosity, and surface roughness can significantly influence the mechanical flexibility, conductivity, and overall integration of nanofibers with other device components. For instance, reducing the fiber diameter from the micrometer to the nanometer scale significantly enhances the specific surface area, porosity, and pore connectivity of the fibrous mesh, leading to distinct properties in terms of light, heat, magnetism, and electrical performance.[76] Specifically, a very very common approach to enhancing the flexibility of flexible electronic devices is to reduce material thickness,[77] making nanofibers with small sizes highly advantageous.

3.2.1. Polymer Features. Polymer types predominantly determine the features of the resulting nanofibers. Natural biopolymers, such as silk fibroin (SF), chitosan (CS), and collagen, are commonly employed in electrospinning.[25] Natural polymers exhibit favorable biocompatibility and biodegradability, and their varied functional groups provide customized functions for implementation across diverse fields.[78−80] Moreover, by incorporating nanoscale components into polymer solutions, electrospun nanocomposites can be created, amalgamating the characteristics of both components.[81,82] Synthetic polymers offer more solvent options for preparing electrospinning solutions.[83,84] Various electrospun nanofibers have been developed from materials such as polyacrylonitrile (PAN), polyurethane (PU), poly(methyl methacrylate) (PMMA), polycarbonate, poly(lactic-*co*-glycolic acid) (PLGA), polyvinylidene fluoride (PVDF), poly(vinyl chloride), and polycaprolactone (PCL).[85,86] Many synthetic polymers, such as polylactic acid, PCL, and polylactic acid-hydroxyacetic acid copolymers, exhibit exceptional biocompatibility and biodegradability. Electrospun nanofibers composed of biodegradable polymers have also been produced and extensively utilized in biomedical fields, including tissue engineering, drug release, wound dressings, and implantable devices.[87,88]

Other polymer attributes affecting electrospinning include molecular weight, polymer solubility, *etc.*[89] Moreover, the rheological properties of the polymer solution, which encompass electrical conductivity and surface tension, also influence the structure of the electrospun nanofibers.[90] To ensure a smooth electrospinning process, selecting an appropriate solvent is essential. Besides, high conductivity and low surface tension are not sufficient for electrospinning of polymer solutions.[91] The fiber refinement principle shows that increasing the electrical conductivity of polymer solution could reduce the diameter of the formed nanofibers.[92] In certain cases, a high surface tension may serve as a negative factor for electrospinning.[91] This is because electrospinning can only occur when the electrostatic force from the applied electric

https://doi.org/10.1021/acsnano.4c13106
ACS Nano 2024, 18, 31737−31772

field overcomes the surface tension of the liquid. These factors interact with each other, and their specific combination ultimately determines the final nanofiber diameter and surface morphology.[93]

3.2.2. Processing Parameters. The processing conditions of the electrospinning process significantly influence the nanofiber formation.[94] The applied voltage plays an essential role in the electrospinning process since it can influence the electric field strength. An increase in voltage typically results in a higher electrostatic force, which can lead to the formation of thinner fibers. However, excessively high voltage can lead to bead formation or irregular fibers. Thus, optimizing the voltage is critical for obtaining consistent nanofibers.[95] The flow rate of the polymer solution also significantly affects fiber formation. A higher flow rate generally results in thicker fibers, as more material is ejected from the needle tip. However, if the flow rate is too high, defects may be produced due to incomplete solvent evaporation. On the other hand, lower flow rates allow for more controlled fiber formation, often resulting in finer fibers with fewer defects. Therefore, controlling the flow rate is also crucial to achieving uniform nanofiber.[96]

Increasing the concentration can increase the polymer chain entanglement and solution viscosity. The solution viscosity influences the nanofiber diameter, therefore, reducing the solution concentration results in a smaller nanofiber diameter. The viscosity of a polymer solution is determined by the degree of entanglement between the polymer chains in the solution. Viscous solutions are indispensable for overcoming the electrostatic and Coulombic repulsion forces that elongate the electrospinning jet. At lower viscosities, the jet partially breaks apart, causing the solvent molecules not bound in the solution to clump together into spherical formations, resulting in the formation of beads.[97] However, significantly lowering the concentration may disrupt stable jet formation and diminish the quality of the nanofibers. The distance between the needle tip and the collector affects the solvent evaporation, nanofiber diameter, and nanofiber deposition pattern. Research has shown that decreasing the collection distance improves the interconnectivity of the nanofibers.[98] Additionally, rotating the collector during deposition generated electron beam alignment.[99] Furthermore, increasing the collector rolling speed within an optimal range was associated with improved alignment and neatness of the nanofibers.[100] Aligned nanofibers can create an efficient pathway for electron transport with improved energy storage capacity and charging/discharging speeds. Therefore, using aligned electrospun nanofibers in organic solar cells improved the device performance and efficiency.[101] Other key processing parameters are voltage and flow rate.

Moreover, environmental factors, like temperature and humidity, also influence the nanofiber properties. For instance, elevated temperature has several effects on the electrospinning process. First, higher temperatures can reduce the surface tension and viscosity of the polymer solution, resulting in nanofibers with a more uniform size. Moreover, increased temperature can accelerate the evaporation of solvents from the fluid jet and the solidification of the nanofibers. However, too high a temperature can cause premature cessation of electro-stretching of the fluid jet, resulting in larger nanofiber diameters.[102] Thus, the effect of temperature on the electrospinning process is a balance between promoting nanofiber formation and the potential negative impact on nanofiber diameter. For humidity, it may influence the electrospinning process by influencing solvent evaporation rates.[103] In most cases, higher relative humidity can result in slower solvent evaporation rates. On the other hand, higher humidity levels can provide more opportunities for polymer chains to align and form organized structures, leading to larger nanofiber diameters. Consequently, lower relative humidity may accelerate the evaporation process, thereby speeding up solvent removal. This results in an increase in the porosity of nanofibers and surface roughness.[104]

3.3. Electrospinning Techniques to Prepare Flexible Electronic Devices. *3.3.1. Single-Fluid Electrospinning.* The electrospinning technique available for the preparation of composite fibers can be categorized into three types according to the different solutions or fluids involved: single-fluid electrospinning, double-fluid electrospinning, and multifluid electrospinning (Figure 2b).[105] Single-fluid electrospinning offers a straightforward method for fabricating flexible devices.[106] A typical single-fluid electrospinning experimental setup consists of a high-voltage power supply, a solution supply system, and a grounded collector (Figure 2c).[107] The high surface area and porosity of these nanofibers facilitate the incorporation of various sensing elements, enabling multifunctional detection capabilities within a single sensor.[108] Guo et al. prepared flexible and water-resistant PVA nanofibers using single-fluid electrospinning and annealing techniques. They coated the nanofiber surface surface with polypyrrole (PPy) nanoparticles *via in situ* polymerization. After three rounds of polymerizations, the PPy@PVA nanofiber membrane exhibited a conductivity of 32.1 mS cm^{-1} and a resistance of 840 Ω sq^{-1}. However, the study discovered that the elongation properties of pure PVA nanofiber membranes were inadequate.

In particular, single-fluid electrospinning can be combined with certain advanced fabrication techniques to create multifunctional devices. For instance, the development of covalent organic framework (COF), metal−organic framework (MOF), and zeolite imidazolium framework nanofibers through precursor electrospinning and subsequent sol−gel reaction has attracted much attention. In these processes, the polymer phase typically serves as a binder or substrate for MOF or COF composite fibers, providing flexibility to the overall composite system.[109−112] However, adding supplementary polymer components to the COF film can occasionally compromise its flexibility and mechanical durability. Ding et al. addressed this issue using a template-assisted framework (TAF) process. In this approach, an electrospun porous polymer membrane serves as a sacrificial template for the COF membrane. The TAF process involves removing the template polymer, resulting in a self-supporting COF membrane that offers high flexibility and mechanical stability. COF membranes created using the TAF process demonstrate exceptional flexural stability, remaining unchanged even after 10,000 cycles of flexural testing. Additionally, these COF membranes feature a layered and permeable structure, which facilitates efficient gas flow with minimal pressure drop, making them suitable for gas separation and adsorption applications.[113] Recently, Wang et al. presented a simple and robust method for fabricating flexible ephemeral circuits for human-computer interaction.[114] The method involved using stencil-printed liquid metal conductors on water-soluble electrospun films. The resulting circuit exhibited high resolution, feasibility of customized patterning, superior permeability, excellent conductivity, and superior mechanical stability. Furthermore, the circuit exhibited reliable noncontact proximity sensing capabilities

https://doi.org/10.1021/acsnano.4c13106
ACS Nano 2024, 18, 31737−31772

Table 1. Summary of Flexible Sensors Based on Electrospun Nanofibers

preparation method	solvent	polymer	nanofiber diameter	application areas	ref
Single-fluid electrospinning	1,2-Dichloroethane	Poly(styrene-*block*-butadiene-*block*-styrene)	1 μm	E-skin soft robotics and bioelectronics	18
Centrifugal electrospinning	Hexafluoroisopropanol, ethanol	PU		Voice signal monitoring and recognition	21
Single-fluid electrospinning	dimethylformamide (DMF), tetrahydrofuran	polyurethane (TPU)	55 nm	Wearable electronic devices	41
Electrospinning and annealing	DMF	PVA, PPy	170−250 nm	Medical monitoring, human movement detection	108
Single-fluid electrospinning	DMF	PAN	200−300 nm	HMI and monitoring body movement	123
Single-fluid electrospinning	DMF	PAN, PPy	253 nm	Volatile organic compound sensors	124
Single-fluid electrospinning	DMF	PDMS, Anisotropic carbon nanofiber		Soft, flexible electronics	125
Single-fluid electrospinning	DMF/Acetone (3:2)	PVDF-co-trifluoroethylene (P(VDF-TrFE))	260 nm	Self-powered micromechanical components	126
Single-fluid electrospinning	DMF	TPU, Carbon nanotubes (CNTs)	200 nm	E-skin	127
Single-fluid electrospinning	Isopropanol	TPU, Liquid metal	600 nm	E-skin	128
Single-fluid electrospinning	DMF, tetrahydrofuran	TPU, TiO_2	1 μm	Human psychological signal monitoring and wearable transmission system	129
Single-fluid electrospinning	1,1,1,3,3,3-Hexafluoro-2-propanol (HFIP)	SF PLGA, PANI		Human motion detection	130
Single-fluid electrospinning	Deionized water	PVA, PU		Smart wearables and pneumatic pressure monitoring	131
	Deionized water	PVA	1 μm	Wearable devices	132
Single-fluid electrospinning	DMF	Polystyrene	180 nm	Wearable electronic devices	133
Single-fluid electrospinning	Acetone, DMF	PVDF-TrFE		Smart home appliances	134
Single-fluid electrospinning	DMF	PU		Long-term, high-precision electrophysiological monitoring	135
Single-fluid electrospinning	Acetone, DMF	PVDF	652 nm	Capacitive touch sensors	136
Single-fluid electrospinning	Acetone, DMF	PVDF, PAN	200−300 nm	Human-machine interaction, and soft robots	137
Single-fluid electrospinning	DMF	TPU	500−700 nm	Virtual reality, human−machine interface	138
Single-fluid electrospinning	DMF	TPU, PAN	200 nm	Personal healthcare and intelligent robots	139
Single-fluid electrospinning	Tetrahydrofuran	PU	2.5 μm	E-skin	140
Single-fluid electrospinning	Acetone, DMF	PVDF, Ag	2 μm	Real-time human motion sensing and pulse monitoring	141
Single-fluid electrospinning	DMF	poly(ionic liquid), CNTs	300 nm	E-skin	142
Single-fluid electrospinning and calcination treatment	DMF	Polyvinylpyrrolidone (PVP), $SbCl_3$, $SnCl_4{\cdot}5H_2O$	166 nm	Wearable strain sensors	143
Single-fluid electrospinning	DMF, DCM	TPU		Human-machine interaction, soft robotics, and wearable devices	144
Single-fluid electrospinning	DMF	TPU, Ag	1 μm	Multifunctional strain sensors	145

while maintaining satisfactory contact sensing performance, a feat that is unattainable with traditional systems. As a result, this flexible circuit can be utilized as a wearable sensor for information transfer, smart identification, and trajectory monitoring. Additionally, by using a straightforward water dissolution technique, the circuit can be recycled rapidly and effectively, providing significant economic and environmental benefits.

A bubble electrospinning system, consisting of an air injection pump, a high-voltage power supply, a bipolymer solution supply device, a grounded collector (represented by a revolving disc), and a solution reservoir system, can also be referred to as a single-fluid electrospinning (Figure 2d).[105] However, its applications in device design have not yet been reported. Besides, the single-fluid electrospun nanofibers can be used as the substrate and integrated with other layers to get flexible devices. For example, to prepare the wearable moisture-electric generator (MEG), the PVA/phytic acid nanofiber membrane was electrospun onto a silver-plated fabric, while the PVDF nanofiber membrane was electrospun onto porous aluminum foil. Polyethylene oxide (PEO) was used as an adhesive to bond these two layers, forming the power generation layer. The MEG device was then assembled and heated at 60 °C under pressure for 10 min to securely bond the porous aluminum foil electrode to the PVA/phytic acid nanofiber membrane.[66]

3.3.2. Multifluid Electrospinning. Multifluid electrospinning is a technique used to produce composite nanofibers with tailored release kinetics. Coaxial electrospinning, a common type of double-fluid electrospinning, involves using two types of fluids within a single concentric spinneret. This method is regarded as one of the most significant advancements in the field (Figure 2e).[115] The primary advantage of coaxial electrospinning is its ability to create composite nanofibers with precisely controlled compositions and structures. By simultaneously extruding multiple solutions through coaxial needles, this technique enables the formation of complex nanofibrous architectures, such as core−shell, hollow, or

https://doi.org/10.1021/acsnano.4c13106
ACS Nano 2024, 18, 31737−31772

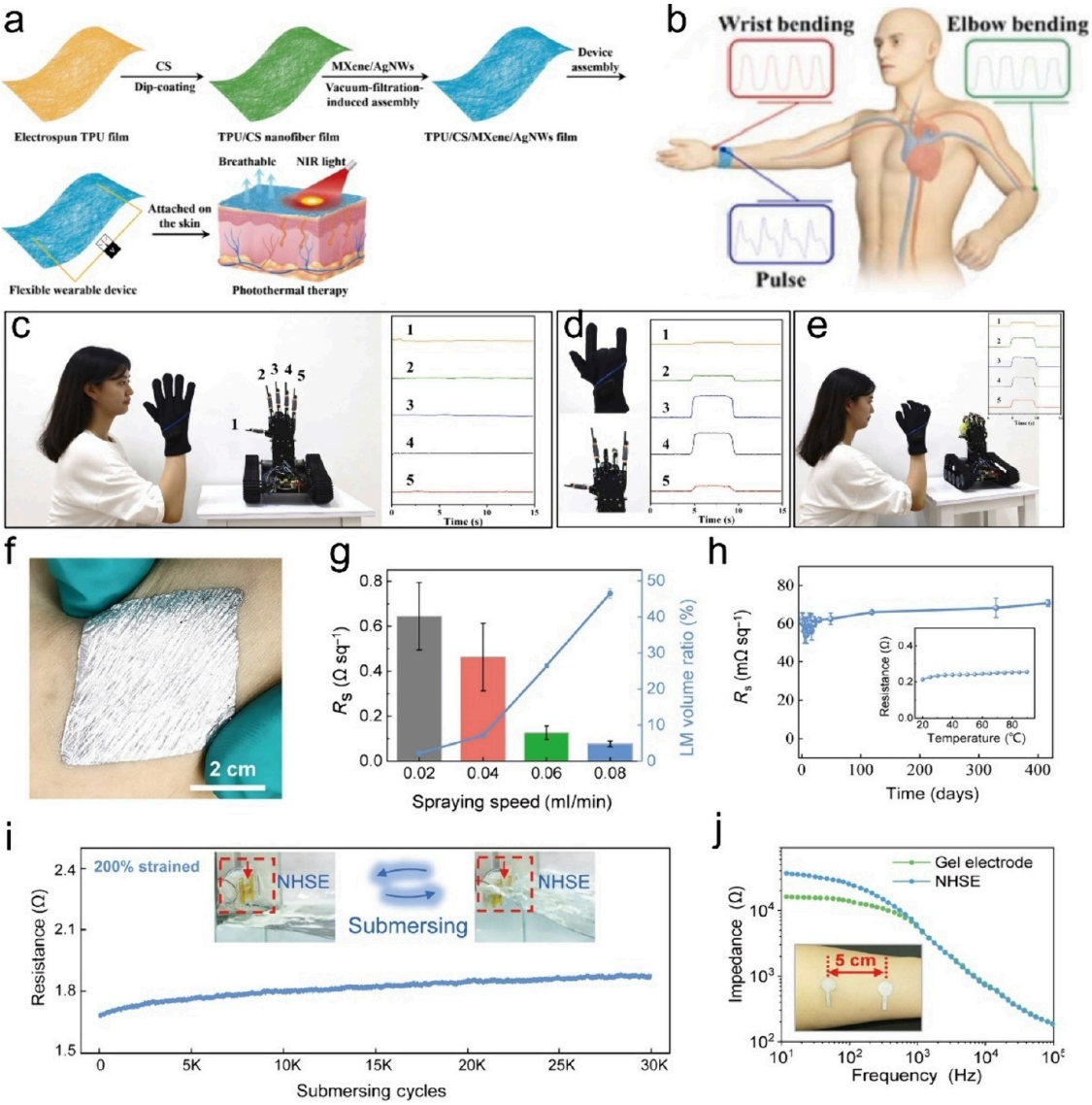

Figure 3. (a) A schematic illustration of electronic sensors designed for wearable human motion detection and highly sensitive human−machine interfaces. (b−e) These sensors were successfully utilized for comfortable human motion tracking and ultrasensitive human−machine interaction. (a−e) Reprinted from ref 41 with permission. Copyright 2023 Elsevier. (f) A photo of the highly conformal NHSE attached to a forearm. (g) The sheet resistance of the NHSE and the volume ratio of LM in the liquid metal nanoparticle/TPU scaffold composite as a function of the electrospray speed of the EGaIn nanoparticles solution. (h) The sheet resistance of the NHSE after being exposed to air for 420 days with an inset showing resistance variation as the temperature increases from 20 to 90 °C. (i) The resistance of the NHSE stretched to 300% over 30,000 water immersion cycles (initial sample size: 1 cm × 1 cm). (j) A comparison of electrode−skin contact impedance between the commercial gel electrode and NHSE. (f−j) Reprinted with permission under a Creative Commons [CC BY] License from ref 128. Copyright 2022 The Authors. Published by UESTC and Wiley-VCH.

multilayered structures, which are difficult to achieve with conventional electrospinning methods. For example, using coaxial electrospinning, researchers created highly porous and flexible materials by using polyethylene terephthalate (PET) and a PET composite with titanium dioxide (PET-TiO_2) in core−shell nanofibrous mats. The core solution was a mixture of PET dissolved in trifluoroacetic acid (TFA) and dichloromethane (DCM), while the shell solution contained TiO_2 (in the form of nanobars and nanorhombics) dispersed in a PET solution also dissolved in TFA and DCM. Incorporating TiO_2 into the shell layer enhanced the optical, thermal, and mechanical properties of the fibrous mats, making them suitable alternatives to the currently used brittle porous TiO_2-based photoelectrodes.[116] Using a similar technique, PU@Fe_3O_4−PU@CNT coaxial fiber membrane[117] and poly(ether imide)@polyaniline (PANI) core−shell fibrous membrane[118] were designed for flexible devices.

Side-by-side electrospinning is also a kind of multifluid electrospinning approach. Side-by-side electrospinning can overcome the limitations of the thermodynamic mixability and interactions between polymer components, enabling the formation of Janus fibers (Figure 2f).[119] In side-by-side electrospinning, a pair of Taylor cones and jets was formed between the polymer solutions, which experienced strong electrostatic repulsion. It is essential to prevent the two polymer solutions from coming into contact with each other before spinning to ensure the proper functionality of the nanofibers. Ensuring that the internal, intermediate, and

https://doi.org/10.1021/acsnano.4c13106
ACS Nano 2024, 18, 31737−31772

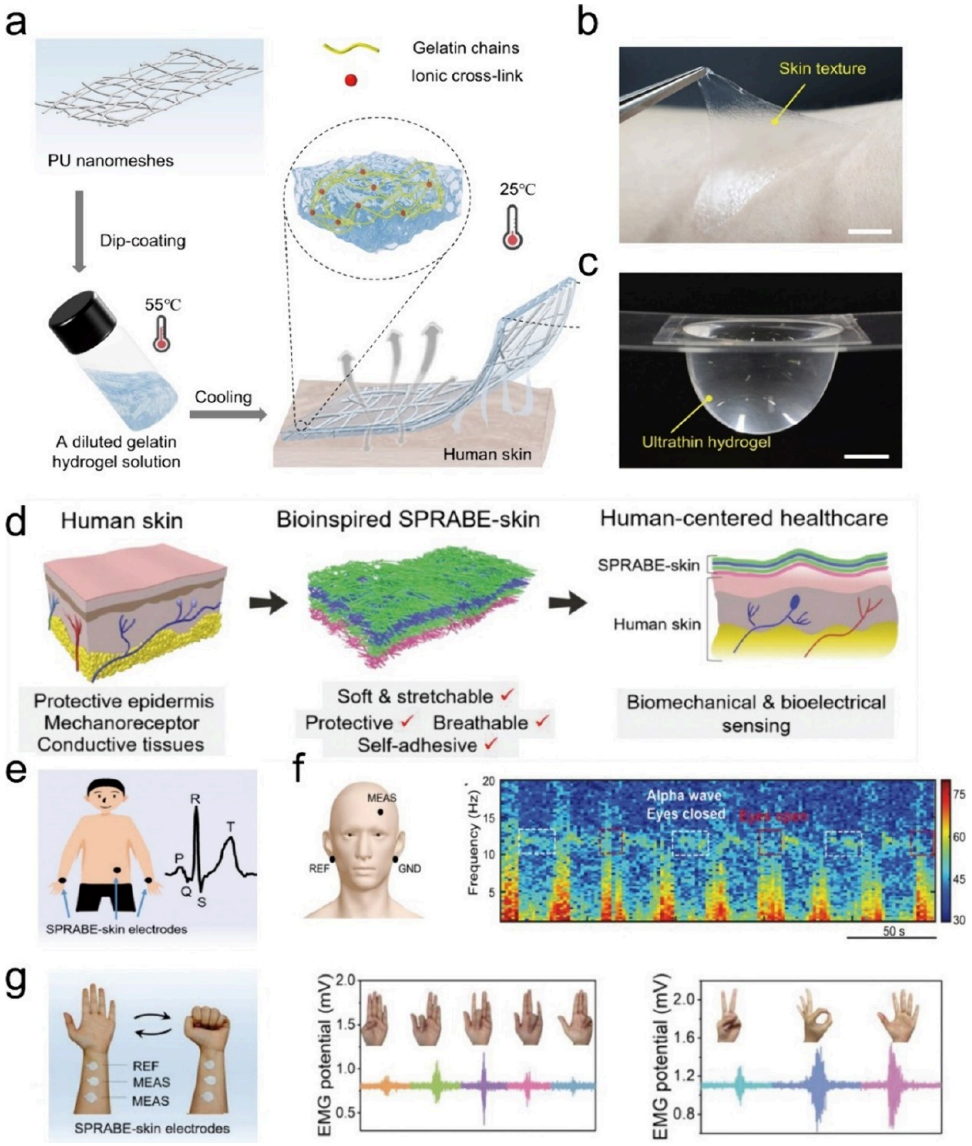

Figure 4. (a) An illustration showing the design principles of hydrogels reinforced with PU nanomesh. (b) An image of a superthin hydrogel being removed from human skin, highlighting its exceptional adhesion and elasticity. (c) An image showing that the ultrathin hydrogel, when suspended, retains a significant amount of water. (a–c) Reprinted from ref 135 with permission. Copyright 2024 The Authors, some rights reserved; exclusive licensee American Association for the Advancement of Science. Distributed under a Creative Commons Attribution NonCommercial License 4.0 (CC BY-NC) https://creativecommons.org/licenses/by-nc/4.0/. (d) A schematic of the bioinspired design of SPRABE-skin. (e) A diagram of SPRABE-skin electrocardiogram detection and the amplification curve of a single cardiac cycle. (f) The SPRABE-skin electrode positioned at the Fp1 location and earlobe for EEG measurement, including spectral analysis to differentiate between open and closed eye events. (g) The SPRABE-skin electrode on the wrist flexor muscle used for electromyography, capturing EMG signals generated by various finger movements, including flexions, extensions, and gestures. (d–g) Reprinted from ref 127 with permission. Copyright 2023 Wiley-VCH.

external laminar flow fluids form a complex of Taylor cones and maintain concentric alignment throughout the electrospinning process is crucial for the effectiveness of triaxial electrospinning.[120] In another study, using a trifluid side-by-side electrospinning, Liao and co-workers presented a trilayer eccentric Janus nanofiber system for the treatment of periodontitis. The nanofibers are composed of PCL, PVA, and CS, forming distinct layers that deliver multiple therapeutic agents. The PCL layer provided structural support and controlled release of anti-inflammatory drugs, while the PVA layer offered a rapid release of antibacterial agents. The CS layer enhanced the biocompatibility and promoted tissue regeneration.[121]

Through programmatic design, a trilayer concentric spinneret can facilitate the execution of one-fluid uniaxial, two-fluid coaxial, and three-fluid coaxial electrospinning techniques, yielding nanofibers with monolithic, core–shell, and trilayer core–shell structures.[122] For instance, Yu et al. designed a trilayer core–shell medicated nanofiber using the concentric spinneret-assisted electrospinning. Using a trilayer concentric spinneret, double-working fluids can be arranged in three configurations. If the outer fluid consists solely of a pure solvent, monolithic nanofibers are produced regardless of the middle or inner fluid composition. Alternatively, when the outer fluid flow is stopped, the central and inner fluids can

https://doi.org/10.1021/acsnano.4c13106
ACS Nano 2024, 18, 31737–31772

participate in a conventional coaxial electrospinning process, leading to the formation of core−shell nanofibers.

4. FLEXIBLE SENSORS

Flexible sensors are widely used in smart homes, environmental conservation, health monitoring, and other fields. This section highlights the recent advances in flexible biosensors, pressure sensors, and strain sensors using electrospun nanofibers as the substrate. Table 1 lists more details about these typical electrospun nanofiber-based flexible sensors.

4.1. Biosensors. Biosensors are analytical devices designed to detect biological or chemical substances by converting a biological response into a measurable electrical, optical, or mechanical signal. These devices typically consist of a biological sensing element, a transducer to convert biological responses into measurable signals, and a signal processor for data analysis.[146] Recent advancements in biosensor technology have led to the development of flexible, stretchable, and highly durable biosensors, particularly those based on electrospun nanofibers.[134,147,148] The high surface area and porosity of electrospun nanofibers enable biosensors to evolve into flexible and biocompatible intelligent systems with high breathability.[149]

For example, Wan et al. developed a multifunctional, flexible, wearable, and breathable electronic sensor for comfortable human motion detection and ultrasensitive human−machine interaction.[41] In their research, a flexible and breathable electronic sensor was developed by incorporating conductive MXene nanosheets and Ag NWs onto a breathable, chitosan-coated electrospun thermoplastic TPU nanofiber network. This sensor, which boasts excellent durability and a wide sensing range (Figure 3a,b), benefits from the reversible movement of MXene and AgNWs. As a result, it is capable of detecting subtle human motions and physiological signals across a broad strain range (approximately 120% strain), ultrahigh calibration coefficients (up to 4720), and low detection limits (∼0). The device has excellent reliability and durability, making it suitable for monitoring small physiological signals such as pulse and more significant movements like wrist flexion and elbow bending. More interestingly, the device can aid in smart disease diagnosis. A volunteer demonstrated various hand gestures and ball grasping using a wireless somatosensory glove on her right-hand. Observers could instantly see the robotic fingers flexing and extending in response to the volunteer's hand movements, facilitated by the intelligent wireless somatosensory glove (Figure 3c-e).

To enhance the permeability of liquid-metal-based flexible devices, Zheng and co-workers reported a highly permeable superelastic "liquid-metal fiber mat" (LMFM). This innovative design facilitated the creation of biocompatible and versatile monolithic stretchable electronics, such as electrocardiography (ECG) sensors, sweat sensors, and heaters in a vertical stack.[18] The LMFM was created by applying liquid metal onto an electrospun elastomeric mat using coating and printing techniques, followed by a straightforward mechanical activation. In this process, the liquid metal arranged itself into a film with a laterally porous structure and vertical buckling that adhered to the fibers. The LMFM exhibited exceptional air, moisture, and liquid permeability while retaining superelastic properties (withstanding over 1,800% strain) and ultrahigh conductivity (up to 1,800,000 S m^{-1}) over 10,000 cycles of tensile testing. However, the high surface tension of liquid metal and its poor substrate interaction make it difficult to maintain conductivity under significant strain. In another study, Li and Zhu introduced a nanoliquid metal-based robust and highly stretchable electrode (NHSE), featuring a self-adaptive interface that mimics the interaction of water with a net (Figure 3f). This NHSE is created by the *in situ* integration of electrospun elastic nanofiber frameworks with electrosprayed liquid metal nanoparticles. It boasted an exceptionally low sheet resistance of 52 mΩ sq^{-1} (Figure 3g) and was not significantly impacted by substantial mechanical stretching or repeated deformation. Its durability and stability were demonstrated under various conditions, including long-term high-temperature exposure (20−90 °C, 420 days, Figure 3h) and repeated submersion (30,000 cycles, Figure 3i). Therefore, the NHSE is well-suited for integration into epidermal devices designed to capture physiological signals from the body (Figure 3j).[128]

Additionally, the combination of electrospun nanofibers and hydrogels holds promise for yielding e-skin characterized by customizable thickness, transparency, and superior gas-permeability. Hydrogels have garnered significant interest in the realm of skin bioelectronics due to their resemblance to biological tissues and their versatility in mechanical, electrical, and biofunctional applications.[150,151] Given that human skin continuously loses both sensible and insensible sweat at a rate of approximately 600 g/m^2/day, engineering ultrathin, robust, gas-permeable, and skin-adherable hydrogel sensors to prevent dryness for long-term daily use (>7 days) is of significant.[18] In a pioneer study, the electrospun PU nanomeshes were prepared from the PU/DMF/methyl ethyl ketone solution using a simple room temperature electrospinning process.[135] The ultrathin hydrogel was developed by PU nanomeshes into a type A gelatin hydrogel solution that underwent a thermal-controlled phase transition, followed by gelation at either physiological temperature or in ambient conditions (Figure 4a). Suca a thick PU nanomesh-reinforced hydrogel sensor (thickness: ∼ 10-μm) with gas-permeability was able to adhere to human skin autonomously (Figure 4b), enabling sustained and reliable electrophysiological monitoring for up to 8 days in real-life conditions. The resulting ultrathin hydrogels demonstrated superior mechanical strength, excellent skin adhesion, gas permeability, and resistance to drying (Figure 4c).

The advent of electronic skin (e-skin) technology has revolutionized the field of biosensors, presenting a convergence of flexible electronics and biological sensing capabilities.[152] A key advantage of electrospun nanofibers-based e-skin is that it can mimic the properties of human skin, offering high breathability and biocompatibility, which are essential for continuous and noninvasive monitoring of physiological parameters.[153] By integrating various types of biosensors, such as electrochemical, optical, and piezoelectric sensors, into a single e-skin platform, it becomes possible to detect a wide range of biomarkers (e.g., glucose, lactate, and pH levels, as well as physical parameters like temperature and pressure).[69] This synergy enables real-time, on-body health monitoring and diagnostics for advanced healthcare applications. Furthermore, the development of self-healing and biodegradable materials in e-skin technology enhances its practicality and sustainability for durable applications. One of the most frequently used building materials for e-skin is PU.[140] For example, Cheng and Wang reported a scalable bioinspired SPRABE-skin. For preparation, a fibrous TPU membrane was created using electrospinning. Next, a hybrid MXene-CNTs solution was sprayed onto the TPU membrane to form a strain-sensitive

https://doi.org/10.1021/acsnano.4c13106
ACS Nano 2024, 18, 31737−31772

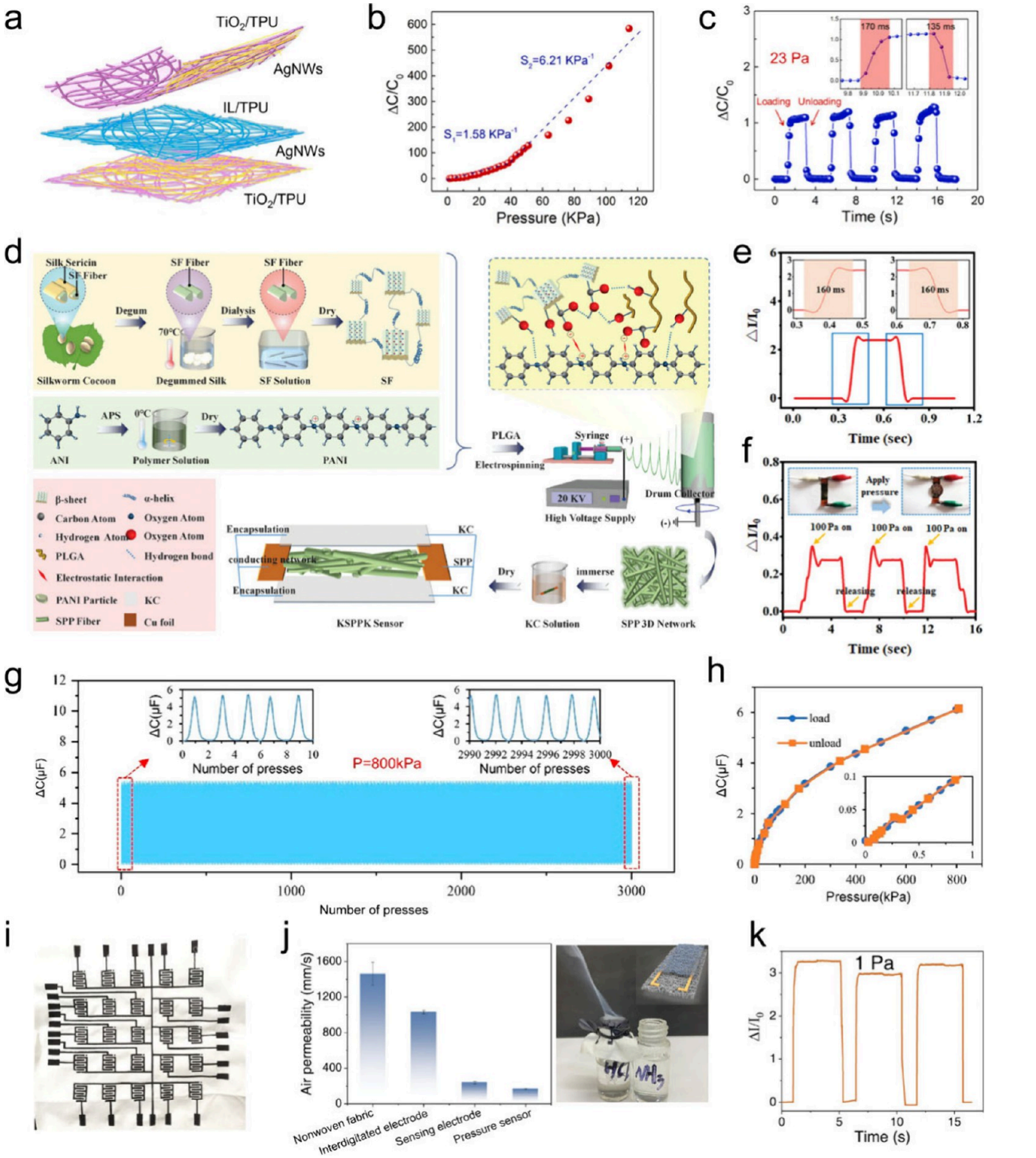

Figure 5. (a) Structural diagram of the structure of the developed flexible pressure sensor. (b) Capacitance changes of the sensor as a function of varying pressures. (c) Response of the sensor to the application and removal of a load (23 Pa) with an inset displaying the sensor's response and recovery times. (a–c) Reprinted from ref 129 with permission. Copyright 2023 Elsevier. (d) Production of the sensor involves several stages: a schematic representation details the extraction of SF protein, synthesis of PANI powder, electrospinning procedure, and subsequent encapsulation. The blue dotted box highlights the interactions among the SPP nanofibers. (e) The sensor's response and recovery times under a pressure of 920 Pa are measured from the *I*–*t* curve. (f) The *I*–*t* curve also illustrates the sensor's response to the application and release of a coin, indicating a pressure of just 100 Pa. (d–f) Reprinted from ref 130 with permission. Copyright 2021 Wiley-VCH. (g) Evaluating the durability of pressure sensors through up to 3000 cycles. (h) Measuring the capacitive response of the sensor during a single load and unload cycle. (g,h) Reprinted from ref 132 with permission. Copyright 2023 American Chemical Society. (i) Optical image of a single interdigitated electrode and screen-printed MXene-based interdigitated arrays for e-skin with 5 × 5 pixels. (j) Air permeability of nonwoven fabric, textile-based interdigitated electrode, BMTPU sensing electrode, and the assembled pressure sensor. Demonstrations of air permeability of the assembled pressure sensor. (k) Relative current response of the device under 1 Pa. (i–k) Reprinted from ref 22 with permission. Copyright 2024 Wiley-VCH.

https://doi.org/10.1021/acsnano.4c13106
ACS Nano 2024, 18, 31737–31772

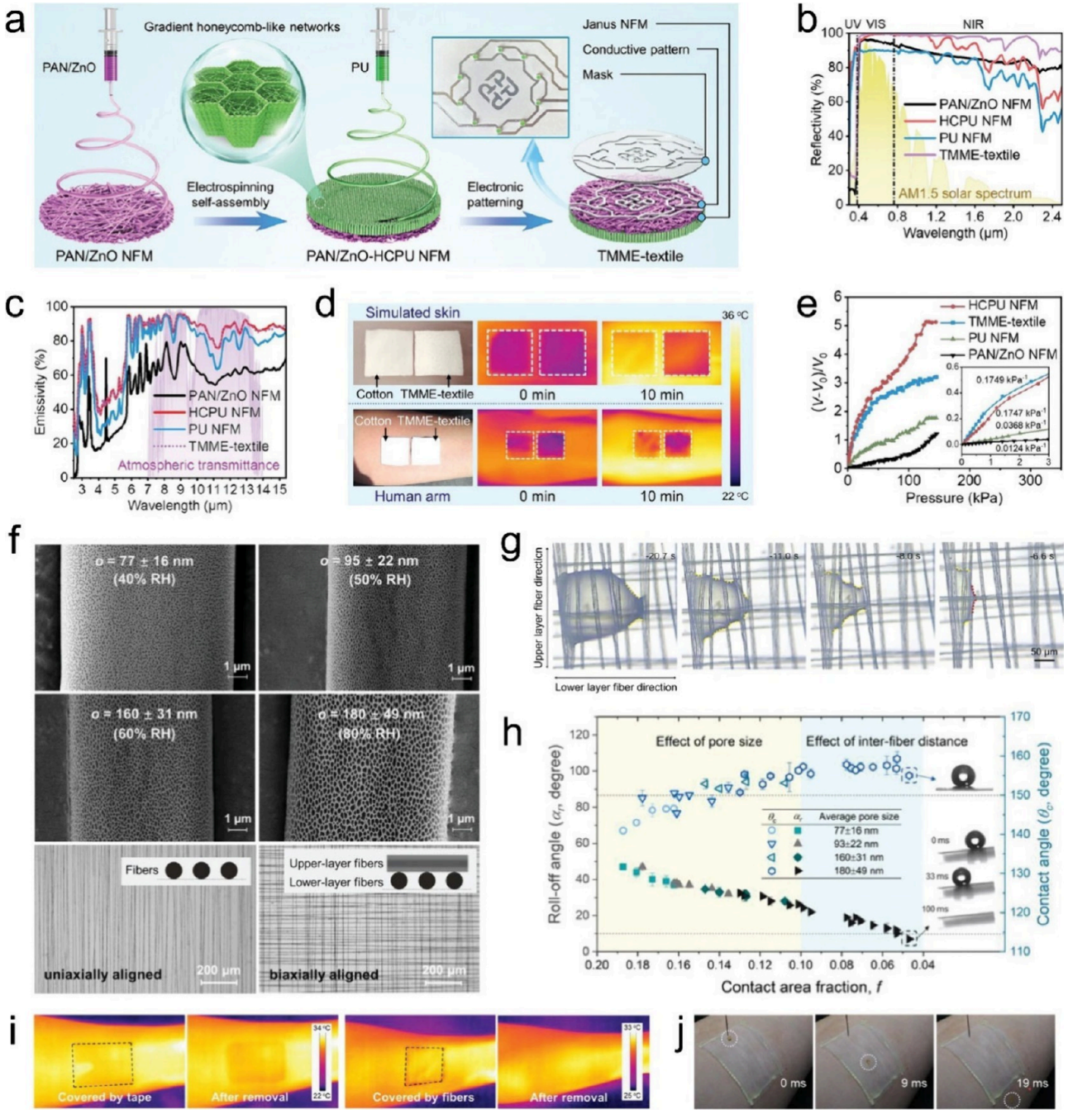

Figure 6. (a) Illustration of the process to fabricate TMME-textile featuring gradient honeycomb-like networks. (b) Reflectivity spectra measurements for PAN/ZnO, HCPU, PU nanofiber films (NFMs), and TMME-textile within the solar wavelength range. (c) Emissivity spectra measurements for PAN/ZnO, hydrophobic gradient honeycomb-like PU, PU NFMs, and TMME-textile in the IR wavelength range. (d) Optical and infrared images of TMME-textile on the skin and cotton before and after approximately 10 min of direct sunlight exposure. The environment temperature during the test was 23−24 °C. (e) Relative voltage change, $(V - V_0)/V_0$ versus applied pressure on strain sensors based on TMME-textile and various NFMs. The inset displays the sensitivities of these strain sensors for pressures ranging from 0 to 3 kPa. (a−e) Reprinted from ref 123 with permission. Copyright 2024 Wiley-VCH. (f) Images from SEM and optical microscopy of electrospun fibers produced at 40%−80% relative humidity reveal surfaces with varying pore sizes and two distinct alignment patterns. (g) The final stages of droplet-free evaporation on biaxially aligned porous fibers with droplet diameters reduced to below 300 μm. (h) Examination of how the size of the upper-layer pores and the average distance between fibers influence water contact and roll-off angles. (i) Thermal images comparing the effects of applying nonbreathable adhesive tape versus biaxially aligned porous fibers on human forearm skin for 60 min, followed by removal. (j) The superhydrophobic properties of the forearm skin area covered with biaxially aligned porous fibers. (f−j) Reprinted with permission under a Creative Commons [CC BY] License from ref 133. Copyright 2023 The Authors. Published by Wiley-VCH.

layer (S-layer) (Figure 4d). Both sides were deposited with electrospun TPU to create the protective and isolating layers (P-layer and I-layer). Finally, an electrode layer (E-layer) for biopotential sensing was created by applying a coating of

https://doi.org/10.1021/acsnano.4c13106
ACS Nano 2024, 18, 31737−31772

MXene-waterborne polyurethane onto the I-layer. The MXene-CNT@TPU strain sensing layer exhibited ultrahigh sensitivity over a wide range (gauge factor at 485% strain reaches 63,494). The fibrous TPU scaffold endowed the SPRABE-skin with the tissue-like softness (Young's modulus: 3.36 MPa), along with enhanced stretchability, permeability, and self-protection against damaging forces. The MXene-waterborne polyurethane E-layer ensured a highly adhesive interface for acquiring biopotentials like ECG, electromyo-graph (EMG), and electroencephalo-graph (EEG) with enhanced fidelity despite dynamic interferences. Ultimately, a human-centered healthcare system utilizing SPRABE-skin technology was showcased, achieving continuous, wireless monitoring of ECG and physical activities over extended periods (Figure 4e−g).[127] Other polymers like PVDF and PDMS have also been employed as substrate materials for the e-skin construction.[154−157] However, the thickness and transparency of the designed electrospun nanofiber substrates may significantly impact their performance.

4.2. Pressure Sensors. Pressure sensors have four different modes of operation which are capacitive,[138] piezoelectric,[126] triboelectric,[141] and resistive.[124] Accurately assessing external stimuli on curved and dynamic surfaces (e.g., human skin), requires precise measurement of weak pressures. Electrospun nanofibers are used in pressure sensors as electrode media, conductive layers, or dielectric layers.[158] These nanofibers confer exceptional sensitivity to mechanical stimuli and breathability, which allows for precise pressure detection.[22,132] Their inherent flexibility allows for the fabrication of conformal and adaptable sensor devices, ensuring comfortable integration with irregular surfaces.[159]

Recent research has focused on enhancing the performance of electrospun nanofiber-based pressure sensors through various strategies.[22] For example, incorporating conductive substances into electrospun nanofibers improved the electrical conductivity and sensitivity of nanofibers.[129,130] To accelerate the piezoelectric reaction, Zhu et al. created an electronic pressure sensor made of a breathable and self-cleaning TPU material. The self-cleaning capability arises from the inclusion of TiO_2 nanoparticles in the TPU, which safeguarded it from bacterial and UV damage (Figure 5a). The sensor showed sensitivities of approximately 1.58 kPa^{-1} (0−40 kPa) and 6.21 kPa^{-1} (40−120 kPa), and can detect pressure signals as small as 23 Pa (Figure 5b). It has rapid response and recovery speeds, with an instantaneous response time of 170 mS and a recovery time of 135 mS (Figure 5c).[129] In another study, Li and colleagues developed a breathable and biodegradable piezoresistive sensor. To construct the sensor, they used SF and PANI to create a 3D network of intertwined nanofibers. The nanofibers were then incorporated into an intelligent skin sensor (Figure 5d).[130] The sensor exhibited a maximum sensitivity of 2.54 kPa^{-1} and a wide linear detection range of 165.3 kPa, and can support over 2000 detection cycles, facilitating the rapid detection of subtle pressure changes. More interestingly, the sensor boasted a response time of 160 mS (Figure 5e), allowing it to quickly detect and respond to changes in pressure. Additionally, the sensor is capable of detecting minimal pressures as low as 100 Pa, equivalent to the weight of a freely falling coin (Figure 5f). The sensor was fully biodegradable because of the natural biodegradability of SF and its eco-friendly polymer encapsulation technique. Further, the physical properties of electrospun nanofibers also significantly influence the performance of sensors. For example, researchers investigated how the porosity of the electrospun electrode and ion membrane affects the sensor's sensitivity.[132] The thickness and porosity of the nanofibers were precisely adjusted by controlling the electrospinning parameters and precursor ratio. The results indicated that smaller nanofiber sizes and higher porosity resulted in more significant deformation of the dielectric layer and increased sensor sensitivity under the same pressure. Even after 3000 repetitions, the sensor maintained its initial capacitive response without any significant degradation in performance (Figure 5g). Moreover, the curves for both the loading and unloading processes are essentially identical, indicating that the ion membrane pressure sensor exhibits excellent recoverability (Figure 5h).

In addition, the bionic design also provides an outlet to enhance the performance of nanofiber-based pressure sensors. For instance, a biomimetic flexible pressure sensor inspired by the spinosum microstructure of human skin was designed using MXene-based sensing and interdigitated electrodes (Figure 5i). The sensor demonstrated good flexibility and air permeability (165.6 mm s^{-1}, Figure 5j), similar to typical breathable garments. The bionic intermittent structure exhibited a two-stage amplification effect, resulting in ultrahigh sensitivity (1368.9 kPa^{-1}), ultrafast response (20 ms), low detection limit (1 Pa, Figure 5k), and high linearity (R^2 = 0.997) across the sensing range. Additionally, the sensor can detect a wide range of human motions in real-time through close skin contact.[22]

A major challenge in pressure sensing is to monitor finger touches without diminishing the natural sense of touch. It is crucial to track finger movements while preserving the natural functionality to fully understand and replicate the sensation of touch. However, placing any object, even a very thin layer, over the human finger significantly reduces the natural sense of touch. This interference affects sensory feedback and alters the inherent control.[160] Hassani et al. developed an innovative Au nanomesh pressure sensor designed to monitor finger movements while preserving the natural sense of touch.[131] The Au nanomesh was created by depositing a 100 nm thick gold layer onto the surface of electrospun PVA nanofibers. The ultrathin and flexible PVA nanomesh conformed closely to the skin, minimizing mechanical mismatch and sensory interference. When applied to the finger, it achieved grip forces comparable to those of a bare finger, with a 14% increase in grip force due to a 2-μm-thick polymeric film. In addition, thermal comfort is also essential for the prolonged use of flexible sensors.

Besides, creating flexible electronics that effectively combine electrical performance with thermal and moisture management remains a challenging task.[142] Zheng et. al designed a thermal and moisture-managing e-textile (TMME-textile), by integrating directional water movement and daytime radiative cooling, combined with highly responsive sensing abilities. This design enabled the textile to effectively transport excess sweat away, ensuring a dry and comfortable environment for the user (Figure 6a). The TMME-textile features high solar reflectivity (98.3%, Figure 6b) and mid-infrared (MIR) emissivity (89.2%, Figure 6c), which helped to lower skin temperature by approximately 7.0 °C under a solar intensity of 1 kW m^{-2} (Figure 6d). The strain sensor in the TMME-textile demonstrates high sensitivity (174.9 Pa^{-1}, Figure 6e) and a quick response time (170 ms), facilitating continuous monitoring, particularly during high-intensity outdoor activities

https://doi.org/10.1021/acsnano.4c13106
ACS Nano 2024, 18, 31737−31772

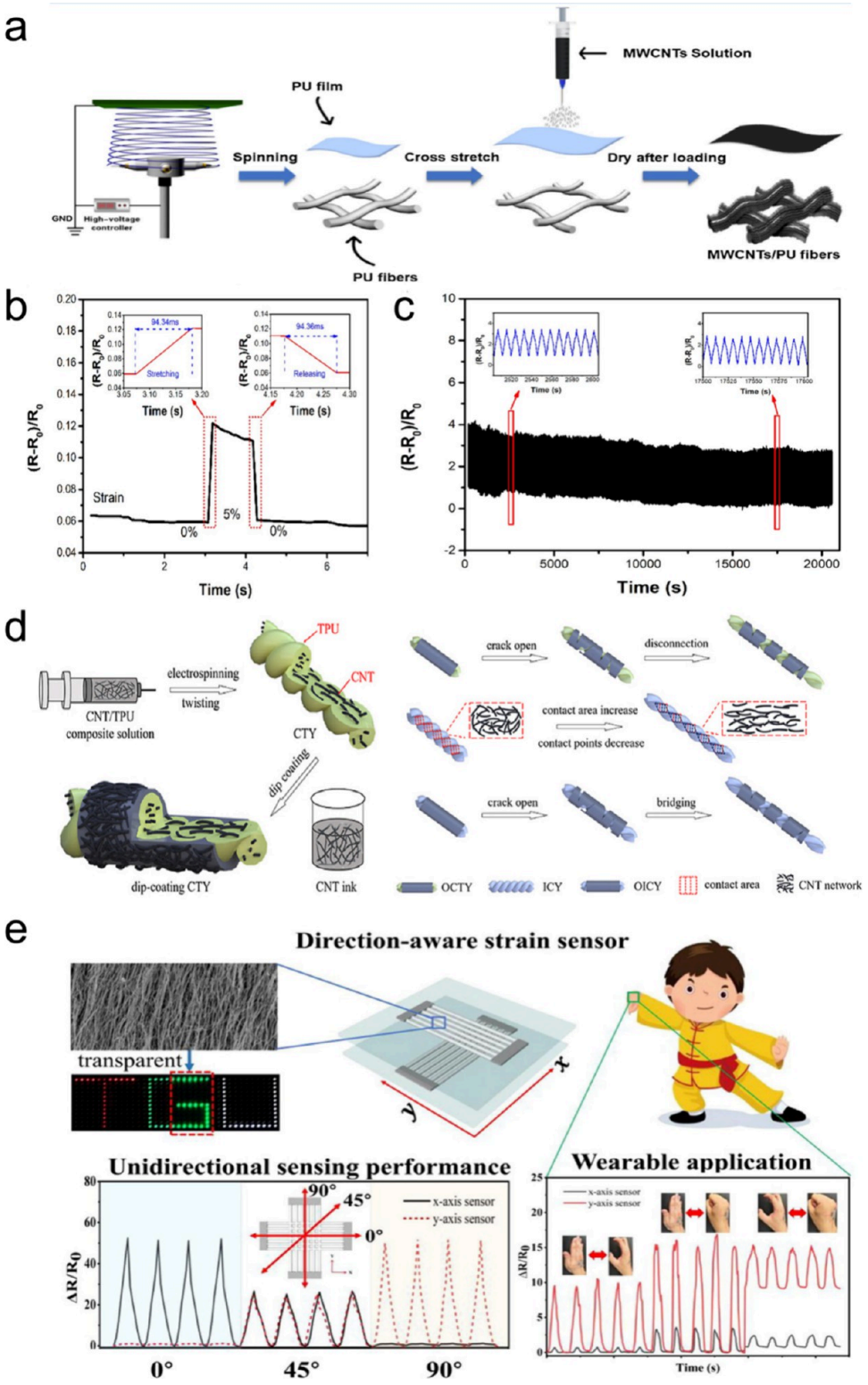

Figure 7. (a) The process for creating the MWCNTs/PU stretchable fibrous membrane sensor. (b) Sensor response time with insets showing enlarged details. (c) Performance of the sensor under 200% strain over 10,000 stretch−release cycles at 5 mm/s with insets displaying sensing behavior at various intervals. (a−c) Reprinted from ref 21 with permission. Copyright 2021 Elsevier. (d) Flowchart depicting the construction of dual CNT networks via dip-coating CTY, along with schematics of sensing mechanisms for OCTY, ICY, and OICY. Reprinted from ref 164 with permission. Copyright 2022 Elsevier. (e) Diagram of a high-performance directional sensing strain sensor based on directional electrospun nanofibers. Reprinted from ref 143 with permission. Copyright 2022 Elsevier.

where traditional e-textiles often face challenges with thermal and moisture management.[123]

To enhance user comfort and extend the lifespan of devices, a breathable and superhydrophobic outer layer can be incorporated into wearable electronics, which promotes

https://doi.org/10.1021/acsnano.4c13106
ACS Nano 2024, 18, 31737−31772

sweat evaporation and reduces the risk of skin irritation and inflammation from prolonged wear. Additionally, this layer protects the electronics from moisture damage. For instance, a fibrous structure was developed using basic electrospinning techniques, featuring two layers of porous polystyrene fibers arranged in both warp and weft directions. (Figure 6f). A wetting phenomenon termed Cassie−Baxter "restoring" (CaRe) wetting mechanism was therefore proposed in this structure, which ensured that droplets remain on the upper-layer fibers even when spaced sparsely, contributing to a stable Cassie−Baxter state (Figure 6g). This distinctive property enables the attainment of superhydrophobicity by strategically decreasing the structural solidity (Figure 6h). A flexible nylon web with such a structure was covered on a human forearm. The covered area showed no significant change in temperature after 60 min, indicating good breathability for wearables (Figure 6i). Furthermore, the developed surface layer is semitransparent (83.6 ± 3.1% light transmittance), allowing for direct observation and monitoring of wearable electronic.[133] Furthermore, nanofiber-reinforced structures exhibit enhanced mechanical durability, exhibiting high tolerance to repeated external pressure.[139] Recently, researchers developed a perpendicularly assembled piezoresistive pressure sensor based on oriented electrospinning TPU/PAN nanofibers (OETPN). The interdigital electrode was created by spraying AgNWs on OETPN using a mask plate. The active layer, consisting of MXene-coated OETPN, was encapsulated by a PU film. The porous nanofiber membrane exhibited a broad measurement range (0.02−700 kPa) and enhanced sensitivity (6.71 kPa^{-1}, 0.02−2 kPa) owing to its compressibility. This allows it to detect weak signals, such as those from the radial artery.[139]

4.3. Strain Sensors. There is an increasing demand for highly flexible and sensitive wearable strain sensors to monitor motion for health, robotics, prosthetics, visual reality, professional sports, and entertainment. Based on their operational principles, various types of flexible strain sensors exist, encompassing resistive, capacitive, piezoelectric, and triboelectric sensors.[61,143] The ideal strain sensor should have high flexibility, sensitivity, and ruggedness to withstand prolonged use without degrading performance.[161] Decorating or depositing functional layers on nanofiber scaffolds is an effective way to fabricate strain sensors with enhanced intelligence.[108,144]

CNTs are frequently utilized as conductive fillers in flexible strain-sensing materials due to their outstanding electrical, thermal, mechanical, and chemical attributes.[162] Recently, Li and colleagues created a highly flexible and breathable PU nanofiber membrane sensor designed for tracking human movements and recognizing speech signals.[21] The sensor consisted of multiwalled carbon nanotubes (MWCNTs) loaded onto a PU nanofiber membrane as a substrate. The PU nanofibers were produced via centrifugal electrospinning (Figure 7a). Excellent electrical conductivity endowed MWCNTs/PU stretchable nanofiber membrane sensors with a low resistance of 800 Ω, high elongation at a break of 272%, a wide response test range from 0 to 203%, and a sensitivity of up to 4177 at 190% strain. The response and recovery times were 94.34 mS and 94.36 mS, respectively (Figure 7b). The sensor exhibited outstanding mechanical durability and an exceptional water vapor transmission rate as demonstrated by the multicycle test of 10,000 cycles (Figure 7c).

Compared with the common nanofibers, sensors designed in a yarn shape can be seamlessly incorporated into fabrics using conventional textile techniques like knitting, weaving, and embroidery, making them particularly suitable for smart textiles.[163] Multifluid electrospinning technology can produce nanofiber yarn. A composite nanofiber yarn (CTY) with exceptional stretchability was created by embedding CNTs into a flexible TPU matrix. This mixture was then twisted into yarns through a multineedle liquid-bath electrospinning process (Figure 7d).[164] The twisting process not only provided mechanical strength but also aligned the CNTs within the TPU matrix, enhancing the electrical conductivity of the yarn. The CNT/TPU nanofiber yarn exhibited excellent flexibility, high sensitivity, and robust mechanical properties. Specifically, the sensor demonstrated a high gauge factor of 14.3 at 50% strain, a wide sensing range of up to 100%, and durability over 5000 stretching-releasing cycles. These attributes make it highly suitable for real-time monitoring of strain and movement in sports and rehabilitation applications.

In addition, MWCNTs can be used to enhance the mechanical properties and electrical conductivity of sensors. Styrene ethylene butylene styrene (SEBS), despite its flexibility, exhibits limited compatibility and weak adhesion with inorganic materials due to its minimal surface energy and lack of polarity. Yu and co-workers developed a SEBS/dopamine/MWCNTs sensor. In their study, the modification with dopamine enhanced the adhesion between SEBS fibers and MWCNTs. The resulting strain sensor exhibited high stretchability and sensitivity, with a gauge factor of 20 at a strain of 100%. Additionally, the sensor demonstrated excellent durability, maintaining consistent performance over 1000 cycles of stretching and releasing.[106] Except for CNTs, other conductive materials, including PANI, PPy, and poly(3,4-ethylenedioxythiophene) (PEDOT), graphene, and metal nanoparticles, have also been incorporated into the nanofibers for the device construction.[165] For instance, Guo and colleagues developed an innovative strain sensor employing PVA fibers as a matrix, which were coated with PPy nanoparticles. These fibers underwent annealing followed by an *in situ* polymerization process to apply the PPy coating. Experiments assessing the sensor's response to stretching and releasing showed that the changes in resistance ($\Delta R/R_0$, where ΔR is the difference between detection and initial resistance) exhibited a linear correlation with the applied strain.[108]

A challenge of the practical application of strain sensors is their inability to detect multidegree-of-freedom strains, as they are affected by interference from multidirectional strains.[145] For applications requiring precise quantification of complex strains, it is essential to design a single strain sensor capable of reliable direction recognition.[166] To achieve separate electrical characteristics, innovative anisotropic structural designs have been employed. These designs effectively minimize interference from various stimuli and allow for sensing in multiple directions. One method involves constructing stretchable matrices with variable stiffness, combined with a cross-shaped conductive network, to develop strain sensors that are sensitive to directional changes.[167] For instance, Yang et al. developed a strain sensor that integrates high sensitivity, directional awareness, and transparency, making it ideal for seamless incorporation into wearable devices. They employed electrospinning to create oriented nanofibers, which enhanced the sensor's mechanical and electrical properties. This approach addresses the limitations of existing sensors, offering a more

https://doi.org/10.1021/acsnano.4c13106
ACS Nano 2024, 18, 31737−31772

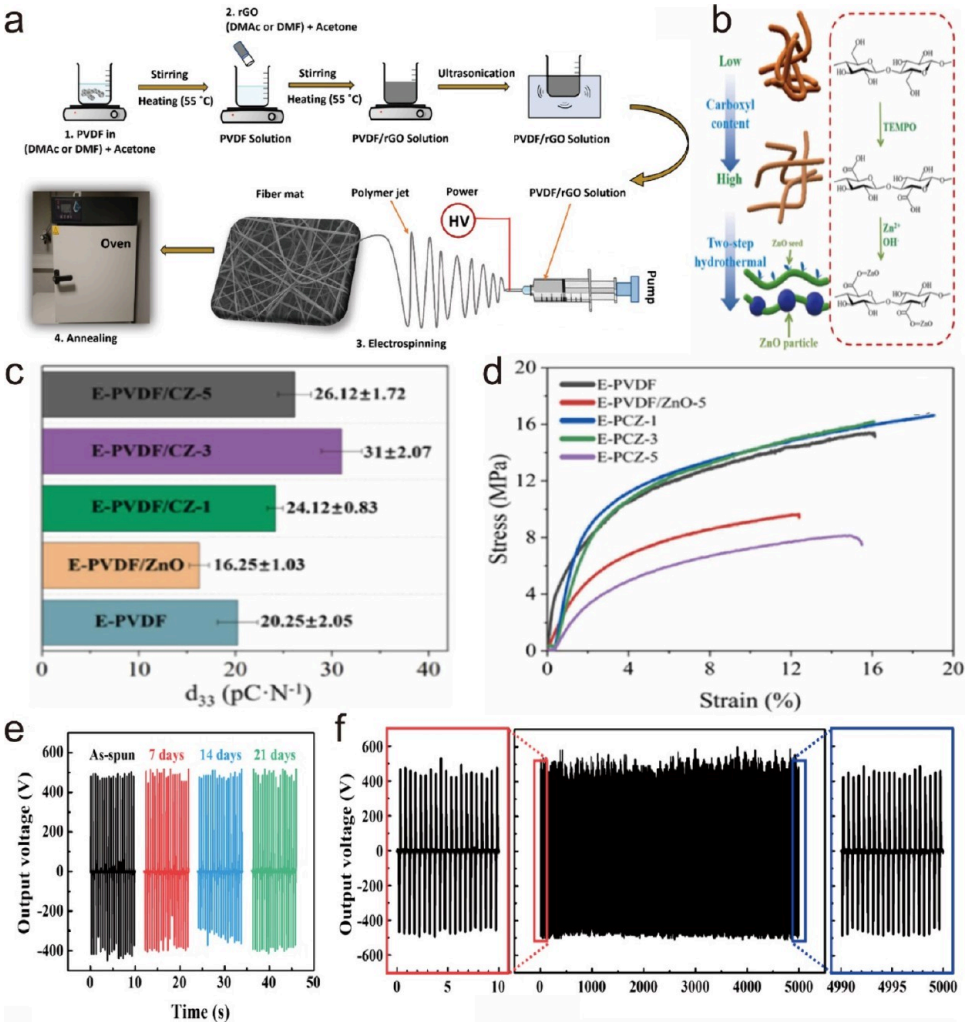

Figure 8. (a) A schematic of the steps involved in preparing PVDF/rGO composite fibers: (1) preparing PVDF solutions in DMAc/acetone and DMF/acetone, (2) creating PVDF/rGO solutions in DMAc/acetone and DMF/acetone, (3) electrospinning these solutions, and (4) annealing the resulting fiber mats. Reprinted with permission under a Creative Commons [CC BY] License from ref 174. Copyright 2023 The Authors. Published by Wiley-VCH. (b) The 2,2,6,6-tetramethylpiperidine-1-oxyl (TEMPO) oxidation method and the preparation process of CNF@ZnO. (c) The dielectric loss properties of CNF@ZnO. (d) The piezoelectric constant of the CNF@ZnO composite membrane. (b–d) Reprinted from ref 175 with permission. Copyright 2024 Elsevier. (e) Measurement of the TENG's output voltage every 7 days over 3 weeks. (f) Using a motorized tapping machine, continuous output voltage testing for 10,000 cycles at 2 Hz. (e,f) Reprinted from ref 177 with permission. Copyright 2023 Elsevier.

effective solution for real-time monitoring in diverse applications, from health tracking to interactive electronics (Figure 7e).[143]

5. FLEXIBLE ENERGY MODULES

In recent years, flexible energy modules have captured increasing attention due to their good stretchability, portability, ultrathinness, and lightweight characteristics.[168] These modules serve as power suppliers in flexible electronic systems, capable of collecting various forms of energy such as solar, wind, and mechanical energy through devices converting it into electrical energy. The generated electrical energy was then stored in flexible energy storage units (e.g., batteries and supercapacitors) for use by other functional units. Electrospinning technology offers a low-cost, highly efficient, and scalable method for manufacturing highly flexible electrospun nanofiber-based energy modules.[169] This section will explore the latest advancements in the preparation of electrospun nanofiber-based flexible energy modules.

5.1. Energy Harvester. Energy harvesting devices capable of collecting mechanical energy on a microscale through deformation have seen rapid development.[154] Energy harvesting devices can be divided into nanogenerators, polymer solar cells, moist-electric generators, thermoelectric generators, *etc.*[170,171] Nanogenerators present additional opportunities for self-powered flexible electronic devices, with electrospinning technology widely used in the production of fiber-structured nanogenerators. Currently, the two main nanogenerators—piezoelectric nanogenerators (PENGs) and triboelectric nanogenerators (TENGs)—have become focal points of research.[172] In 2006, Wang and colleagues designed the PENGs based on zinc oxide nanowire arrays, offering an effective method for converting weak mechanical energy into electrical energy.[173] Since then, PENGs have garnered significant attention, primarily being fabricated from PVDF due to its high piezoelectric coefficients.[174] For example, a PVDF/reduced graphene oxide (rGO) composite fibers mat was prepared using a four-step method (Figure 8a). Using

https://doi.org/10.1021/acsnano.4c13106
ACS Nano 2024, 18, 31737–31772

PVDF combined with rGO in a dimethylacetamide (DMAc) solvent substantially enhances the piezoelectric coefficient, resulting in a notable 4-fold increase in power density relative to pure PVDF. In another study, piezoelectric barium titanate nanoparticles were affixed onto P(VDF-TrFE) nanofibers, significantly amplifying the PENG's output to 6 V and 1.5 μA. Compared to the standard electrospun P(VDF-TrFE), the PENGs featuring polydopamine-modified barium titanate ($BaTiO_3$)@P(VDF-TrFE) demonstrated a 4.8-fold increase in output voltage and a 2.5-fold increase in current. The optimized PENG exhibited a maximum power density of approximately 8.78 mW m^{-2}, showcasing the immense potential for wearable, self-powered sensors capable of harvesting mechanical energy and monitoring human kinetics

PVDF/CNF@ZnO composite membrane (E-PVDF/CZ), the β phase in PVDF was effectively increased to 87.36% (Figure 8b), further enhancing its piezoelectric response to 24.65 pm V^{-1}. The longitudinal piezoelectric coefficient (d_{33}) of E-PVDF/CZ reached 31 ± 2.07 pC/N, higher than that of E-PVDF (20.25 ± 2.05 pC/N) (Figure 8c). The composite membrane also exhibited excellent mechanical performance and flexibility, with a tensile strength of 16.12 ± 2.35 MPa and elongation at a break of 16.21 ± 2.17% (Figure 8d). Under a force of 45 N, the open-circuit voltage (V_{OC}) and short-circuit current (I_{SC}) of E-PVDF/CZ reached 11.8 V and 452 nA, respectively. Additionally, the flexible sensor achieved a VOC of 31.2 V under fist impact and 1.68 V when stimulated by water droplets, sufficient to weakly light an LED.[175]

In 2012, Wang and colleagues further demonstrated the feasibility of TENGs by combining the triboelectric effect with electrostatic induction.[176] Recently, Oh et al. developed a methodology for the synthesis of flexible TENGs with enhanced surface adhesion properties.[177] The fabrication process involved the direct electrospinning of P(VDF-TrFE) to construct TENGs on pliable multiwalled CNTs/PDMS/silver nanowire (MWCNTs/PDMS/AgNWs) composite electrodes. Notably, the TENGs output performance exhibited good stability, with no significant changes observed over a period ranging from 7 days to 3 weeks. Furthermore, the output voltage remained stable through 5,000 cycles of contact and separation at a frequency of 2 Hz (Figure 8e,f). Except for the PVDF, other polymers have also been employed to fabricate the TENGs. Recently, researchers reported a fully biodegradable TENG composed of aligned PLLA (aPLLA) fibers and CS as active layers. The aPLLA fiber-based TENG (aPL-TENG) showed superior output voltage and current (45 V and 9 μA, respectively) due to enhanced 10_3 helix chain conformation. Further, the aPL-TENG demonstrated excellent mechanical stability over 24,000 cycles and produced an output power density of 6.5 Mw m^{-2}. As a proof-of-concept, the aPL-TENG output was used to charge a capacitor, successfully powering a commercial wristwatch and stopwatch. The straightforward fabrication process and use of sustainable materials make the aPL-TENG a promising solution for green energy harvesting, capable of powering portable devices on a large scale without concerns over electronic waste management.[178]

For polymer solar cells, electrospun nanofibers offer a promising approach for enhancing the efficiency and flexibility due to their high surface area and tunable morphology.[179] In addition, in contrast to planar solar cells, which can only absorb light from one direction, fiber-shaped solar cells have the potential to capture sunlight from all angles owing to their special structure.[180] Therefore, electrospinning has been chosen as a fabrication technique for the hole transport material. Researchers presented an approach to fabricating a hole transport material for organic solar cells. By combining electrospinning and electropolymerization techniques, the researchers developed a composite material consisting of carbon nanofibers (CNFs), PANI, and copper. This composite material exhibited enhanced electrical conductivity and stability, making it an efficient and durable option for transporting positive charges within the solar cell. The innovation lies in the integration of these techniques to create a versatile and high-performance hole transport material, thereby advancing the field of organic solar cell technology.[181] In the PET-TiO_2 core/shell nanofibrous mats, TiO_2 served as a critical component for the photoanode layer. The TiO_2 nanoparticles enhanced the photoanode's ability to facilitate efficient charge transfer and minimize the recombination of photogenerated charges, thereby improving the overall efficiency and performance of the dye-sensitized solar cells more efficiently than TiO_2 nanorhombics.[116] Besides their application as flexible solar cells, electrospun nanofibers can also serve as building blocks for solar thermoelectric generators, showcasing significant potential for self-powered wearable electronics.[182] Recently, scientists created a flexible and wearable MEG with excellent power output, breathability, and flame resistance. This was achieved by designing an asymmetrical nanofiber assembly using hydrophobic PVDF and hydrophilic PVA/phytic acid nanofiber mats. The device benefited from the combined effects of strong water absorption, improved ion release, and numerous micronano transport channels. As a result, a single MEG with a 1 cm^2 area consistently delivered high direct current power, with a voltage of 1.0 V, a current of 15.5 μA, and a power density of 3.0 μW cm^{-2}. Additionally, the asymmetric nanofiber structure effectively maintained moisture circulation, ensuring stable voltage output for up to 1 week without any degradation.[66]

5.2. Batteries. The application of electrospun membranes in batteries has been gaining increasing attention, particularly as electrodes or separators. To enhance the mechanical, electrochemical, and safety features, researchers have developed a series of electrodes, diaphragms, and electrolytes based on electrospun nanofibers.[183−186] The high specific surface area, good porous structure, thermal stability, and mechanical stability of electrospun nanofibers provide significant advantages in the field of lithium-ion, predominantly as separators or electrodes.[187−189]

A high-performance separator with good mechanical and thermal properties is essential for lithium-ion batteries. Lithium-ion batteries, characterized by their lightweight design, portability, high safety profile, substantial capacity, and extended lifespan, have the lowest reduction potential and emerged as the optimal power source for different flexible electronic devices.[25,190] An innovative approach to enhance battery safety involves utilizing an organic flame-retardant-loaded separator. Despite its potential, this technology faces significant challenges due to inadequate thermal stability. A core−shell nanofibrous membrane was developed via coaxial electrospinning. The membrane's shell comprised a blend of GO, polyvinylidene fluoride, and silicon dioxide (SiO_2), while its core contained GO, triphenyl phosphate (TPP), and SiO_2 were incorporated to bolster electrochemical performance and thermal stability. TPP encapsulated within the core mitigated heat transfer and preserved electrochemical integrity by

https://doi.org/10.1021/acsnano.4c13106
ACS Nano 2024, 18, 31737−31772

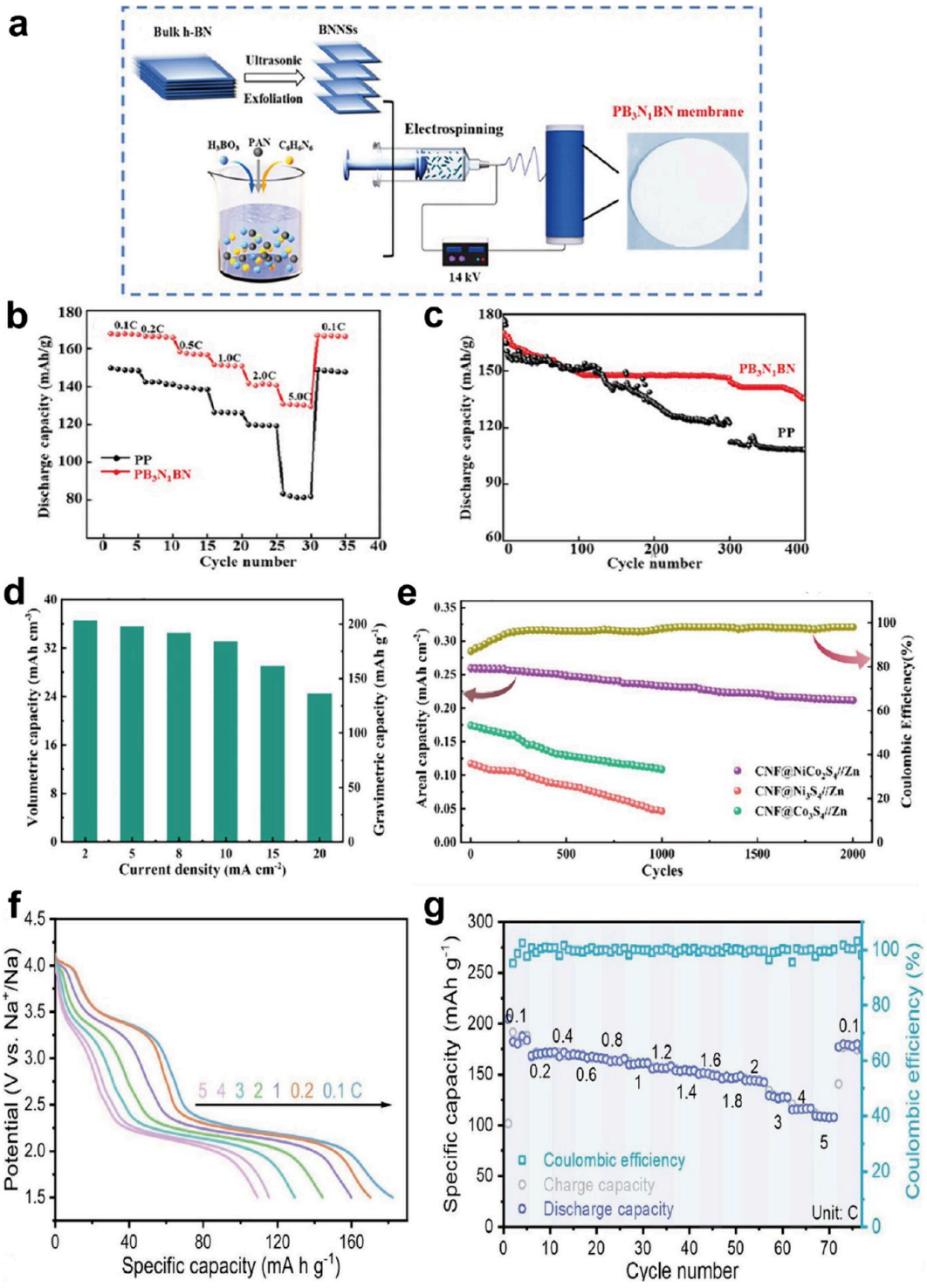

Figure 9. (a) A schematic illustration of the fabrication process for the PB_3N_1BN electrospun membrane, which exhibits robust mechanical properties, outstanding electrolyte wettability, excellent fire resistance, and high thermal stability, created using the electrospinning method. (b) The rate performance at various current densities and (c) the cycle stability after 400 cycles, comparing the commercial PP separator with the PB_3N_1BN electrospun fiber membrane. (a–c) Reprinted from ref 189 with permission. Copyright 2024 Wiley-VCH. (d) Gravimetric and volumetric capacities of the CNF@$NiCo_2S_4$//Zn battery at various current densities. (e) The performance of the CNF@$NiCo_2S_4$//Zn battery at 10 mA cm^{-2} for 2000 cycles. (d,e) Reprinted from ref 191 with permission. Copyright 2021 Elsevier. (f) The corresponding discharge behaviors. (g) The rate capability. (f,g) Reprinted from ref 192 with permission. Copyright 2024 Elsevier.

preventing direct dissolution. This separator resisted combustion and retained 91.2% integrity after exposure to an open flame for 15 s and enabled an initial capacity of 164 mAh g^{-1}, maintaining 95% capacity retention after 100 charge–discharge cycles.[186] In another study, PVDF was blended with the synthesized fluorinated polyimide (FPI) to improve the mechanical strength and thermal stability of electrospun composite nanofibrous membranes (CNMs). As the content of FPI increased, the tensile strength of the CNMs rose from 1.57 MPa (0% FPI) to 2.30 MPa (30% FPI). Additionally, the

https://doi.org/10.1021/acsnano.4c13106
ACS Nano 2024, 18, 31737–31772

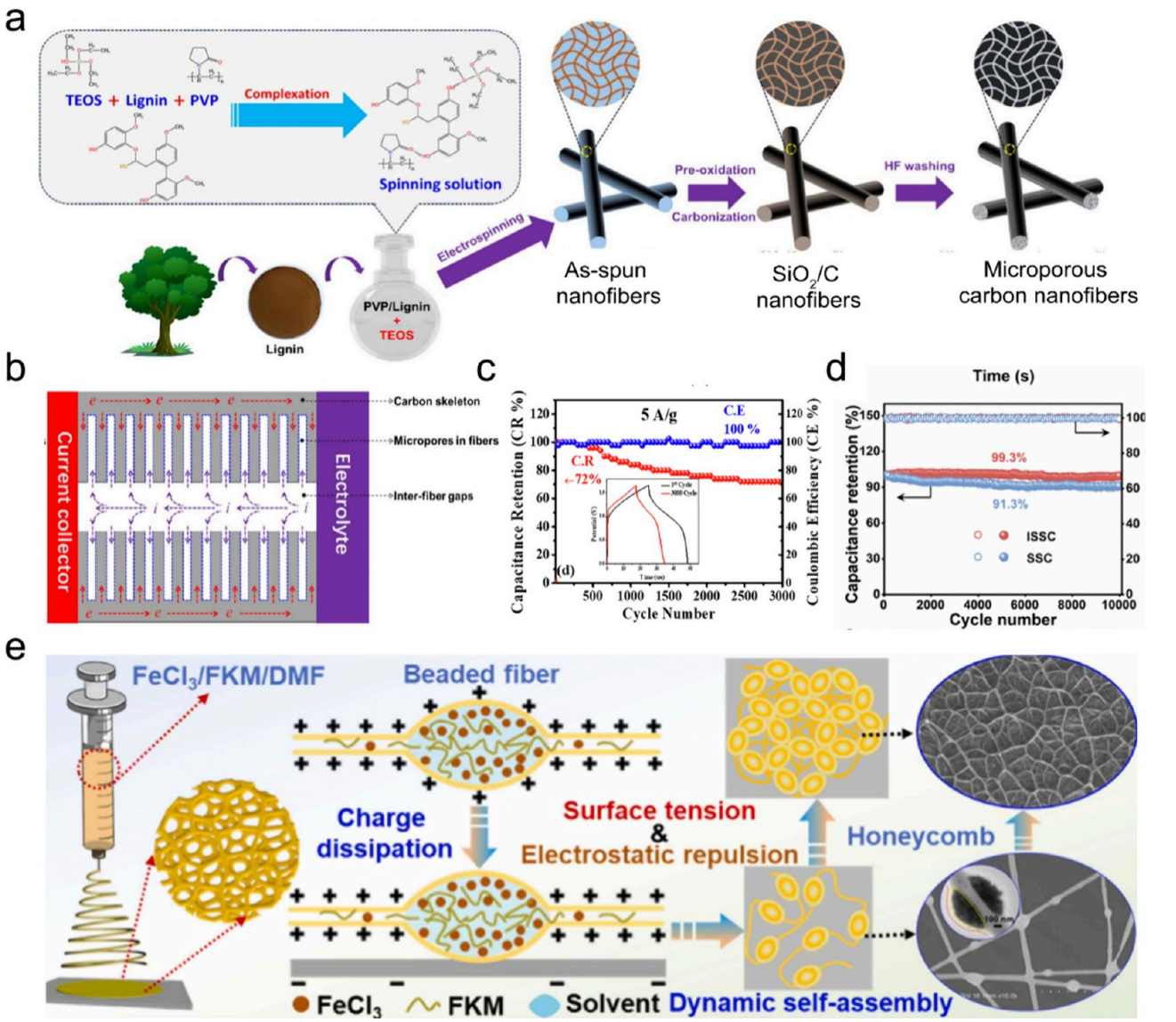

Figure 10. Typical instances of electrospun fibers utilized in supercapacitors. (a) Illustration depicting the manufacturing process of carbon nanofiber supercapacitors. (b) Diagram showing a potential charge density distribution for the electrode. (a,b) Rreprinted from ref 40 with permission. Copyright 2024 Elsevier. (c) Performance during cycling and Coulombic efficiency were measured at a current density of 5 A g^{-1}. Reprinted from ref 199 with permission. Copyright 2024 Elsevier. (d) Stretched configuration of PEDOT@FKM stretchable supercapacitors. (e) Illustration of the fabrication process for PEDOT@FKM films. (d,e) Reprinted from ref 203 with permission. Copyright 2024 Elsevier.

CNM-30, which contains 30 wt % FPI, exhibited almost no dimensional shrinkage after the heat treatment (1 h, 160 °C). Furthermore, the electrochemical performance of the prepared CNMs was superior to that of commercial Celgard and pure PVDF membranes. The ionic conductivity and electrolyte uptake of the CNMs reached 1.14 mS cm^{-1} and 522.4%, respectively.[188] Recently, a PAN/boric acid/melamine/delaminated BN nanosheets electrospun fiber membrane (PB_3N_1BN) was developed by electrospinning a homogeneous viscous suspension of PAN/DMF/H_3BO_3/$C_3H_6N_6$/delaminated BN nanosheets (BNNSs) followed by heat treatment (Figure 9a). The PB_3N_1BN electrospun nanofibers exhibited exceptional properties, including high thermal stability (exhibiting almost no size contraction at 200 °C), superior electrolyte wettability (with a contact angle of approximately 0°), excellent mechanical strength (19.1 MPa), and outstanding flame retardancy (with a minimum total heat release of 3.2 MJ m^{-2}). Additionally, the assembled $LiFePO_4/PB_3N_1BN/Li$ asymmetrical battery demonstrated high capacity (169 mAh g^{-1} at 0.5 C), exceptional rate capability (129 mAh g^{-1} at 5 C, Figure 9b), excellent cycling stability without significant decay after 400 cycles (Figure 9c), and good discharge capacity of 152 mAh g^{-1} at 80 °C.[189]

The advantage of electrospun membranes as electrodes lies in their high specific surface area and tailored porosity, enhancing electrochemical performance in energy storage devices.[184] There is currently a significant demand for lightweight, flexible, and binder-free cathode electrodes for aqueous Ni−Zn batteries. Researchers introduced electrospinning CNFs functionalized with ternary $NiCo_2S_4$ nanoparticles (designated as CNF@$NiCo_2S_4$) as lightweight, flexible, and binder-free electrodes.[191] As a cathode, the self-supporting CNF@$NiCo_2S_4$ film delivered a high capacity of 0.32 mAh cm^{-2} and 35.9 mAh cm^{-3} at 2 mA cm^{-2}, along with

https://doi.org/10.1021/acsnano.4c13106
ACS Nano 2024, 18, 31737−31772

impressive rate capability (0.21 mAh cm^{-2} at 20 mA cm^{-2}, Figure 9d) and long-term cycling stability (83% capacity retention at 10 mA cm^{-2} over 2000 cycles, Figure 9e). When assembled in a quasi-solid-state CNF@$NiCo_2S_4$//Zn battery, it demonstrated an energy density of 362.3 Wh/kg and volumetric energy densities of 58.2 mWh cm^{-3} (liquid) and 45.4 mWh cm^{-3} (quasi-solid-state). In another study, electrospun V_2O_5 nanofibers (VNFs) were coated with conductive carbon (VNF-C-120), serving as cathode materials in photorechargeable lithium-ion batteries.[184] These materials exhibited a discharge capacity of 160 mAh g^{-1}, which can increase to 184 mAh g^{-1} (C rate of 0.75) under light, demonstrating their photoresponsive behavior. The carbon coating not only enhanced conductivity but also stabilized the structure and morphology of V_2O_5 fibers, leading to improved capacity retention (43.85% for VNF and 61.13% for VNF-C-120 after 300 cycles of testing). Unlike the noncoated VNF electrode, which failed after 400 cycles, the carbon-coated electrodes prevented cell failure. Moreover, under a UV lamp, the photorechargeability achieved a conversion efficiency of 4.24% for VNF and 5.07% for VNF-C-120. $Na_3MnTi(PO_4)_3$ has attracted significant attention due to its exceptional theoretical capacity, strong structural stability, and abundant resource availability in sodium-ion batteries, cao et al. prepared the electrospun hierarchical carbon-decorated $Na_3MnTi(PO_4)_3$ nanofibers, followed by pyrolysis, as a sodium-ion battery cathode, which demonstrated excellent electronic conductivity and superior Na^+ transport capability (Figure 9f). The battery showed a notable reversible capacity of 171.4 mAh g^{-1} at 0.2 C (Figure 9g) and maintained outstanding cyclic stability with 63.7% capacity retention after 6300 cycles at 1 C. When integrated into a full cell with an independent $Na_3MnTi(PO_4)_3$/C cathode and hard carbon anode, the cell delivered a reversible capacity of 153.7 mAh g^{-1} at a current density of 10 mA g^{-1}.[192]

5.3. Supercapacitors. Supercapacitors, also known as electrochemical capacitors, not only allow rapid charge−discharge cycles but also exhibit higher energy and power densities compared to traditional capacitors. Moreover, they have longer lifespans and wider operating temperature ranges than traditional capacitors.[193] To achieve high energy density, supercapacitors rely on charge separation at the electrode−electrolyte interface, forming a nanostructured self-assembled electric double layer as the primary source of capacitance. Some supercapacitors also exhibit Faradaic pseudocapacitance, where reversible chemical adsorption, desorption, oxidation, and reduction reactions occur on the two-dimensional (2D) surface of the electrode.[158] The capacitance is directly proportional to the electrode's surface area. Therefore, increasing the electrode's surface area is crucial for supercapacitor fabrication.

Electrospinning, in the context of supercapacitors, has emerged as a revolutionary method. Electrospun nanofibers can serve as excellent scaffolds for active materials such as conductive polymers, metal oxides, or carbon-based substances, enhancing overall electrode capacitance and energy density.[194,195] Furthermore, the interconnected porous network of electrospun nanofibers facilitates ion transport, which is essential for rapid charge−discharge cycling characteristics in supercapacitors.[196,197] To make vanadium/cobalt oxide (VCO) and carbon nanofiber electrodes, researchers combined PAN with DMF and then added Cobalt(II) acetate tetrahydrate and vanadyl acetylacetonate in the electrospinning solution. The preparation of VCO/CNFs electrodes exhibited a specific surface area of 118.9 m^2 g^{-1}. The specific surface capacitance was 1.83 F cm^{-2} at a current density of 8 mA cm^{-2}, with negligible capacitance degradation observed at a bending angle of 180°. After 10,000 cycles of charging and discharging, the Coulombic efficiency remained at 100% and the specific surface capacitance retention rate reached 95.2%, with a high energy density of 44.2 μWh cm^{-2} under a power density of 2.8 mW cm^{-2}.[198]

In a recent study, Ma et al. utilized wood lignin as a precursor and tetraethyl orthosilicate (TEOS) as an additive to fabricate microporous carbon nanofiber membranes via electrospinning (Figure 10a). Under the influence of TEOS, the resulting lignin-based nanofiber membrane exhibited an impressive specific surface area of up to 1197 m^2 g^{-1}, an 84.1% micropore volume, and significantly improved diameter retention. When used as a self-supporting electrode for supercapacitors, it demonstrated an impressive specific capacitance of 282 F g^{-1} at 0.2 A g^{-1}. Figure 10b shows the schematic diagram of the possible charge distribution inside the electrode. This supercapacitor material boasts advantages such as renewable raw materials, simple processing, and excellent performance, making it a promising alternative for supercapacitor electrodes.[40] In another study, Abdel-Salam et al. employed a straightforward one-step hydrothermal technique to grow $NiCo_2S_4$ on porous electrospun nitrogen-dopedCNFs, resulting in a layered $NiCo_2S_4$@CNF structure.[199] The manufactured $NiCo_2S_4$@CNF composite exhibited a large surface area and high porosity, serving as an effective ion diffusion pathway. The energy density of supercapacitors prepared using $NiCo_2S_4$@CNF reached 65.6 and 52.5 W kg^{-1}, with corresponding power densities of 665 and 1313.8 W kg^{-1}. Furthermore, the device displayed excellent stability after 3000 charge−discharge cycles, maintaining 72% of its initial capacitance (Figure 10c). These results position the designed $NiCo_2S_4$@CNF layered structure as a promising electrode material for supercapacitors.

Conductive polymer typically combines the flexibility of the polymer with the conductive properties of the conductor. One can imagine that using a conductive polymer as an auxiliary may further enhance the application performance of supercapacitors. For instance, PANI, the most frequently used fabric for the flexible supercapacitor, can be electrospun to form a nanofiber mesh as an electrode.[200] Researchers have used electrospray and chemical polymerization techniques to create a PANI coating on electrospun CNFs. The resultant hybrid structure offered advantages such as increased surface area, enhanced electrical conductivity, structural stability, and resilience to external strain.[201] Furthermore, because of their extensive surface area, porous and intertwined nanofibers have the potential to be infused with significant amounts of active capacitive media to enhance the capacitive performance.[202] Mu et al. proposed an innovative self-selecting in situ gas-phase polymerization strategy for one-step assembly of stretchable supercapacitors (SSCs).[203] The assembled SSCs exhibited excellent stability, with a capacitance retention rate of 99.5% after 500 cycles of stretching (Figure 10d). Additionally, these SSCs demonstrated outstanding flame-retardant properties. To prepare these SSCs, authors employed electrospinning technology to construct a multilayered in situ precursor membrane of fluorinated elastomer m$FeCl_3$@nonflammable fluoroelastomer (m$FeCl_3$@FKM) with a dual-scale porous honeycomb structure. Next, using vapor-phase polymerization,

https://doi.org/10.1021/acsnano.4c13106
ACS Nano 2024, 18, 31737−31772

Table 2. Summary of Flexible Energy Modules Based on Electrospun Nanofibers

preparation method	solvent	polymer type	fiber diameter	application areas	ref
Single-fluid electrospinning	DMF	Lignin		Self-supporting electrode	40
Single-fluid electrospinning	Distilled water, HFIP	PVA, SF	PVA/MXene 160 nm SF 400 nm	Drug delivery, environmental monitoring, and other fields	55
Single-fluid electrospinning	DMF, dimethyl sulfoxide (DMSO)	PVA, phytic acid	1 μm	Moist-electric generators	68
Coaxial electrospinning	TFA and DCM	PET	477 nm	Dye-sensitized solar cells	116
Single-fluid electrospinning	DMF, Acetone	P(VDF-TrFE), PDMS		LED lights, flexible sensors, microcapacitors, digital multifunction clocks, and other fields	155
Single-fluid electrospinning and gas-phase cross-linking	DMSO	PVDF, PVA	840 nm	Artificial intelligence, monitoring human health	168
Single-fluid electrospinning	DMF	Tourmaline, PVDF	1 μm	Portable electronic devices	172
Single-fluid electrospinning	DMAc, DMF	PVA, rGO		Energy harvesting applications	173
Single-fluid electrospinning	DMF	PVDF	500−700 nm	Energy harvesting, environmental monitoring.	175
Single-fluid electrospinning	DCM	PDMS	1 μm	Flexible and high efficient power sources	176
Single-fluid electrospinning	DMF	aPLLA, CS		Degradable capacitors	178
Single-fluid electrospinning	DMSO, NMP	PANI		Solar cell	181
Single-fluid electrospinning	DMF	PAN, CNTs	538 nm	Solar cells	182
Single-fluid electrospinning and postcalcination	Acetic acid	PVP, V_2O_5	100−200 nm	Rechargeable batteries	184
Single-fluid electrospinning	DMF	PAN, TPU, CNTs	500−1000 nm	Batteries.	187
Coaxial electrospinning	DMSO, Distilled water	PVDF		Flame retardant capacitors	186
Single-fluid electrospinning		FPI, PVDF		Flexible capacitors	188
Single-fluid electrospinning	DMF	PAN, polystyrene, $NiCo_2S_4$	1 μm	Aqueous Ni−Zn batteries	191
Single-fluid electrospinning	DMF	$Na_3MnTi(PO_4)_3$, PVP	192 nm	Sodium-ion batteries	192
Single-fluid electrospinning	DMF	PAN, CNTs	200−300 nm	Multifunctional supercapacitors	195
Single-fluid electrospinning and postcalcination	DMF	PEI, CNTs	300−500 nm	Supercapacitors	196
Single-fluid electrospinning	DMF	PAN, Zeolite imidazole frameworks-67	200 nm	Lithium-ion supercapacitors	197
Single-fluid electrospinning and carbonization treatment	DMF	PAN, vanadium/cobalt oxides, CNTs	600−700 nm	Flexible capacitive energy storage units	198
Single-fluid electrospinning	DMF	PAN, $NiCo_2S_4$, CNTs	300 nm	Supercapacitors	199
Single-fluid electrospinning	DMF	PANI	200 nm	Supercapacitors	200
Single-fluid electrospinning	DMF	PANI, PEO	1 μm	Wearable devices.	201
Single-fluid electrospinning	DMF	PAN, $Ti_3C_2T_x$ MXene	400−600 nm	Flexible symmetric and asymmetric supercapacitor devices	202
In situ layer-by-layer electrospinning	DMF	FKM	1 μm	SSCs	203
Single-fluid electrospinning	DMF	PEO, PEDOT:PSS,	1 μm	Supercapacitors	204
Single-fluid electrospinning	Distilled water	PDMS, PVA	200 nm	Health sensors, strain-insensitive pressure sensors	205
Single-fluid electrospinning	DMF	PAN, PEDOT	300 nm	Wearable biosensor platform	206
Single-fluid electrospinning	Methyl alcohol	PVP, AlO_3	130 nm	High-temperature flexible sensors	207

they in situ polymerized PEDOT in the $mFeCl_3$@FKM region containing an oxidant (Figure 10e). This strategy provides a systematic solution for scalable manufacturing of wearable devices and holds promise in the field of flexible electronic devices. Table 2 lists more details about these typical electrospun nanofiber-based flexible energy modules.

6. FLEXIBLE ACCESSORIES FOR ELECTRONIC DEVICES

6.1. Flexible Display. Fibertronic strategies for wearable applications have garnered significant attention due to their ability to integrate various functions into textiles while preserving their inherent properties. Among the various features, display capability is particularly desirable in wearable electronics.[208] Electrospinning technology is a comparatively common technique for creating porous fiber membranes due to its accessibility, flexibility, breathability, mass production, and environmental friendliness. Researchers have successfully prepared SrY_2O_4 electrospun nanofibers (SYO:Eu NFs) doped with Eu^{3+} ions (Figure 11a).[209] These nanofibers exhibited red light emission under near-ultraviolet excitation. The researchers were able to effectively control the diameter of the nanofibers by regulating the temperature and Eu^{3+} doping concentration throughout the electrospinning process. Moreover, the nanofibers exhibited superior properties compared to the bulk counterparts, including a high specific surface area and reduced internal scattering, which collectively enhanced their fluorescence characteristics (Figure 11b). Consequently, the synthesized nanofiber can be utilized in flexible display applications.

Organic Light Emitting Diodes (OLEDs) employ specific organic compounds as luminescent materials that emit visible

https://doi.org/10.1021/acsnano.4c13106
ACS Nano 2024, 18, 31737−31772

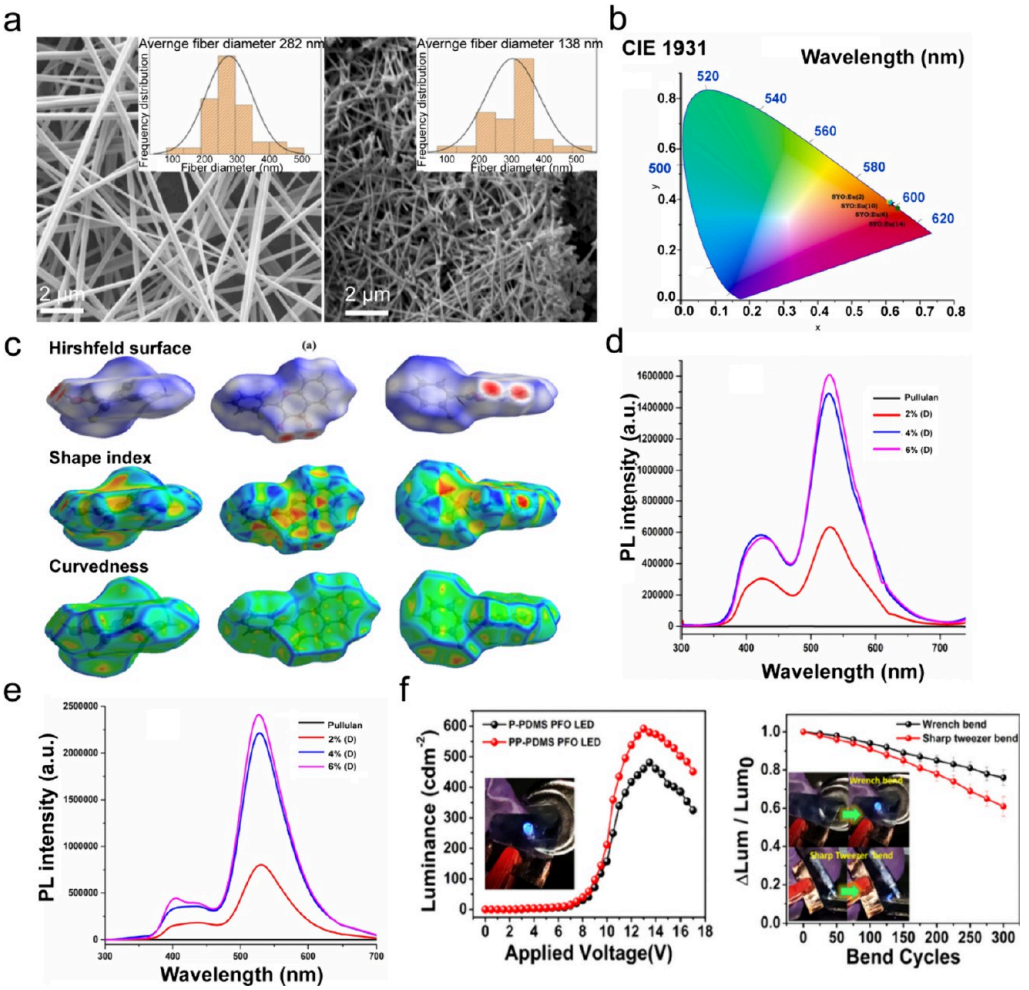

Figure 11. (a) SEM images and corresponding histogram of SYO nanofibers pre- and postcalcination. (b) CIE plot displaying SYO nanofibers at various concentrations. (a,b) Reprinted from ref 209 with permission. Copyright 2022 Elsevier. (c) Hirshfeld surface analysis of a single crystal. (d,e) Fluorescence emission spectra of the fabricated nanofiber mat excited at (d) 296 nm and (e) 336 nm. (c–e) Reprinted from ref 214 with permission. Copyright 2023 Elsevier. (f) Luminance versus voltage graph and repetitive bend cycle test results for the PFO OLED device. (f) Reprinted from ref 205 with permission. Copyright 2022 Elsevier.

light when excited by an electric current.[210] Despite Sony's launch of the first OLED television in 2004 marking the commencement of its commercialization, OLEDs continue to encounter many challenges, including lack of elasticity, low luminous efficiency, and limited color uniformity.[211] Particularly, the short lifespan of blue light-emitting materials has restricted their application scope.[212] The advent of electrospun nanofiber technology offers potential solutions to these issues. Electrospun nanofibers hold a broad prospect for application in OLED technology. Electrospun nanofibers can be directly used for OLED fabrication as an emissive layer. For example, Xue et al. developed an electrospinning supramolecular hybrid nanofibers.[213] These fibers were composed of poly(*N*-vinylcarbazole) (PVK) and poly{9-[4(octyloxy)-phenyl]-2,7-fluoren-9-ol} (PPFOH). By adjusting the PPFOH content, they achieved tunable supramolecular aggregation within the PVK matrix. This process enabled the intelligent transfer of energy, resulting in the manifestation of multicolor emission characteristics. The research revealed that these nanofibers, under hydrogen bonding interactions, display strong aggregation-induced quasi-molecular emission in the 500 to 600 nm range. As the concentration of PPFOH in the PPFOH/PVK composite electrospun fibers decreased, the intensity of green-yellow emission significantly diminished, while the blue emission increased. This shift resulted in a spectrum of fluorescent colors within the nanofibers, ranging from deep blue to sky blue, near white, cyan, green, and yellow. Furthermore, these PPFOH-doped blended nanofibers demonstrated the ability to modulate conductive properties effectively, showing their application potential in the field of organic optoelectronics. In a recent study, Sarojini et al. created nonfluorescent Prussian blue nanofibers through electrospinning, incorporating 2-(2-fluorophenyl)-3-hydroxy-4H-chromen-4-one as a dopant.[214] Upon forming dimers with neighboring molecules via intermolecular hydrogen bonding, the dopant molecular chain exhibited a slip pattern characterized as J-aggregation (Figure 11c). This twisting nature of the J-aggregation is likely a crucial factor influencing the material's photophysical properties. These electrospun nanofiber films exhibited a bandgap that varies from 2.41 to 2.91 eV, indicating versatile electronic properties. The films achieved an impressive quantum yield, ranging from 32.1% to 36.72%, and boasted a high refractive index. When nanofiber films were used as a dual-emission layer in OLED materials, they unveiled an emission at 426 and 532 nm when it was excited both at 296 and 336 nm respectively (Figure 11d,e),

https://doi.org/10.1021/acsnano.4c13106
ACS Nano 2024, 18, 31737–31772

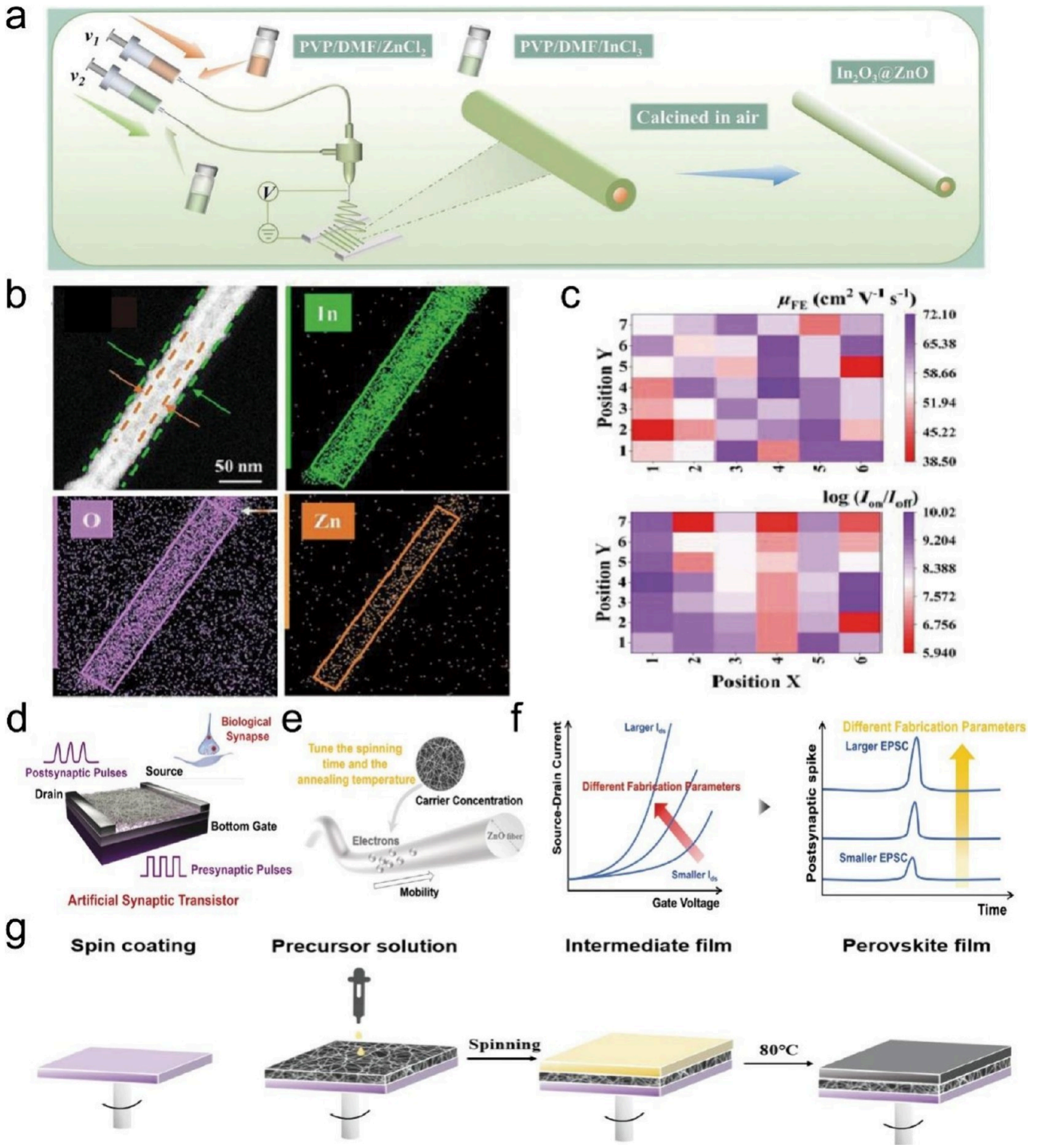

Figure 12. (a) A simplified schematic showing the process for preparing In_2O_3@ZnO core−shell nanowires. (b) Elemental maps illustrating the distribution of indium (In), zinc (Zn), and oxygen (O). (c) Graphs displaying the distribution of In, O, and Zn. (a−c) Reprinted from ref 216 with permission. Copyright 2024 Wiley-VCH. (d) A diagram illustrating the comparison between a biological synapse and a synaptic transistor made from ZnO nanofibers. (e) A single nanofiber sample with inner electrons is shown to explain the electrical characteristic mechanism. (f) Adjustable electrical and synaptic properties based on various process parameters for the created artificial synapse. (g) The manufacturing procedure for the transistor is based on ZnO nanofibers doped with perovskite. (d−g) Reprinted from ref 38 with permission. Copyright 2022 Wiley-VCH.

significantly improved luminous efficiency and stability. Additionally, these films simplified the OLED device architecture, potentially leading to more streamlined manufacturing processes and lower production costs.

Besides, electrospun nanofibers can serve as a sacrificial template to support the formation of carrier transport layers, emissive layers, or encapsulation layers.[215] As a template, electrospun nanofibers can impart a fibrous structure to these aforementioned layers, which can provide faster carrier migration paths, enhance light extraction efficiency, and enhance device response speed and efficiency. Moreover, these sacrificial nanofiber templates can help form nano-

https://doi.org/10.1021/acsnano.4c13106
ACS Nano 2024, 18, 31737−31772

patterned structures that enhance the performance of OLEDs, particularly in terms of light outcoupling or electrode structuring. For example, Veeramuthu et al. developed a strain-insensitive conductive structure for OLEDs using electrospun PVA nanofibers as a template.[205] To fabricate the OLEDS, a well-dispersed PDMS solution was drop-casted onto the PVA nanofibers and annealed to form PVA-embedded PDMS thin films. Then, the PVA nanofibers were etched using water to form nanofibrous patterned PDMS (P-PDMS). The PEDOT:PSS and PEO solution was spin-coated onto the nanofiber-patterned PDMS, assembled with the poly[9,9-dioctylfluorenyl-2,7-diyl] (PFO) emission layer and EGaIn metal to form the PFO LED. This PFO LED maintained good brightness performance even after 300 bending cycles. Specifically, brightness retention was approximately 61% when measured with tweezers (at a 2 mm bending radius) and 76% with a wrench (at a 5 mm bending radius, Figure 11f). As a result, these PFO LED exhibited excellent color quality and uniform emission characteristics, offering promising solutions to challenges faced by the next generation of OLED technology.

6.2. Transistors. The invention of field-effect transistors (FETs) has propelled the miniaturization and integration of flexible electronic devices. The compactness and flexibility of these devices not only significantly expand their application domains but also bring immense convenience to applications.[216] However, FETs constructed from solid-state semiconductor trenches lack the necessary flexibility for wearable electronics applications. Furthermore, the manufacturing process of these conventional FETs generally entails costly photolithographic methods. Nonetheless, there has been considerable advancement in the development of inherently stretchable FETs. This progress is attributed to the innovative combination of thermoplastic elastomers with organic polymers like PEDOT polystyrenesulfonate (PEDOT:PSS). This synthesis has been crucial in addressing the rigidity limitations of traditional FETs, thereby expanding their applicability in the growing field of flexible and wearable electronic devices.[206]

Electrospinning technology presents significant advantages in fabricating FETs. This technique can produce highly ordered nanofibers, crucial for enhancing carrier mobility, with increases of more than 3 orders of magnitude. Compared to traditional photolithography, electrospinning not only offers significant cost benefits but also improves the flexibility and breathability of FETs, making them more suitable for fully deformable and wearable applications.[217] Besides, these electrospun nanofibers can be precisely deposited onto a polymer substrate, serving a dual function as a sacrificial mask in creating semiconductor trenches within FETs.[218] An active channel comprised of a single electrospun semiconducting elongated NWs with a diameter of 675 ± 40 nm was reported.[67] The NWs were created using a fused thiophene-diketopyrrolopyrrole-based polymer as the semiconducting element and a poly(ethylene oxide)-based polymer as a molecular adhesive and formability enhancer. Notably, the fully deformable NW FETs demonstrated the ability to withstand 3D volume changes exceeding 1700% while maintaining a constant current output when attached to the surface of a rubber balloon, subsequently returning to their original state.

In addition to the single nanofibers, core−shell electrospun semiconductor nanofibers can also serve as channel materials.[68] Using the coaxial electrospinning process, He and Wang designed the In_2O_3@ZnO coaxial NW arrays-based FETs (Figure 12a,b). Capitalizing on the robust carrier effusion efficiency facilitated by the circular heterogeneous interface of In_2O_3@ZnO, the field effect mobility (ε_{FE}) experienced a significant intrinsic enhancement, achieving an impressive value of 202.3 $cm^2\ V^{-1}\ s^{-1}$, with an I_{on}/I_{off} of more than 10^8 and a competitive mobility of 58.16 $cm^2\ V^{-1}\ s^{-1}$ (Figure 12c). Moreover, the structural attributes of In_2O_3@ZnO coaxial NW arrays FETs endowed them with outstanding optoelectronic coupling capabilities. Consequently, optoelectronic detection systems and artificial photonic synaptic devices were successfully constructed, accompanied by functional simulations to validate their performance.[216] For the fabrication of artificial synaptic transistors, the utilization of electrospun nanofibers presents benefits including lightweight, flexibility, affordability, and customizable chemical and physical attributes. For example, Ren and colleagues developed a transistor utilizing electrospun ZnO nanofibers that demonstrated flexible plasticity to replicate changing synaptic functions. Their study revealed that variations in carrier concentration and mobility affect both the electrical and synaptic characteristics of the device (Figure 12d,e). The device's fiber-based architecture enabled the modulation of short-term plasticity behaviors such as paired-pulse facilitation, spike duration-dependent plasticity, and dynamic filtering, thereby showcasing its adjustable electrical and synaptic performance (Figure 12 f). Moreover, perovskite-doped devices were prepared with the $MAPbI_3$ pin-coated on the ZnO nanofiber after high-temperature annealing (Figure 12g) and demonstrated ultra-low energy consumption down to approximately 0.2554 fJ, offering a prospective method for constructing intricate neuromorphic systems.[38]

7. FLEXIBLE ENVIRONMENTAL MONITORING DEVICES

7.1. Temperature Sensors. Electrospun nanofibers provide many benefits for flexible electronic temperature sensors compared to conventional mercury and infrared thermometers. Their high surface area enhances thermal responsiveness and sensitivity, enabling accurate temperature measurements.[219] For flexible temperature sensors, the primary mechanisms include thermosensitive, thermoelectric, and pyroelectric effects.[220] Currently, the primary challenge hindering the advancement of flexible body or ambient temperature sensors lies in the selection of suitable substrate materials. Thin-film sensors offer the benefits of compact size, seamless integration, in situ, and field measurements. However, finding flexible substrates that can withstand high temperatures is challenging, limiting the practical application of flexible sensors in industries like aerospace, steel, and metallurgy.[221,222] For example, the temperature sensors using carbon-based materials exhibit sensitivities that fall below 1.00% $°C^{-1}$. Shen and Kim presented an approach to fabricating temperature sensors using aligned electrospun carbon nanofiber films. These sensors exhibited exceptional sensitivity and selectivity toward temperature due to their structural properties and high surface area-to-volume ratio. The method involves electrospinning PAN precursor solution onto a flexible substrate, followed by carbonization to produce aligned carbon nanofiber films. Three key mechanisms determine the performance of the aligned carbon nanofiber (ACNF) temperature sensor. First, the size and orientation of sp^2 carbon crystallites dictate the

https://doi.org/10.1021/acsnano.4c13106
ACS Nano 2024, 18, 31737−31772

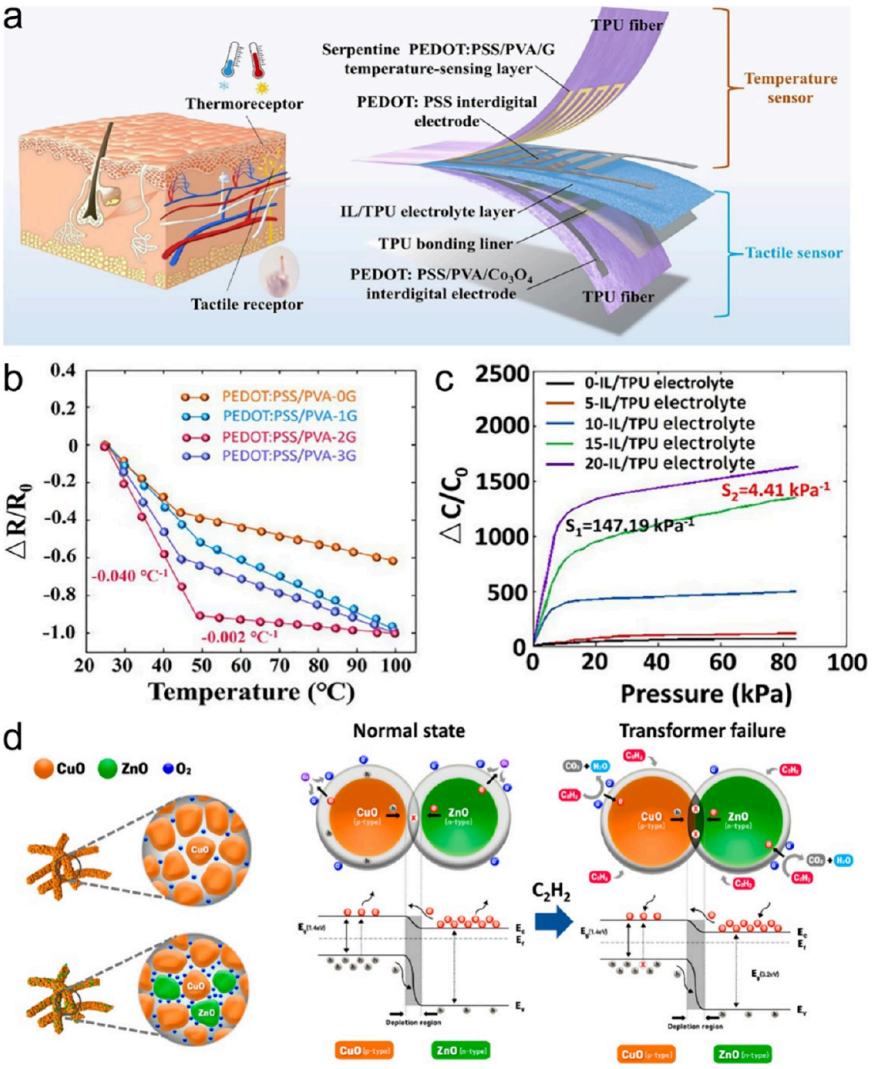

Figure 13. (a) Illustrative representation of human skin highlighting both touch and heat receptors, along with a schematic of the layered structure of the dual-function sensor where the temperature-sensing element is positioned at the top and the touch-sensing element is at the bottom. (b) Variation in relative resistance as a function of temperature for PEDOT electrodes combined with various amounts of graphene. (c) Graphs depicting changes in relative capacitance for ionic nanofiber electrolytes with differing IL concentrations. (a–c) Reprinted from ref 39 with permission. Copyright 2023 Elsevier. (d) Effect of p–n junction by CZ heterostructure. Reprinted from ref 227 with permission. Copyright 2024 American Chemical Society.

semiconducting or metallic nature of ACNFs, affecting their negative temperature coefficient or the positive temperature coefficient characteristics. Second, defects and pyridinic-N groups trap and localize electrons, which activate with sufficient thermal energy, improving sensing performance in ACNFs carbonized at lower temperatures. Lastly, thermal electron transport via variable range hopping is crucial; as temperature increases, charge carriers gain more energy, leading to higher and longer-range hopping between localized sp^2 states. Lower carbonization temperatures result in more sp^3 domains, facilitating longer-range hopping and enhanced charge transport.[223]

Besides, flexible multifunctional sensors face challenges such as signal interference from different stimuli and discomfort during prolonged skin contact.[224−226] Yu and Guo introduced an ultrathin, flexible bifunctional sensor that measured pressure-induced supercapacitance and temperature-induced resistance with minimal crosstalk. The sensor features a planar iontronic supercapacitor beneath a serpentine resistor, comprising a total of seven layers on an electrospun TPU nanofiber platform. The sensing electrodes, made of PEDOT, were patterned using direct ink writing, incorporating graphene nanoflakes and Co_3O_4 nanoparticles to enhance performance (Figure 13a). The sensor achieved high temperature sensitivity (0.040 $°C^{-1}$, 25−50 °C; 0.002 $°C^{-1}$, 50−100 °C, Figure 13b) and pressure sensitivity (147.19 kPa^{-1}, 0−7 kPa; 4.41 kPa^{-1}, 25−85 kPa, Figure 13c). Additionally, it is resistant to humidity, waterproof, and breathable, ensuring wearer comfort.[39]

7.2. Gas Sensors. When used as the substrate of gas sensors, their high surface area-to-volume ratio enhances gas adsorption and sensitivity, enabling rapid and precise detection of trace gas concentrations (e.g., NH_3,[228] CH_4 and CO_2,[229] SO_2,[230] VOC,[231,232] NO_x,[233,234] C_2H_2,[227] H_2S,[235] *etc.*). The flexibility of these nanofibers allows for the creation of adaptable and conformal sensor devices suitable for various surfaces and environments. Additionally, the ability to tailor the substrates (e.g., pure polymers,[236] composites,[237] and

https://doi.org/10.1021/acsnano.4c13106
ACS Nano 2024, 18, 31737−31772

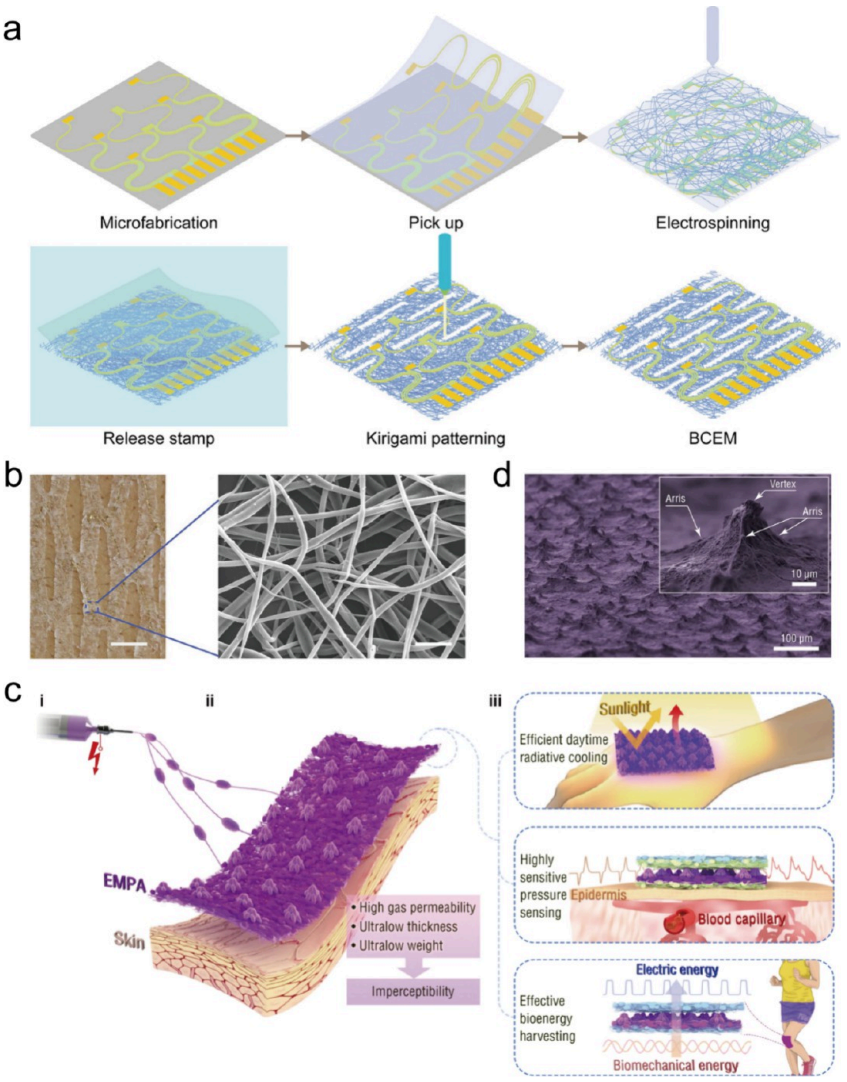

Figure 14. (a) Diagrams depicting the manufacturing process, including stamp-based transfer methods, electrospinning, and kirigami patterning. (b) Images displaying serpentine electronics adhering closely to the skin. Scale bar: 10 mm. Additionally, a scanning electron microscope image reveals the permeable nanofibrous architecture of a BCEM. Scale bar: 5 μm. (a,b) Reprinted from ref 51 with permission. Copyright 2022 Wiley-VCH. (c) Diagrammatic representation of the (i) production, (ii) design, and (iii) usage of EMPAs. (d) Photo of a large-area film made with EMPA. (c,d) Reprinted with permission under a Creative Commons [CC BY] License from ref 53. Copyright 2022 The Authors. Published by Springer Nature.

semiconductors[238]), decorators (e.g., ZnO,[239] NO_2−UiO-66,[240] UiO-66-NH_2,[241] curcumin,[242] and CuO[243]), and morphology (e.g., ring-like, necklace-like, core−shell, multi-channel, tubular, nanowire-in-microtube structures)[147,244,245] of electrospun nanofibers improved the selectivity and response time of gas sensors. Their scalable and cost-effective manufacturing further highlights their potential as high-performance, flexible gas sensors for diverse applications. For example, Jung and co-workers developed high-performance C_2H_2 gas sensors for dissolved gas analysis using CuO/ZnO (CZ) heterostructures made by electrospinning.[227] Their study proved that the CuO = 8:2 (CZ2) sensor had the best performance, with a response of R_g/R_a = 7.6 to 10 ppm of C_2H_2 at 200 °C and good stability (>10 h). The CZ2 sensor also showed high selectivity (>5 times) for coexisting transformer oil gases, including H_2, CH_4, C_2H_4, C_2H_6, CO, and CO_2. Mechanically, the CuO/ZnO heterostructure sensor showed p-type sensing behavior for C_2H_2 detection in lean O_2 conditions. The p-type metal oxide semiconductor formed an insulating core and a hole accumulation layer with O_2, which reduced when reacting with reducing gases, increasing resistance. The heterojunction with n-type ZnO enhanced sensing by forming a depletion layer, where electrons transferred from ZnO to CuO, and holes migrated from CuO to ZnO. When exposed to C_2H_2, electrons trapped by oxygen ions were released back, reacting with both ZnO and CuO, causing an increased depletion layer and higher sensor resistance (Figure 13d). Besides, electrospun nanofiber-based flexible sensors possess the capability to detect a broad spectrum of biological, chemical, and physical hazards. Recent investigations focusing on utilizing electrospun nanofiber-based sensors for the identification of pathogens, pesticide/drug residues, toxins, allergens, and heavy metals have been reviewed[23] and will not be discussed in this review.

8. SUMMARY AND OUTLOOK

Electrospun flexible electronics represent an innovative technology that integrates the benefits of both electrospinning

https://doi.org/10.1021/acsnano.4c13106
ACS Nano 2024, 18, 31737−31772

and flexible electronics for diverse applications. These devices utilize electrospinning to produce nanoscale fibrous or thin-film substrates, enabling the fabrication of intrinsically stretchable electronics, including highly sensitive pressure sensors, efficient energy harvesters, and smart response wearable devices, with skin-like mechanical properties. Electrospinning is an efficient, simple, and scalable method for producing nanofibers, well-suited for creating flexible electronic devices. By modulating nanofiber morphology, diameter, and structure, one can optimize material properties like electrical conductivity, mechanical flexibility, and chemical stability, offering a broad range of opportunities for creating electrospun flexible electronics. While significant progress has been made in developing electrospun flexible electronic devices, challenges persist in both current and future endeavors.

The primary challenge is to overcome the incompatibility of multiple interfaces, including (i) Interfaces at the nano- and microscale between different materials, (ii) Interfaces at the mesoscale between layers or microstructures, and (iii) Interfaces at the macroscale involving unit devices, substrates, electrical connections, and skin.[51,205] Fabrication of nanoelectronics on rough fiber surfaces remains difficult, hindering device performance.[152] Flexible devices must sustain high performance during repeated folding and stretching. The molecules, nanostructures, microstructures, multiple layers, and unit devices forming these interfaces exhibit varying moduli and mechanical hysteresis. Thus, it is essential to systematically study these interfaces according to the appropriate physical scales.[246] One potential solution is to achieve precise control over the nanofiber preparation process or combine it with additional micromachining technology to ensure both structural stability and robust mechanical strength in electrospun nanofibers. For instance, to overcome the incompatibility of multiple interfaces, Xu et al. proposed a stamp-based transferring scheme for the hybrid integration of high-performance micromachined multifunctional kirigami sensors with porous flexible electrospun styrene-ethylene-butylene-styrene nanofibrous substrate. The kirigami architecture was designed by creating precise cuts in nanofibrous substrates using a laser, to form a pattern of breathable and conformal electronic membrane (BCEM, Figure 14a).[51] The fabrication strategy that combined the stamp-based transferring techniques effectively mitigated the processing incompatibility between planar microelectronic devices and porous substrates. The design of the kirigami architecture enhanced the stretchability and conformability of the nanofibrous substrate, allowing for seamless integration with the skin (Figure 14b). This study offers a potential pathway for designing advanced micromachining technologies to develop highly accurate biosensors for electrophysiological signal capture.

Another challenge is the difficulty in developing 3D microstructure sensor arrays with gradient geometry for various imperceptible on-skin devices. An array configuration offers higher spatial resolution, enhances sensitivity by distributing the sensing area for detecting subtle pressure or movement variations, and provides multifunctionality by enabling the simultaneous detection of multiple touch points. The electrospinning process, which deposits fibers in a random pattern, often results in the functional surfaces of these nearly invisible films being 2D flat planes. Therefore, their optical, thermal, mechanical, and electrical properties are typically less than satisfactory.[247,248] Conversely, 3D microstructures with gradient space-filling, stress distribution, and refractive index are advantageous for regulating force, heat, light, and electricity.[249] In this regard, the design of 3D electrospun nanofiber sensor arrays may offer a promising solution for achieving significant advantages in high-performance devices. For instance, electrospinning self-assembly has been used to create multifunctional, ultrathin, and lightweight electrospun micropyramid arrays (EMPAs) that are gas-permeable.[53] These EMPAs demonstrate good efficacy in on-skin applications, such as daytime radiative cooling, pressure sensing, and biomechanical energy harvesting (Figure 14c). By utilizing a series of electrified wet jets, EMPAs of various materials can be structurally tailored (Figure 14d). The EMPA-based fabric cools by 4 °C in sunlight, while the hybrid sensor and nanogenerators exhibit high sensitivity and efficient biomechanical energy capture. This research lays the foundation for constructing adaptable EMPAs, creating possibilities for using on-skin devices in areas such as personal protection, healthcare, precise sensing, powerful self-powered electronics, and seamless human−machine interaction with minimal sensory disruption. In another study, Ma et al. proposed a pressure sensor based on electrospun polyurethane membrane with MXene-embedded ZnO nanowire arrays, for wide-sensing range and high-sensitivity flexible pressure sensor.[250] To enhance the efficiency of TENGs, electrospun amino-functionalized reduced graphene oxide (A-rGO)/Nylon-12 (tribopositive layer) and micropatterned molybdenum disulfide (MoS_2)/Ecoflex (tribonegative layer) were assembled into a sensor array. The optimized TENG array achieved a maximum open-circuit potential of 451 V, a short-circuit current of 13.3 μA, and an instantaneous power density of 1.3 Wm^{-2}, with a mechanical conversion efficiency of 96.7%.[251] Recently, Zhang and colleagues reported the design of a "sandwich" flexible pressure sensor. This sensor is composed of a porous PLA nanofiber network layer and a micropyramid structure PDMS electrodes array.[252] Such a sensor array can accurately monitor different physiological signals in real-time, which is believed to be a strong impetus for the design of the next generation of wearable devices.

Third, many electrospun nanofibers exhibit a lack of robust mechanical properties due to their inherently small diameter and high surface area-to-volume ratio, which can lead to structural weaknesses. Additionally, the random orientation and alignment of the nanofibers during the electrospinning process can result in nonuniform mechanical strength and reduced load-bearing capabilities. Furthermore, the nature of the polymer materials used in electrospinning can also contribute to their insufficient mechanical performance, as some polymers may not provide the necessary strength and durability required for certain applications. Researchers have tried to address these shortcomings by introducing other functional components like polymers and nanoparticles.[66,253,254] For instance, incorporating polyglycolic acid into a nanofiber system enhanced the mechanical properties of the original nanofiber.[255] Nanoparticles can be 1D nanomaterials including metal NWs, metal nanofibers, and CNTs with high conductivity and excellent mechanical deformability, and 2D nanomaterials like graphene, hexagonal boron nitride, and transition metal dichalcogenide have also been applied in flexible electronics.[77,239,242,243] In addition, the limited commercial implementation of these devices necessitates further investigation into the selection of nanofabricants and

https://doi.org/10.1021/acsnano.4c13106
ACS Nano 2024, 18, 31737−31772

process optimization. For instance, traditional PAN-based electrospun nanofibers possess relatively low electrical conductivity and are insufficient to compete with conventional electrode materials. To address these challenges, researchers have proposed various potential strategies, such as doping with heteroatoms or combining nanofibers with conductive polymers and other materials to enhance their electrical and mechanical properties. For batteries, despite their advantages, several challenges persist in practical applications. For instance, volumetric expansion during prolonged charge−discharge cycles can compromise the cyclic stability of batteries. Moreover, when compared to other flexible nanomaterials such as graphene and CNTs, electrospun nanofibers have room for improvement in conductivity. Insufficient battery penetrability also significantly limits performance.[256,257] To address these issues, one potential solution is the structural optimization of electrospun nanofibers, such as adopting core−shell or sandwich structures. In addition, integrating electrospinning with other techniques like chemical vapor deposition, and modifying the principles of electrospinning, can enhance the structural and compositional attributes of battery materials. For OLEDs, although its fabrication using the electrospun nanofibers as sacrificial templates has been successful on a laboratory scale, scaling it to industrial production faces several challenges. First, the electroluminescence efficiency of these electrospun conjugated polymer nanofibers within the OLED architecture is limited. There is a need to enhance the electroluminescent performance and emission color tunability of this hybrid bilayer structure.[258] To this end, one can reduce the percolation threshold by extending the conjugation length and alignment of the conjugated polymers. Besides, designing band-like microstructural patterns and altering the filling within the electrospun nanofibers can also enhance the charge balance in the nanofiber-thin film composite bilayer, achieving optimal luminescent performance and color.[259] Second, surface roughness is a critical issue in OLEDs. The incorporation of metal fibers (such as Ag NWs) during the electrospinning process can lead to defects due to fiber bending or transfer, affecting OLED performance.[260] A potential solution is employing wet etching of overdeposited Ag film, with electrospun polymer fibers serving as etching masks to avoid complex transfer processes or high-temperature treatments. By adjusting the thickness of the Ag film, surface roughness can be controlled, eliminating junction resistance.[261]

Future research should focus on achieving high conductivity without compromising flexibility, improving durability during repeated deformations, and integrating multifunctionality. This is difficult due to the mechanical mismatch between polymeric fibers and conductive fillers, which degrades performance during stretching. Additionally, the high surface roughness of nanofiber assemblies hinders the fabrication of micro/nanoelectronics, limiting functional integration. On the manufacturing side, scaling up production from lab-scale to industrial-scale while maintaining uniformity and functionality is challenging, with larger devices needed for practical applications. Moreover, integrating multifunctionality, such as sensing, self-powering, and wireless communication, remains more complex compared to film-based flexible electronics. Nevertheless, this integration is anticipated to enhance the performance and versatility of existing devices while laying the groundwork for next-generation solutions that transcend conventional boundaries. These innovations will substantially contribute to the advancement of science and bring convenience and advancements to human society and technology.

AUTHOR INFORMATION

Corresponding Authors

Guisheng Li − *School of Materials and Chemistry, University of Shanghai for Science and Technology, Shanghai 200093, P. R. China*; Email: liguisheng@usst.edu.cn

Lizhi Xu − *Department of Mechanical Engineering, The University of Hong Kong, Hong Kong SAR 999077, P. R. China; Advanced Biomedical Instrumentation Centre, Hong Kong SAR 999077, P. R. China; Materials Innovation Institute for Life Sciences and Energy (MILES), The University of Hong Kong Shenzhen Institute of Research and Innovation (HKU-SIRI), Shenzhen 518057, P. R. China*; orcid.org/0000-0001-6888-0524; Email: xulizhi@hku.hk

Authors

Shige Wang − *School of Materials and Chemistry, University of Shanghai for Science and Technology, Shanghai 200093, P. R. China; Department of Mechanical Engineering, The University of Hong Kong, Hong Kong SAR 999077, P. R. China; Advanced Biomedical Instrumentation Centre, Hong Kong SAR 999077, P. R. China*; orcid.org/0000-0002-7639-6035

Peng Fan − *School of Materials and Chemistry, University of Shanghai for Science and Technology, Shanghai 200093, P. R. China*

Wenbo Liu − *Department of Mechanical Engineering, The University of Hong Kong, Hong Kong SAR 999077, P. R. China*

Bin Hu − *School of Materials and Chemistry, University of Shanghai for Science and Technology, Shanghai 200093, P. R. China*

Jiaxuan Guo − *School of Materials and Chemistry, University of Shanghai for Science and Technology, Shanghai 200093, P. R. China*

Zizhao Wang − *School of Materials and Chemistry, University of Shanghai for Science and Technology, Shanghai 200093, P. R. China*

Shengke Zhu − *School of Materials and Chemistry, University of Shanghai for Science and Technology, Shanghai 200093, P. R. China*

Yipu Zhao − *Department of Mechanical Engineering, The University of Hong Kong, Hong Kong SAR 999077, P. R. China; Advanced Biomedical Instrumentation Centre, Hong Kong SAR 999077, P. R. China*

Jinchen Fan − *School of Materials and Chemistry, University of Shanghai for Science and Technology, Shanghai 200093, P. R. China*; orcid.org/0000-0002-8905-1693

Complete contact information is available at: https://pubs.acs.org/10.1021/acsnano.4c13106

Notes

The authors declare no competing financial interest.

ACKNOWLEDGMENTS

This study was supported by the National Natural Science Foundation of China (82073386, 22476131, 22176127) and the Health@InnoHK program of the Innovation and Technology Commission of the Hong Kong SAR Government.

https://doi.org/10.1021/acsnano.4c13106
ACS Nano 2024, 18, 31737−31772

VOCABULARY

electrospun nanofibers: technique that uses direct current to create nanometer-scale polymer fibers from polymer solutions or melts.

flexible sensor: a sensor with flexibility and bendability.

energy harvesting: the process of transforming the energy available in the surrounding environment into electrical energy.

supercapacitors: a high-capacity capacitor with a capacitance value significantly higher than that of traditional capacitors.

wearable electronics: a category of electronic devices that can be worn as accessories embedded in clothing or even implanted in the body.

flexible display: an electronic visual display designed to be flexible, foldable, or rolling.

REFERENCES

(1) Liu, L.; Li, R.; Liu, F.; Huang, L.; Liu, W.; Wang, J.; Wu, Z.; Reddy, N.; Cui, W.; Jiang, Q. Highly elastic and strain sensing corn protein electrospun fibers for monitoring of wound healing. *ACS Nano* **2023**, *17* (10), 9600−9610.

(2) Zhong, D.; Wu, C.; Jiang, Y.; Yuan, Y.; Kim, M.-g.; Nishio, Y.; Shih, C.-C.; Wang, W.; Lai, J.-C.; Ji, X.; Gao, T. Z.; Wang, Y.-X.; Xu, C.; Zheng, Y.; Yu, Z.; Gong, H.; Matsuhisa, N.; Zhao, C.; Lei, Y.; Liu, D.; Zhang, S.; Ochiai, Y.; Liu, S.; Wei, S.; Tok, J. B. H.; Bao, Z. High-speed and large-scale intrinsically stretchable integrated circuits. *Nature* **2024**, *627* (8003), 313−320.

(3) Arwani, R. T.; Tan, S. C. L.; Sundarapandi, A.; Goh, W. P.; Liu, Y.; Leong, F. Y.; Yang, W.; Zheng, X. T.; Yu, Y.; Jiang, C.; Ang, Y. C.; Kong, L.; Teo, S. L.; Chen, P.; Su, X.; Li, H.; Liu, Z.; Chen, X.; Yang, L.; Liu, Y. Stretchable ionic−electronic bilayer hydrogel electronics enable in situ detection of solid-state epidermal biomarkers. *Nat. Mater.* **2024**, *23*, 1115−1122.

(4) Zhuang, Q.; Yao, K.; Zhang, C.; Song, X.; Zhou, J.; Zhang, Y.; Huang, Q.; Zhou, Y.; Yu, X.; Zheng, Z. Permeable, three-dimensional integrated electronic skins with stretchable hybrid liquid metal solders. *Nat. Electron.* **2024**, *7*, 598−609.

(5) Weng, W.; Yang, J.; Zhang, Y.; Li, Y.; Yang, S.; Zhu, L.; Zhu, M. A route toward smart system integration: from fiber design to device construction. *Adv. Mater.* **2020**, *32* (5), No. 1902301.

(6) Babu, A.; Aazem, I.; Walden, R.; Bairagi, S.; Mulvihill, D. M.; Pillai, S. C. Electrospun nanofiber based TENGs for wearable electronics and self-powered sensing. *Chem. Eng. J.* **2023**, *452*, No. 139060.

(7) Peng, S.; Yu, Y.; Wu, S.; Wang, C.-H. Conductive polymer nanocomposites for stretchable electronics: material selection, design, and applications. *ACS Appl. Mater. Interfaces* **2021**, *13* (37), 43831−43854.

(8) Guan, X.; Xu, B.; Gong, J. Hierarchically architected polydopamine modified $BaTiO_3$@P(VDF-TrFE) nanocomposite fiber mats for flexible piezoelectric nanogenerators and self-powered sensors. *Nano Energy* **2020**, *70*, No. 104516.

(9) Choi, M.; Bae, S. R.; Hu, L.; Hoang, A. T.; Kim, S. Y.; Ahn, J. H. Full-color active-matrix organic light-emitting diode display on human skin based on a large-area MoS_2 backplane. *Sci. Adv.* **2020**, *6* (28), No. eabb5898.

(10) Someya, T.; Bao, Z.; Malliaras, G. G. The rise of plastic bioelectronics. *Nature* **2016**, *540* (7633), 379−385.

(11) Chortos, A.; Liu, J.; Bao, Z. Pursuing prosthetic electronic skin. *Nat. Mater.* **2016**, *15* (9), 937−950.

(12) Guo, M.; Xiong, J.; Jin, X.; Lu, S.; Zhang, Y.; Xu, J.; Fan, H. Mussel stimulated modification of flexible Janus PAN/PVDF-HFP nanofiber hybrid membrane for advanced lithium-ion batteries separator. *J. Membr. Sci.* **2023**, *675*, No. 121533.

(13) Fukuda, K.; Yu, K.; Someya, T. The future of flexible organic solar cells. *Adv. Energy Mater.* **2020**, *10* (25), No. 2000765.

(14) Sim, K.; Rao, Z.; Ershad, F.; Yu, C. Rubbery electronics fully made of stretchable elastomeric electronic materials. *Adv. Mater.* **2020**, *32* (15), No. 1902417.

(15) Matsuhisa, N.; Chen, X.; Bao, Z.; Someya, T. Materials and structural designs of stretchable conductors. *Chem. Soc. Rev.* **2019**, *48* (11), 2946−2966.

(16) Rogers, J. A.; Someya, T.; Huang, Y. Materials and mechanics for stretchable electronics. *Science* **2010**, *327* (5973), 1603−1607.

(17) Wang, P.; Ma, X.; Lin, Z.; Chen, F.; Chen, Z.; Hu, H.; Xu, H.; Zhang, X.; Shi, Y.; Huang, Q.; Lin, Y.; Zheng, Z. Well-defined in-textile photolithography towards permeable textile electronics. *Nat. Commun.* **2024**, *15* (1), 887.

(18) Ma, Z.; Huang, Q.; Xu, Q.; Zhuang, Q.; Zhao, X.; Yang, Y.; Qiu, H.; Yang, Z.; Wang, C.; Chai, Y.; Zheng, Z. Permeable superelastic liquid-metal fibre mat enables biocompatible and monolithic stretchable electronics. *Nat. Mater.* **2021**, *20* (6), 859−868.

(19) Miyamoto, A.; Lee, S.; Cooray, N. F.; Lee, S.; Mori, M.; Matsuhisa, N.; Jin, H.; Yoda, L.; Yokota, T.; Itoh, A.; Sekino, M.; Kawasaki, H.; Ebihara, T.; Amagai, M.; Someya, T. Inflammation-free, gas-permeable, lightweight, stretchable on-skin electronics with nanomeshes. *Nat. Nanotechnol.* **2017**, *12* (9), 907−913.

(20) Zhuang, Q.; Yao, K.; Wu, M.; Lei, Z.; Chen, F.; Li, J.; Mei, Q.; Zhou, Y.; Huang, Q.; Zhao, X.; Li, Y.; Yu, X.; Zheng, Z. Wafer-patterned, permeable, and stretchable liquid metal microelectrodes for implantable bioelectronics with chronic biocompatibility. *Sci. Adv.* **2023**, *9* (22), No. eadg8602.

(21) Shen, Y.; Yang, F.; Lu, W.; Chen, W.; Huang, S.; Li, N. A highly stretchable and breathable polyurethane fibrous membrane sensor for human motion monitoring and voice signal recognition. *Sens. Actuators A-Phys.* **2021**, *331*, No. 112974.

(22) Zheng, X.; Zhou, D.; Liu, Z.; Hong, X.; Li, C.; Ge, S.; Cao, W. Skin-inspired textile electronics enable ultrasensitive pressure sensing. *Small* **2024**, *20*, No. 2310032.

(23) Akhavan-Mahdavi, S.; Mirbagheri, M. S.; Assadpour, E.; Sani, M. A.; Zhang, F.; Jafari, S. M. Electrospun nanofiber-based sensors for the detection of chemical and biological contaminants/hazards in the food industries. *Adv. Colloid Interface Sci.* **2024**, *325*, No. 103111.

(24) Ji, D.; Lin, Y.; Guo, X.; Ramasubramanian, B.; Wang, R.; Radacsi, N.; Jose, R.; Qin, X.; Ramakrishna, S. Electrospinning of nanofibres. *Nat. Rev. Methods Prim.* **2024**, *4* (1), 1.

(25) Yang, T.; Wan, C. W.; Zhang, X. Y.; Liu, T.; Niu, L.; Fang, J.; Liu, Y. Q. High-efficiency preparation of multifunctional conjugated electrospun graphene doped PVDF/CF yarns for energy harvesting and human movement monitoring in TENG textile. *Nano Res.* **2024**, *17*, 4478−4488.

(26) Lin, L.; Wang, L.; Li, B.; Luo, J.; Huang, X.; Gao, Q.; Xue, H.; Gao, J. Dual conductive network enabled superhydrophobic and high performance strain sensors with outstanding electro-thermal performance and extremely high gauge factors. *Chem. Eng. J.* **2020**, *385*, No. 123391.

(27) Zeng, Z.; Jiang, F.; Yue, Y.; Han, D.; Lin, L.; Zhao, S.; Zhao, Y. B.; Pan, Z.; Li, C.; Nyström, G.; et al. Flexible and ultrathin waterproof cellular membranes based on high-conjunction metal-wrapped polymer nanofibers for electromagnetic interference shielding. *Adv. Mater.* **2020**, *32* (19), No. 1908496.

(28) Zhao, J.; Liu, Z.; Low, S. C.; Xu, Z.; Tan, S. H. Electrospinning technique meets solar energy: electrospun nanofiber-based evaporation systems for solar steam generation. *Adv. Fiber Mater.* **2023**, *5* (4), 1318−1348.

(29) Ding, J.; Zhang, J.; Li, J.; Li, D.; Xiao, C.; Xiao, H.; Yang, H.; Zhuang, X.; Chen, X. Electrospun polymer biomaterials. *Prog. Polym. Sci.* **2019**, *90*, 1−34.

(30) Wu, T.; Ding, M.; Shi, C.; Qiao, Y.; Wang, P.; Qiao, R.; Wang, X.; Zhong, J. Resorbable polymer electrospun nanofibers: History, shapes and application for tissue engineering. *Chin. Chem. Lett.* **2020**, *31* (3), 617−625.

(31) Ram, N.; Kaarthik, J.; Singh, S.; Palneedi, H.; Prasad, P. D.; Venkateswarlu, A. Boosting energy harvesting of fully flexible

https://doi.org/10.1021/acsnano.4c13106
ACS Nano 2024, 18, 31737−31772

magnetoelectric composites of PVDF-AlN and NiO-decorated carbon nanofibers. *Ceram. Int.* **2024**, *50* (10), 17465−17474.
(32) Zhu, M.; Wang, H.; Li, S.; Liang, X.; Zhang, M.; Dai, X.; Zhang, Y. Flexible electrodes for in vivo and in vitro electrophysiological signal recording. *Adv. Healthc. Mater.* **2021**, *10* (17), No. 2100646.
(33) Xia, Y.; Shi, F.; Liu, R.; Zhu, H.; Liu, K.; Ren, C.; Li, J.; Yang, Z. In situ electrospinning MOF-derived highly dispersed α-cobalt confined in nitrogen-doped carbon nanofibers nanozyme for biomolecule monitoring. *Anal. Chem.* **2024**, *96* (3), 1345−1353.
(34) Amiri, A.; Conlee, B.; Tallerine, I.; Kennedy, W. J.; Naraghi, M. A novel path towards synthesis of nitrogen-rich porous carbon nanofibers for high performance supercapacitors. *Chem. Eng. J.* **2020**, *399*, No. 125788.
(35) Uzabakiriho, P. C.; Wang, M.; Ma, C.; Zhao, G. Stretchable, breathable, and highly sensitive capacitive and self-powered electronic skin based on core-shell nanofibers. *Nanoscale* **2022**, *14* (17), 6600−6611.
(36) Lv, B.; Zhao, G.; Wang, H.; Wang, Q.; Yang, B.; Ma, W.; Li, Z.; Li, J. Ionogel fiber-based flexible sensor for friction sensing. *Adv. Mater. Technol.* **2023**, *8* (10), No. 2201617.
(37) Pan, C.-T.; Dutt, K.; Kumar, A.; Kumar, R.; Chuang, C.-H.; Lo, Y.-T.; Wen, Z.-H.; Wang, C.-S.; Kuo, S.-W. PVDF/AgNP/MXene composites-based near-field electrospun fiber with enhanced piezoelectric performance for self-powered wearable sensors. *Int. J. Bioprinting* **2023**, *9* (1), No. 647.
(38) Guo, Y.; Wu, F.; Dun, G.-H.; Cui, T.; Liu, Y.; Tan, X.; Qiao, Y.; Lanza, M.; Tian, H.; Yang, Y.; Ren, T.-L. Electrospun nanofiber-based synaptic transistor with tunable plasticity for neuromorphic computing. *Adv. Funct. Mater.* **2023**, *33* (5), No. 2208055.
(39) Wang, P.; Yu, W.; Li, G.; Meng, C.; Guo, S. Printable, flexible, breathable and sweatproof bifunctional sensors based on an all-nanofiber platform for fully decoupled pressure−temperature sensing application. *Chem. Eng. J.* **2023**, *452*, No. 139174.
(40) Ma, C.; Song, G.; Li, Z.; Wu, H.; Wang, C.; Wang, Y.; Zhang, X.; Song, Y.; Shi, J. High-areal-capacitance electrode constructed by lignin-based microporous carbon nanofibers for supercapacitors. *J. Energy Storage* **2024**, *88*, No. 111465.
(41) Chao, M.; Di, P.; Yuan, Y.; Xu, Y.; Zhang, L.; Wan, P. Flexible breathable photothermal-therapy epidermic sensor with MXene for ultrasensitive wearable human-machine interaction. *Nano Energy* **2023**, *108*, No. 108201.
(42) Jang, K.-I.; Chung, H. U.; Xu, S.; Lee, C. H.; Luan, H.; Jeong, J.; Cheng, H.; Kim, G.-T.; Han, S. Y.; Lee, J. W.; Kim, J.; Cho, M.; Miao, F.; Yang, Y.; Jung, H. N.; Flavin, M.; Liu, H.; Kong, G. W.; Yu, K. J.; Rhee, S. I.; Chung, J.; Kim, B.; Kwak, J. W.; Yun, M. H.; Kim, J. Y.; Song, Y. M.; Paik, U.; Zhang, Y.; Huang, Y.; Rogers, J. A. Soft network composite materials with deterministic and bio-inspired designs. *Nat. Commun.* **2015**, *6* (1), 6566.
(43) Fan, J. A.; Yeo, W.-H.; Su, Y.; Hattori, Y.; Lee, W.; Jung, S.-Y.; Zhang, Y.; Liu, Z.; Cheng, H.; Falgout, L.; Bajema, M.; Coleman, T.; Gregoire, D.; Larsen, R. J.; Huang, Y.; Rogers, J. A. Fractal design concepts for stretchable electronics. *Nat. Commun.* **2014**, *5* (1), 3266.
(44) Han, S.; Kim, M. K.; Wang, B.; Wie, D. S.; Wang, S.; Lee, C. H. Mechanically reinforced skin-electronics with networked nanocomposite elastomer. *Adv. Mater.* **2016**, *28* (46), 10257−10265.
(45) Maneeratana, V.; Bass, J. D.; Azaïs, T.; Patissier, A.; Vallé, K.; Maréchal, M.; Gebel, G.; Laberty-Robert, C.; Sanchez, C. Fractal inorganic−organic interfaces in hybrid membranes for efficient proton transport. *Adv. Funct. Mater.* **2013**, *23* (22), 2872−2880.
(46) Park, S.-H.; Lee, H. B.; Yeon, S. M.; Park, J.; Lee, N. K. Flexible and stretchable piezoelectric sensor with thickness-tunable configuration of electrospun nanofiber mat and elastomeric substrates. *ACS Appl. Mater. Interfaces* **2016**, *8* (37), 24773−24781.
(47) Kakunuri, M.; Wanasekara, N. D.; Sharma, C. S.; Khandelwal, M.; Eichhorn, S. J. Three-dimensional electrospun micropatterned cellulose acetate nanofiber surfaces with tunable wettability. *J. Appl. Polym. Sci.* **2017**, *134* (15), No. 44709.
(48) Sun, B.; McCay, R. N.; Goswami, S.; Xu, Y.; Zhang, C.; Ling, Y.; Lin, J.; Yan, Z. Gas-permeable, multifunctional on-skin electronics based on laser-induced porous graphene and sugar-templated elastomer sponges. *Adv. Mater.* **2018**, *30* (50), No. 1804327.
(49) Parida, K.; Thangavel, G.; Cai, G.; Zhou, X.; Park, S.; Xiong, J.; Lee, P. S. Extremely stretchable and self-healing conductor based on thermoplastic elastomer for all-three-dimensional printed triboelectric nanogenerator. *Nat. Commun.* **2019**, *10* (1), 2158.
(50) Thrasher, C. J.; Farrell, Z. J.; Morris, N. J.; Willey, C. L.; Tabor, C. E. Mechanoresponsive polymerized liquid metal networks. *Adv. Mater.* **2019**, *31* (40), No. 1903864.
(51) Li, H.; Wang, Z.; Sun, M.; Zhu, H.; Liu, H.; Tang, C. Y.; Xu, L. Breathable and skin-conformal electronics with hybrid integration of microfabricated multifunctional sensors and kirigami-structured nanofibrous substrates. *Adv. Funct. Mater.* **2022**, *32* (32), No. 2202792.
(52) Li, Y.; Xiao, S.; Zhang, X.; Jia, P.; Tian, S.; Pan, C.; Zeng, F.; Chen, D.; Chen, Y.; Tang, J.; Xiong, J. Silk inspired in-situ interlocked superelastic microfibers for permeable stretchable triboelectric nanogenerator. *Nano Energy* **2022**, *98*, No. 107347.
(53) Zhang, J.-H.; Li, Z.; Xu, J.; Li, J.; Yan, K.; Cheng, W.; Xin, M.; Zhu, T.; Du, J.; Chen, S.; An, X.; Zhou, Z.; Cheng, L.; Ying, S.; Zhang, J.; Gao, X.; Zhang, Q.; Jia, X.; Shi, Y.; Pan, L. Versatile self-assembled electrospun micropyramid arrays for high-performance on-skin devices with minimal sensory interference. *Nat. Commun.* **2022**, *13* (1), 5839.
(54) Sengupta, D.; Lu, L.; Gomes, D. R.; Jayawardhana, B.; Pei, Y.; Kottapalli, A. G. P. Fabric-like electrospun pvac−graphene nanofiber webs as wearable and degradable piezocapacitive sensors. *ACS Appl. Mater. Interfaces* **2023**, *15* (18), 22351−22366.
(55) Jiang, C.; Wu, C.; Li, X.; Yao, Y.; Lan, L.; Zhao, F.; Ye, Z.; Ying, Y.; Ping, J. All-electrospun flexible triboelectric nanogenerator based on metallic MXene nanosheets. *Nano Energy* **2019**, *59*, 268−276.
(56) Gao, J.; Li, B.; Huang, X.; Wang, L.; Lin, L.; Wang, H.; Xue, H. Electrically conductive and fluorine free superhydrophobic strain sensors based on SiO_2/graphene-decorated electrospun nanofibers for human motion monitoring. *Chem. Eng. J.* **2019**, *373*, 298−306.
(57) Lee, S.; Liang, X.; Kim, J. S.; Yokota, T.; Fukuda, K.; Someya, T. Permeable bioelectronics toward biointegrated systems. *Chem. Rev.* **2024**, *124* (10), 6543−6591.
(58) Huang, Q.; Zheng, Z. Pathway to Developing Permeable Electronics. *ACS Nano* **2022**, *16* (10), 15537−15544.
(59) Jiang, Y.; Zhang, Z.; Wang, Y.-X.; Li, D.; Coen, C.-T.; Hwaun, E.; Chen, G.; Wu, H.-C.; Zhong, D.; Niu, S.; et al. Topological supramolecular network enabled high-conductivity, stretchable organic bioelectronics. *Science* **2022**, *375* (6587), 1411−1417.
(60) Chiang, C.-H.; Won, S. M.; Orsborn, A. L.; Yu, K. J.; Trumpis, M.; Bent, B.; Wang, C.; Xue, Y.; Min, S.; Woods, V.; et al. Development of a neural interface for high-definition, long-term recording in rodents and nonhuman primates. *Sci. Transl. Med.* **2020**, *12* (538), No. eaay4682.
(61) Gao, Z.; Xiao, X.; Carlo, A. D.; Yin, J.; Wang, Y.; Huang, L.; Tang, J.; Chen, J. Advances in wearable strain sensors based on electrospun fibers. *Adv. Funct. Mater.* **2023**, *33* (18), No. 2214265.
(62) Wang, M.; Ma, C.; Uzabakiriho, P. C.; Chen, X.; Chen, Z.; Cheng, Y.; Wang, Z.; Zhao, G. Stencil printing of liquid metal upon electrospun nanofibers enables high-performance flexible electronics. *ACS Nano* **2021**, *15* (12), 19364−19376.
(63) Wu, Y.-G.; Wang, Z.-B.; Xu, J.-B.; Chen, Z.; Zeng, G.-L.; Xu, Z.-J.; Zhou, J.-H.; Chen, X.-Q.; Tan, Q.-L.; Chen, Q.-N.; Yang, Y.; Chen, S.-Y.; Wang, L.-Y.; Wu, D.-Z. Direct writing of liquid metal onto an electrospun graphene oxide composite polymer nanofiber membrane for robust and stretchable electrodes. *Adv. Mater. Technol.* **2023**, *8* (9), No. 2201935.
(64) Bian, Y.; Shi, H.; Yuan, Q.; Zhu, Y.; Lin, Z.; Zhuang, L.; Han, X.; Wang, P.; Chen, M.; Wang, X. Patterning techniques based on metallized electrospun nanofibers for advanced stretchable electronics. *Adv. Sci.* **2024**, *11*, No. 2309735.
(65) Luo, G.; Zhang, Q.; Luo, Y.; Wang, S.; Yang, P.; Zhao, L.; Jiang, Z. Gold sputtering-assisted conductive electrospun nanofibers mat decorated with MnO_2 nanospheres for flexible, high-performance

https://doi.org/10.1021/acsnano.4c13106
ACS Nano 2024, 18, 31737−31772

supercapacitor electrodes. *Int. J. Electrochem. Sci.* **2020**, *15* (1), 515−525.
(66) Xing, R.; Liu, Y.; Yan, J.; Wang, R.; Zhuang, X.; Yang, G. High-performance, breathable and flame-retardant moist-electric generator based on asymmetrical nanofiber membrane assembly. *J. Colloid Interface Sci.* **2024**, *671*, 205−215.
(67) Lee, Y.; Oh, J. Y.; Kim, T. R.; Gu, X.; Kim, Y.; Wang, G. J. N.; Wu, H. C.; Pfattner, R.; To, J. W.; Katsumata, T.; et al. Deformable organic nanowire field-effect transistors. *Adv. Mater.* **2018**, *30* (7), No. 1704401.
(68) Wu, H. B.; Shi, S.; Zhou, H. Q.; Zhi, C. W.; Meng, S.; Io, W. F.; Ming, Y.; Wang, Y. C.; Lei, L. Q.; Fei, B.; Hao, J. H.; Hu, J. L. Stem cell self-triggered regulation and differentiation on polyvinylidene fluoride electrospun nanofibers. *Adv. Funct. Mater.* **2024**, *34* (4), No. 2309270.
(69) Zarei, M.; Lee, G.; Lee, S. G.; Cho, K. Advances in biodegradable electronic skin: Material progress and recent applications in sensing, robotics, and human−machine interfaces. *Adv. Mater.* **2023**, *35* (4), No. 2203193.
(70) Wang, P.; Liu, J.; Li, Y.; Li, G.; Yu, W.; Zhang, Y.; Meng, C.; Guo, S. Recent advances in wearable tactile sensors based on electrospun nanofiber platform. *Adv. Sens. Res.* **2023**, *2* (7), No. 2200047.
(71) Dou, Y. B.; Zhang, W. J.; Kaiser, A. Electrospinning of metal-organic frameworks for energy and environmental applications. *Adv. Sci.* **2020**, *7* (3), No. 21.
(72) Zhang, J. L.; Yang, T.; Tian, G.; Lan, B. L.; Deng, W. L.; Tang, L. H.; Ao, Y.; Sun, Y.; Zeng, W. H.; Ren, X. R.; Li, Z. Y.; Jin, L.; Yang, W. Q. Spatially confined MXene/PVDF nanofiber piezoelectric electronics. *Adv. Fiber Mater.* **2024**, *6* (1), 133−144.
(73) Alali, K. T.; Tan, S.; Zhu, J.; Liu, J.; Yu, J.; Liu, Q.; Wang, J. High mechanical property and hydrophilic electrospun poly amidoxime/poly acrylonitrile composite nanofibrous mats for extraction uranium from seawater. *Chemosphere* **2024**, *351*, No. 141191.
(74) Majd, M.; Gholami, M.; Fathi, A.; Sedghi, R.; Nojavan, S. Thin-film solid-phase microextraction of pesticides from cereal samples using electrospun polyvinyl alcohol/modified chitosan/porous organic framework nanofibers. *Food Chem.* **2024**, *444*, No. 138647.
(75) Jirofti, N.; Hashemi, M.; Moradi, A.; Kalalinia, F. Fabrication and characterization of 3D printing biocompatible crocin-loaded chitosan/collagen/hydroxyapatite-based scaffolds for bone tissue engineering applications. *Int. J. Biol. Macromol.* **2023**, *252*, No. 126279.
(76) Gong, M.; Zhang, L.; Wan, P. Polymer nanocomposite meshes for flexible electronic devices. *Prog. Polym. Sci.* **2020**, *107*, No. 101279.
(77) Park, J.; Hwang, J. C.; Kim, G. G.; Park, J.-U. Flexible electronics based on one-dimensional and two-dimensional hybrid nanomaterials. *InfoMat* **2020**, *2* (1), 33−56.
(78) Gruppuso, M.; Turco, G.; Marsich, E.; Porrelli, D. Polymeric wound dressings, an insight into polysaccharide-based electrospun membranes. *Appl. Mater. Today* **2021**, *24*, No. 101148.
(79) Raza, Z. A.; Munim, S.; Ayub, A. Recent developments in polysaccharide-based electrospun nanofibers for environmental applications. *Carbohydr. Res.* **2021**, *510*, No. 108443.
(80) Yan, S.; Qian, Y.; Haghayegh, M.; Xia, Y.; Yang, S.; Cao, R.; Zhu, M. Electrospun organic/inorganic hybrid nanofibers for accelerating wound healing: A review. *J. Mater. Chem. B* **2024**, *12*, 3171−3190.
(81) Chinnathambi, A.; Alharbi, S. A.; Meganathan, V.; Renuka, J.; Palaniappan, S. Fabrication of drugs loaded UiO-66 nanoparticles loaded core-shell nanofibers: investigation of antiproliferative activity and apoptosis induction in lung cancer cells. *Mater. Technol.* **2024**, *39* (1), No. 2304437.
(82) Sensini, A.; Stamati, O.; Marchiori, G.; Sancisi, N.; Gotti, C.; Giavaresi, G.; Cristofolini, L.; Focarete, M. L.; Zucchelli, A.; Tozzi, G. Full-field strain distribution in hierarchical electrospun nanofibrous poly-L(lactic) acid/collagen scaffolds for tendon and ligament regeneration: A multiscale study. *Heliyon* **2024**, *10* (5), No. e26796.
(83) Madruga, L. Y. C.; Kipper, M. J. Expanding the repertoire of electrospinning: New and emerging biopolymers, techniques, and applications. *Adv. Healthc. Mater.* **2022**, *11* (4), No. 27.
(84) Kailasa, S.; Reddy, M. S. B.; Maurya, M. R.; Rani, B. G.; Rao, K. V.; Sadasivuni, K. K. Electrospun nanofibers: Materials, synthesis parameters, and their role in sensing applications. *Macromol. Mater. Eng.* **2021**, *306* (11), No. 2100410.
(85) Zheng, Q. L.; Xi, Y. W.; Weng, Y. X. Functional electrospun nanofibers: fabrication, properties, and applications in wound-healing process. *RSC Adv.* **2024**, *14* (5), 3359−3378.
(86) Doostmohammadi, M.; Niknezhad, S. V.; Forootanfar, H.; Ghasemi, Y.; Jafari, E.; Adeli-Sardou, M.; Amirsadeghi, A.; Ameri, A. Development of Ag NPs/allantoin loaded PCL/GEL electrospun nanofibers for topical wound treatment. *J. Biomater. Appl.* **2023**, *38* (5), 692−706.
(87) Kopanska, A.; Brzezinski, M.; Draczynski, Z. Combination of polylactide with cellulose for biomedical applications: a recent overview. *Cellulose* **2024**, *31* (1), 101−145.
(88) Shen, R. J.; Guo, Y. L.; Wang, S. J.; Tuerxun, A.; He, J. Q.; Bian, Y. Biodegradable electrospun nanofiber membranes as promising candidates for the development of face masks. *Int. J. Environ. Res. Public Health* **2023**, *20* (2), No. 1306.
(89) Salunke, M.; Viswalingam, V.; Shinde, V. Electrospun nanofibers of carbohydrate polymers for neoteric wound dressing: a review. *Int. J. Polym. Mater. Polym. Biomater.* **2024**, No. 1.
(90) Loccufier, E.; Verschraegen, S.; Swanckaert, B.; D'Hooge, D. R.; De Buysser, K.; De Clerck, K. A broad spectrum of electrospun organosilica membrane properties by tuning the chemical nature of the precursor building block. *Mater. Today Chem.* **2024**, *36*, No. 101950.
(91) Ardestani, S. A.; Ghanbarzadeh, B.; Moini, S. The improvement of the sodium caseinate based electrospun nanofiber by modifying solvent system: Study of microstructure and physical properties. *Food Hydrocoll.* **2023**, *137*, No. 108387.
(92) Wen, X.; Xiong, J.; Lei, S.; Wang, L.; Qin, X. Diameter refinement of electrospun nanofibers: From mechanism, strategies to applications. *Adv. Fiber Mater.* **2022**, *4* (2), 145−161.
(93) Abdulhussain, R.; Adebisi, A.; Conway, B. R.; Asare-Addo, K. Electrospun nanofibers: Exploring process parameters, polymer selection, and recent applications in pharmaceuticals and drug delivery. *J. Drug Delivery Sci. Tec.* **2023**, *90*, No. 105156.
(94) Sari, B.; Kaynak, C. Parameters influencing electrospun nanofiber diameter of polylactide incorporated with cellulose nanofibrils and nanocrystals. *J. Thermoplast. Compos. Mater.* **2024**, *37* (11), 3570−3590.
(95) Chinnappan, B. A.; Krishnaswamy, M.; Xu, H.; Hoque, M. E. Electrospinning of biomedical nanofibers/nanomembranes: Effects of process parameters. *Polymers* **2022**, *14* (18), No. 3719.
(96) Sivan, M.; Madheswaran, D.; Hauzerova, S.; Novotny, V.; Hedvicakova, V.; Jencova, V.; Kostakova, E. K.; Schindler, M.; Lukas, D. AC electrospinning: impact of high voltage and solvent on the electrospinnability and productivity of polycaprolactone electrospun nanofibrous scaffolds. *Mater. Today Chem.* **2022**, *26*, No. 101025.
(97) Orisawayi, A. O.; Koziol, K.; Hao, S.; Tiwari, S.; Rahatekar, S. S. Development of hybrid electrospun alginate-pulverized moringa composites. *RSC Adv.* **2024**, *14* (12), 8502−8512.
(98) Roldán, E.; Reeves, N. D.; Cooper, G.; Andrews, K. Can we achieve biomimetic electrospun scaffolds with gelatin alone? *Front. Bioeng. Biotechnol.* **2023**, *11*, No. 1160760.
(99) Lamarra, J.; Rivero, S.; Pinotti, A.; Lopez, D. Nanofiber mats functionalized with Mentha piperita essential oil stabilized in a chitosan-based emulsion designed via an electrospinning technique. *Int. J. Biol. Macromol.* **2023**, *248*, No. 125980.
(100) Gabrion, X.; Koolen, G.; Grégoire, M.; Musio, S.; Bar, M.; Botturi, D.; Rondi, G.; de Luycker, E.; Amaducci, S.; Ouagne, P.; et al. Influence of industrial processing parameters on the effective properties of long aligned European hemp fibres in composite materials. *Composites, Part A* **2022**, *157*, No. 106915.

https://doi.org/10.1021/acsnano.4c13106
ACS Nano 2024, 18, 31737−31772

(101) Schofield, R. M.; Maciejewska, B. M.; Dong, S.; Tebbutt, G. T.; McGurty, D.; Bonilla, R. S.; Assender, H. E.; Grobert, N. Driving fiber diameters to the limit: nanoparticle-induced diameter reductions in electrospun photoactive composite nanofibers for organic photovoltaics. *Adv. Compos. Hybrid Mater.* **2023**, *6* (6), No. 229.
(102) Prabhu, N. N.; Rajendra, B. V.; Anandhan, S.; Murthy, K.; Chandra, R. B. J.; George, G.; Kumar, B. S.; Shivamurthy, B. Understanding the interplay of solution and process parameters on the physico-chemical properties of ZnO nanofibers synthesized by sol-gel electrospinning. *Mater. Res. Express* **2023**, *10* (8), No. 085001.
(103) Mailley, D.; Hebraud, A.; Schlatter, G. A review on the impact of humidity during electrospinning: From the nanofiber structure engineering to the applications. *Macromol. Mater. Eng.* **2021**, *306* (7), No. 2100115.
(104) Szewczyk, P. K.; Stachewicz, U. The impact of relative humidity on electrospun polymer fibers: From structural changes to fiber morphology. *Adv. Colloid Interface Sci.* **2020**, *286*, No. 102315.
(105) Aslam, M.; Khan, T.; Basit, M.; Masood, R.; Raza, Z. Polyacrylonitrile-based electrospun nanofibers-A critical review. *Materialwiss. Werkstofftech.* **2022**, *53* (12), 1575−1591.
(106) Zhou, B.; Liu, Z.; Li, C.; Liu, M.; Jiang, L.; Zhou, Y.; Zhou, F.-L.; Chen, S.; Jerrams, S.; Yu, J. A Highly stretchable and sensitive strain sensor based on dopamine modified electrospun SEBS fibers and MWCNTs with carboxylation. *Adv. Electron. Mater.* **2021**, *7* (8), No. 2100233.
(107) Zhang, C.; Feng, F.; Zhang, H. Emulsion electrospinning: Fundamentals, food applications and prospects. *Trends Food Sci. Technol.* **2018**, *80*, 175−186.
(108) Ding, J.; Mei, L.; Guo, X.; Guo, D.; Ma, L.; Gui, Y.; Guo, D. PVA electrospun fibers coated with PPy nanoparticles for wearable strain sensors. *Macromol. Rapid Commun.* **2023**, *44* (12), No. 2300033.
(109) Ren, J.; Musyoka, N. M.; Annamalai, P.; Langmi, H. W.; North, B. C.; Mathe, M. Electrospun MOF nanofibers as hydrogen storage media. *Int. J. Hydrog. Energy* **2015**, *40* (30), 9382−9387.
(110) Yan, Z.; Hu, B.; Li, Q.; Zhang, S.; Pang, J.; Wu, C. Facile synthesis of covalent organic framework incorporated electrospun nanofiber and application to pipette tip solid phase extraction of sulfonamides in meat samples. *J. Chromatogr. A* **2019**, *1584*, 33−41.
(111) Ma, J.; Yu, Z.; Liu, S.; Chen, Y.; Lv, Y.; Liu, Y.; Lin, C.; Ye, X.; Shi, Y.; Liu, M.; et al. Efficient extraction of trace organochlorine pesticides from environmental samples by a polyacrylonitrile electrospun nanofiber membrane modified with covalent organic framework. *J. Hazard. Mater.* **2022**, *424*, No. 127455.
(112) Bechelany, M.; Drobek, M.; Vallicari, C.; Abou Chaaya, A.; Julbe, A.; Miele, P. Highly crystalline MOF-based materials grown on electrospun nanofibers. *Nanoscale* **2015**, *7* (13), 5794−5802.
(113) Ding, C.; Breunig, M.; Timm, J.; Marschall, R.; Senker, J.; Agarwal, S. Flexible, mechanically stable, porous self-standing microfiber network membranes of covalent organic frameworks: preparation method and characterization. *Adv. Funct. Mater.* **2021**, *31* (49), No. 2106507.
(114) Zheng, K.; Gu, F.; Wei, H.; Zhang, L.; Chen, X. a.; Jin, H.; Pan, S.; Chen, Y.; Wang, S. Flexible, permeable, and recyclable liquid-metal-based transient circuit enables contact/noncontact sensing for wearable human−machine interaction. *Small Methods* **2023**, *7* (4), No. 2201534.
(115) Han, D.; Steckl, A. J. Selective pH-responsive core−sheath nanofiber membranes for chem/bio/med applications: targeted delivery of functional molecules. *ACS Appl. Mater. Interfaces* **2017**, *9* (49), 42653−42660.
(116) Gallah, H.; Mighri, F.; Ajji, A.; Bandyopadhyay, J. Flexible PET/(PET-TiO_2) core/shell nanofibrous mats as potential photoanode layer for dye-sensitized solar cells, DSSCs. *Mater. Chem. Phys.* **2023**, *305*, No. 127911.
(117) Fan, S.-T.; Guo, D.-L.; Zhang, Y.-T.; Chen, T.; Li, B.-J.; Zhang, S. Washable and stable coaxial electrospinning fabric with superior electromagnetic interference shielding performance for multifunctional electronics. *Chem. Eng. J.* **2024**, *488*, No. 151051.
(118) Wang, L.; Zhang, C.; Cao, X.; Xu, X.; Bai, J.; Zhu, J.; Li, R.; Satoh, T. Construction of novel coaxial electrospun polyetherimide@polyaniline core-shell fibrous membranes as free-standing flexible electrodes for supercapacitors. *J. Power Sources* **2024**, *602*, No. 234305.
(119) Wang, M.; Li, D.; Li, J.; Li, S.; Chen, Z.; Yu, D.-G.; Liu, Z.; Guo, J. Z. Electrospun Janus zein−PVP nanofibers provide a two-stage controlled release of poorly water-soluble drugs. *Mater. Des.* **2020**, *196*, No. 109075.
(120) Ghosal, K.; Augustine, R.; Zaszczynska, A.; Barman, M.; Jain, A.; Hasan, A.; Kalarikkal, N.; Sajkiewicz, P.; Thomas, S. Novel drug delivery systems based on triaxial electrospinning based nanofibers. *React. Funct. Polym.* **2021**, *163*, No. 104895.
(121) Zhao, P.; Zhou, K.; Xia, Y.; Qian, C.; Yu, D.-G.; Xie, Y.; Liao, Y. Electrospun trilayer eccentric Janus nanofibers for a combined treatment of periodontitis. *Adv. Fiber Mater.* **2024**, *6*, 1053−1073.
(122) Wang, M.; Ge, R.-L.; Zhang, F.; Yu, D.-G.; Liu, Z.-P.; Li, X.; Shen, H.; Williams, G. R. Electrospun fibers with blank surface and inner drug gradient for improving sustained release. *Biomater. Adv.* **2023**, *150*, No. 213404.
(123) Zhang, Y.; Fu, J.; Ding, Y.; Babar, A. A.; Song, X.; Chen, F.; Yu, X.; Zheng, Z. Thermal and moisture managing E-textiles enabled by Janus hierarchical gradient honeycombs. *Adv. Mater.* **2024**, *36* (13), No. 2311633.
(124) Yagmurcukardes, N.; Yardimci, A. I.; Yagmurcukardes, M.; Capan, I.; Erdogan, M.; Capan, R.; Acikbas, Y. Electrospun polyacrylonitrile (PAN)/polypyrrole (PPy) nanofiber-coated quartz crystal microbalance for sensing volatile organic compounds. *J. Mater. Sci.: Mater. Electron.* **2023**, *34* (27), No. 1869.
(125) Lee, J. H.; Kim, J.; Liu, D.; Guo, F.; Shen, X.; Zheng, Q.; Jeon, S.; Kim, J. K. Highly aligned, anisotropic carbon nanofiber films for multidirectional strain sensors with exceptional selectivity. *Adv. Funct. Mater.* **2019**, *29* (29), No. 1901623.
(126) Singh, V.; Rana, S.; Bokolia, R.; Panwar, A. K.; Meena, R.; Singh, B. Electrospun PVDF-$MoSe_2$ nanofibers based hybrid triboelectric nanogenerator for self-powered water splitting system. *J. Alloys Compd.* **2024**, *978*, No. 173416.
(127) Hao, Y.; Yan, Q.; Liu, H.; He, X.; Zhang, P.; Qin, X.; Wang, R.; Sun, J.; Wang, L.; Cheng, Y. A stretchable, breathable, and self-adhesive electronic skin with multimodal sensing capabilities for human-centered healthcare. *Adv. Funct. Mater.* **2023**, *33* (44), No. 2303881.
(128) Cao, J.; Liang, F.; Li, H.; Li, X.; Fan, Y.; Hu, C.; Yu, J.; Xu, J.; Yin, Y.; Li, F.; Xu, D.; Feng, H.; Yang, H.; Liu, Y.; Chen, X.; Zhu, G.; Li, R.-W. Ultra-robust stretchable electrode for e-skin: In situ assembly using a nanofiber scaffold and liquid metal to mimic water-to-net interaction. *InfoMat* **2022**, *4* (4), No. e12302.
(129) Cui, X.; Chen, J.; Wu, W.; Liu, Y.; Li, H.; Xu, Z.; Zhu, Y. Flexible and breathable all-nanofiber iontronic pressure sensors with ultraviolet shielding and antibacterial performances for wearable electronics. *Nano Energy* **2022**, *95*, No. 107022.
(130) Xu, M.; Cai, H.; Liu, Z.; Chen, F.; Chen, L.; Chen, X.; Cheng, X.; Dai, F.; Li, Z. Breathable, degradable piezoresistive skin sensor based on a sandwich structure for high-performance pressure detection. *Adv. Electron. Mater.* **2021**, *7* (10), No. 2100368.
(131) Lee, S.; Franklin, S.; Hassani, F. A.; Yokota, T.; Nayeem, O. G.; Wang, Y.; Leib, R.; Cheng, G.; Franklin, D. W.; Someya, T. Nanomesh pressure sensor for monitoring finger manipulation without sensory interference. *Science* **2020**, *370* (6519), 966−970.
(132) Fan, L.; Yang, X.; Sun, H. Pressure sensors combining porous electrodes and electrospun nanofiber-based ionic membranes. *ACS Appl. Nano Mater.* **2023**, *6* (5), 3560−3571.
(133) Zhang, Y.; Li, Y.; Huang, Y.; Zuo, Z.; Musselman, K.; Duan, X.; Yu, H.; Xu, Z.; Tan, Z. A facile and strategic approach to superhydrophobic fibrous structure with biaxially aligned electrospun porous fibers. *Adv. Mater. Interfaces* **2023**, *10* (34), No. 2300507.
(134) Rana, S. S.; Rahman, M. T.; Salauddin, M.; Sharma, S.; Maharjan, P.; Bhatta, T.; Cho, H.; Park, C.; Park, J. Y. Electrospun PVDF-TrFE/MXene nanofiber mat-based triboelectric nanogenerator

https://doi.org/10.1021/acsnano.4c13106
ACS Nano 2024, 18, 31737−31772

for smart home appliances. *ACS Appl. Mater. Interfaces* **2021**, *13* (4), 4955−4967.
(135) Zhang, Z.; Yang, J.; Wang, H.; Wang, C.; Gu, Y.; Xu, Y.; Lee, S.; Yokota, T.; Haick, H.; Someya, T.; et al. A 10-micrometer-thick nanomesh-reinforced gas-permeable hydrogel skin sensor for long-term electrophysiological monitoring. *Sci. Adv.* **2024**, *10* (2), No. eadj5389.
(136) Zhang, M.; Wang, W. L.; Xia, G. T.; Wang, L. C.; Wang, K. Self-powered electronic skin for remote human-machine synchronization. *ACS Appl. Electron. Mater.* **2023**, *5* (1), 498−508.
(137) Zhi, C. W.; Shi, S.; Zhang, S.; Si, Y. F.; Yang, J. Q.; Meng, S.; Fei, B.; Hu, J. L. Bioinspired all-fibrous directional moisture-wicking electronic skins for biomechanical energy harvesting and all-range health sensing. *Nano-Micro Lett.* **2023**, *15* (1), No. s40820.
(138) Zhao, S.; Ran, W.; Wang, D.; Yin, R.; Yan, Y.; Jiang, K.; Lou, Z.; Shen, G. 3D dielectric layer enabled highly sensitive capacitive pressure sensors for wearable electronics. *ACS Appl. Mater. Interfaces* **2020**, *12* (28), 32023−32030.
(139) Bi, X.; Duan, Z.; Hou, X.; Qian, S.; Yuan, M.; Hu, J.; Zhang, J.; Lu, Y.; Liu, Y.; He, J.; Peng, Z.; Chou, X. Perpendicularly assembled oriented electrospinning nanofibers based piezoresistive pressure sensor with wide measurement range. *Nano Res.* **2024**, *17*, 6493−6501.
(140) Lai, Y.-C.; Ginnaram, S.; Lin, S.-P.; Hsu, F.-C.; Lu, T.-C.; Lu, M.-H. Breathable and stretchable multifunctional triboelectric liquid-metal E-Skin for recovering electromagnetic pollution, extracting biomechanical energy, and as whole-body epidermal self-powered sensors. *Adv. Funct. Mater.* **2024**, *34* (10), No. 2312443.
(141) Lou, M.; Abdalla, I.; Zhu, M.; Yu, J.; Li, Z.; Ding, B. Hierarchically rough structured and self-powered pressure sensor textile for motion sensing and pulse monitoring. *ACS Appl. Mater. Interfaces* **2020**, *12* (1), 1597−1605.
(142) Zheng, S. J.; Li, W. Z.; Ren, Y. Y.; Liu, Z. Y.; Zou, X. Y.; Hu, Y.; Guo, J. N.; Sun, Z.; Yan, F. Moisture-wicking, breathable, and intrinsically antibacterial electronic skin based on dual-gradient poly(ionic liquid) nanofiber membranes. *Adv. Mater.* **2022**, *34* (4), No. 2106570.
(143) Yang, G.; Tang, X.; Zhao, G.; Li, Y.; Ma, C.; Zhuang, X.; Yan, J. Highly sensitive, direction-aware, and transparent strain sensor based on oriented electrospun nanofibers for wearable electronic applications. *Chem. Eng. J.* **2022**, *435*, No. 135004.
(144) Ahmed, S.; Nauman, S.; Khan, Z. M. Electrospun nanofibrous yarn based piezoresistive flexible strain sensor for human motion detection and speech recognition. *J. Thermoplast. Compos. Mater.* **2023**, *36* (6), 2459−2481.
(145) Zhu, G.; Ren, P.; Hu, J.; Yang, J.; Jia, Y.; Chen, Z.; Ren, F.; Gao, J. Flexible and anisotropic strain sensors with the asymmetrical cross-conducting network for versatile bio-mechanical signal recognition. *ACS Appl. Mater. Interfaces* **2021**, *13* (37), 44925−44934.
(146) Ramesh, M.; Janani, R.; Deepa, C.; Rajeshkumar, L. Nanotechnology-enabled biosensors: A review of fundamentals, design principles, materials, and applications. *Biosensors* **2023**, *13* (1), No. 40.
(147) Song, J.; Lin, X.; Ee, L. Y.; Li, S. F. Y.; Huang, M. A review on electrospinning as versatile supports for diverse nanofibers and their applications in environmental sensing. *Adv. Fiber Mater.* **2023**, *5* (2), 429−460.
(148) Javaid, M.; Haleem, A.; Rab, S.; Singh, R. P.; Suman, R. Sensors for daily life: A review. *Sens. Int.* **2021**, *2*, No. 100121.
(149) Chen, X.; Li, H.; Xu, Z.; Lu, L.; Pan, Z.; Mao, Y. Electrospun nanofiber-based bioinspired artificial skins for healthcare monitoring and human-machine interaction. *Biomimetics* **2023**, *8* (2), 223.
(150) Yu, Y.; Feng, Y.; Liu, F.; Wang, H.; Yu, H.; Dai, K.; Zheng, G.; Feng, W. Carbon dots-based ultrastretchable and conductive hydrogels for high-performance tactile sensors and self-powered electronic skin. *Small* **2023**, *19* (31), No. 2204365.
(151) Khan, M.; Shah, L. A.; Ara, L.; Ullah, R.; Yoo, H.-M. Micelle−micelle cross-linked highly stretchable conductive hydrogels for potential applications of strain and electronic skin sensors. *Chem. Mater.* **2023**, *35* (14), 5582−5592.
(152) Gao, Q.; Agarwal, S.; Greiner, A.; Zhang, T. Electrospun fiber-based flexible electronics: Fiber fabrication, device platform, functionality integration and applications. *Prog. Polym. Sci.* **2023**, *137*, No. 101139.
(153) Yin, F.; Niu, H.; Kim, E.-S.; Shin, Y. K.; Li, Y.; Kim, N.-Y. Advanced polymer materials-based electronic skins for tactile and non-contact sensing applications. *InfoMat* **2023**, *5* (7), No. e12424.
(154) Feng, Z. B.; Zhao, Z. Q.; Liu, Y. A.; Liu, Y. K.; Cao, X. Y.; Yu, D. G.; Wang, K. Piezoelectric effect polyvinylidene fluoride (PVDF): from energy harvester to smart skin and electronic textiles. *Adv. Mater. Technol.* **2023**, *8* (14), No. 2300021.
(155) Qiu, X. L.; Bian, Y. Q.; Mei, X. D.; Luo, X. S.; Hu, Z.; Xuan, F. Z.; Xiang, Y. X.; Zhu, G. D. Fully transparent flexible piezoelectric sensing materials based on electrospun pvdf and their device applications. *Adv. Mater. Technol.* **2024**, *9* (5), No. 2301494.
(156) Marchiori, B.; Regal, S.; Arango, Y.; Delattre, R.; Blayac, S.; Ramuz, M. PVDF-TrFE-based stretchable contact and non-contact temperature sensor for E-skin application. *Sensors* **2020**, *20*, 623.
(157) Mahanty, B.; Maity, K.; Sarkar, S.; Mandal, D. Human skin interactive self-powered piezoelectric e-skin based on PVDF/MWCNT electrospun nanofibers for non-invasive health care monitoring. *Mater. Today Proc.* **2020**, *21*, 1964.
(158) Wang, Y.; Yokota, T.; Someya, T. Electrospun nanofiber-based soft electronics. *NPG Asia Mater.* **2021**, *13* (1), No. 22.
(159) Chen, X.; Wang, J.; Zhang, J.; Lin, H.; Tian, M.; Li, M.; Tian, Y. Development and application of electrospun fiber-based multi-functional sensors. *Chem. Eng. J.* **2024**, *486*, No. 150204.
(160) Bilaloglu, S.; Lu, Y.; Geller, D.; Rizzo, J. R.; Aluru, V.; Gardner, E. P.; Raghavan, P. Effect of blocking tactile information from the fingertips on adaptation and execution of grip forces to friction at the grasping surface. *J. Neurophysiol.* **2016**, *115* (3), 1122−1131.
(161) Lu, Y.; Biswas, M. C.; Guo, Z.; Jeon, J. W.; Wujcik, E. K. Recent developments in bio-monitoring via advanced polymer nanocomposite-based wearable strain sensors. *Biosens. Bioelectron.* **2019**, *123*, 167−177.
(162) Yan, T.; Wu, Y.; Yi, W.; Pan, Z. Recent progress on fabrication of carbon nanotube-based flexible conductive networks for resistive-type strain sensors. *Sens. Actuators A-Phys.* **2021**, *327*, No. 112755.
(163) Li, X.; Hu, H.; Hua, T.; Xu, B.; Jiang, S. Wearable strain sensing textile based on one-dimensional stretchable and weavable yarn sensors. *Nano Res.* **2018**, *11* (11), 5799−5811.
(164) Tang, J.; Wu, Y.; Ma, S.; Yan, T.; Pan, Z. Flexible strain sensor based on CNT/TPU composite nanofiber yarn for smart sports bandage. *Compos. B: Eng.* **2022**, *232*, No. 109605.
(165) Wang, X.; Gao, Q.; Schubert, D. W.; Liu, X. Review on electrospun conductive polymer composites strain sensors. *Adv. Mater. Technol.* **2023**, *8* (16), No. 2300293.
(166) Lee, J. H.; Kim, S. H.; Heo, J. S.; Kwak, J. Y.; Park, C. W.; Kim, I.; Lee, M.; Park, H.-H.; Kim, Y.-H.; Lee, S. J.; Park, S. K. Heterogeneous structure omnidirectional strain sensor arrays with cognitively learned neural networks. *Adv. Mater.* **2023**, *35* (13), No. 2208184.
(167) Ha, S.-H.; Ha, S.-H.; Jeon, M.-B.; Cho, J. H.; Kim, J.-M. Highly sensitive and selective multidimensional resistive strain sensors based on a stiffness-variant stretchable substrate. *Nanoscale* **2018**, *10* (11), 5105−5113.
(168) Zheng, Z.; Wang, X.; Hang, G.; Duan, J.; Zhang, J.; Zhang, W.; Liu, Z. Recent progress on flexible poly(vinylidene fluoride)-based piezoelectric nanogenerators for energy harvesting and self-powered electronic applications. *Renewable Sustainable Energy Rev.* **2024**, *193*, 114285−114285.
(169) Yu, Y. R.; Zhao, X. W.; Ge, H. G.; Ye, L. A self-powered piezoelectric poly(vinyl alcohol)/polyvinylidene fluoride fiber membrane with alternating multilayer porous structure for energy harvesting and wearable sensors. *Compos. Sci. Technol.* **2024**, *247*, No. 110429.

https://doi.org/10.1021/acsnano.4c13106
ACS Nano 2024, 18, 31737−31772

(170) Zhang, Z.; Liao, M.; Lou, H.; Hu, Y.; Sun, X.; Peng, H. Conjugated polymers for flexible energy harvesting and storage. *Adv. Mater.* **2018**, *30* (13), No. 1704261.
(171) Thakur, A.; Devi, P. Paper-based flexible devices for energy harvesting, conversion and storage applications: A review. *Nano Energy* **2022**, *94*, No. 106927.
(172) Pan, J.; Jin, A. L. Improvement of output performance of the TENG based on PVDF by doping tourmaline. *ACS Sustainable Chem. Eng.* **2024**, *12* (5), 2092−2099.
(173) Wang, Z. L.; Song, J. Piezoelectric nanogenerators based on zinc oxide nanowire arrays. *Science* **2006**, *312* (5771), 242−246.
(174) Sukumaran, S.; Szewczyk, P. K.; Knapczyk-Korczak, J.; Stachewicz, U. Optimizing piezoelectric coefficient in PVDF fibers: Key strategies for energy harvesting and smart textiles. *Adv. Electron. Mater.* **2023**, *9* (12), No. 2300404.
(175) Zhu, Q.; Song, X.; Chen, X.; Li, D.; Tang, X.; Chen, J.; Yuan, Q. A high performance nanocellulose-PVDF based piezoelectric nanogenerator based on the highly active CNF@ZnO via electrospinning technology. *Nano Energy* **2024**, *127*, No. 109741.
(176) Fan, F.-R.; Lin, L.; Zhu, G.; Wu, W.; Zhang, R.; Wang, Z. L. Transparent triboelectric nanogenerators and self-powered pressure sensors based on micropatterned plastic films. *Nano Lett.* **2012**, *12* (6), 3109−3114.
(177) Lee, C.; Cho, C.; Oh, J. H. Highly flexible triboelectric nanogenerators with electrospun PVDF-TrFE nanofibers on MWCNTs/PDMS/AgNWs composite electrodes. *Compos. B: Eng.* **2023**, *255*, No. 110622.
(178) Khandelwal, G.; Min, G.; Karagiorgis, X.; Dahiya, R. Aligned PLLA electrospun fibres based biodegradable triboelectric nanogenerator. *Nano Energy* **2023**, *110*, No. 108325.
(179) Ke, H.; Gao, M.; Li, S.; Qi, Q.; Zhao, W.; Li, X.; Li, S.; Kuvondikov, V.; Lv, P.; Wei, Q.; Ye, L. Advances and future prospects of wearable textile- and fiber-based solar cells. *Sol. RRL* **2023**, *7* (15), No. 2300109.
(180) Heng, W.; Weihua, L.; Bachagha, K. Recent progress in flexible electrodes and textile shaped devices for organic solar cells. *J. Mater. Chem. A* **2023**, *11* (3), 1039−1060.
(181) Shanmugasundaram, E.; Govindasamy, C.; Khan, M. I.; Ganesan, V.; Narayanan, V.; Vellaisamy, K.; Rajamohan, R.; Thambusamy, S. Electrospun and electropolymerized carbon nanofiber−polyaniline−Cu material as a hole transport material for organic solar cells. *Carbon Lett.* **2023**, *33* (7), 2223−2235.
(182) Zhuo, S.; Jiang, W.; Dong Zhao, Y.; Liu, J.-Z.; Zhao, X.; Ye, J.; Zheng, M.; Wang, Z.-S.; Zhou, X.-Q.; Wang, X.-Q.; Shi, Y.-L.; Chen, W.; Zhang, K.-Q.; Liao, L.-S.; Zhuo, M.-P. Large-area nanofiber membrane of NIR photothermal $Cs_{0.32}WO_3$ for flexible and all-weather solar thermoelectric generation. *Chem. Eng. J.* **2024**, *479*, No. 147571.
(183) Li, X.; Chen, W.; Qian, Q.; Huang, H.; Chen, Y.; Wang, Z.; Chen, Q.; Yang, J.; Li, J.; Mai, Y. W. Electrospinning-based strategies for battery materials. *Adv. Energy Mater.* **2021**, *11* (2), No. 2000845.
(184) Wilhelm, M.; Adam, R.; Bhardwaj, A.; Neumann, I.; Cho, S. H.; Yamada, Y.; Sekino, T.; Tao, J.; Hong, Z.; Fischer, T.; Mathur, S. Carbon-coated electrospun V_2O_5 nanofibers as photoresponsive cathode for lithium-ion batteries. *Adv. Eng. Mater.* **2023**, *25* (1), No. 2200765.
(185) Tang, L.; Wu, Y.; He, D.; Lei, Z.; Liu, N.; He, Y.; De Guzman, M. R.; Chen, J. Electrospun PAN membranes toughened and strengthened by TPU/SHNT for high-performance lithium-ion batteries. *J. Electroanal. Chem.* **2023**, *931*, No. 117181.
(186) Zeng, Z.; Shao, Z.; Shen, R.; Li, H.; Jiang, J.; Wang, X.; Li, W.; Guo, S.; Liu, Y.; Zheng, G. Coaxial electrospun Tai Chi-inspired lithium-ion battery separator with high performance and fireproofing capacity. *ACS Appl. Mater. Interfaces* **2023**, *15* (37), 44259−44267.
(187) Xue, J.; Wu, T.; Dai, Y.; Xia, Y. Electrospinning and electrospun nanofibers: Methods, materials, and applications. *Chem. Rev.* **2019**, *119* (8), 5298−5415.
(188) Li, J.; Zhang, X.; Lu, Y.; Linghu, K.; Wang, C.; Ma, Z.; He, X. Electrospun fluorinated polyimide/polyvinylidene fluoride composite membranes with high thermal stability for lithium ion battery separator. *Adv. Fiber Mater.* **2022**, *4* (1), 108−118.
(189) Shi, H.; Fu, Z.; Xu, W.; Xu, N.; He, X.; Li, Q.; Sun, J.; Jiang, R.; Lei, Z.; Liu, Z.-H. Dual-modified electrospun fiber membrane as separator with excellent safety performance and high operating temperature for lithium-ion batteries. *Small* **2024**, *20* (19), No. 2309896.
(190) Gao, M.; Li, H.; Xu, L.; Xue, Q.; Wang, X.; Bai, Y.; Wu, C. Lithium metal batteries for high energy density: Fundamental electrochemistry and challenges. *J. Energy Chem.* **2021**, *59*, 666−687.
(191) Cui, Z.; Shen, S.; Yu, J.; Si, J.; Cai, D.; Wang, Q. Electrospun carbon nanofibers functionalized with $NiCo_2S_4$ nanoparticles as lightweight, flexible and binder-free cathode for aqueous Ni-Zn batteries. *Chem. Eng. J.* **2021**, *426*, No. 130068.
(192) Ren, W.; Wang, Y.; Hu, X.; Cao, Z.; Xu, Y.; Zhou, Y.; Cao, X.; Liang, S. Electrospun $Na_3MnTi(PO_4)_3$/C film: A multielectron-reaction and free-standing cathode for sodium-ion batteries. *Chem. Eng. J.* **2024**, *487*, No. 150492.
(193) Mun, W. J.; Kim, B.; Moon, S. J.; Kim, J. H. Hydrogen-bonded organic framework-derived, flower-on-fiber-like, carbon nanofiber electrodes for supercapacitors. *J. Mater. Chem. A* **2024**, *12* (11), 6712−6723.
(194) Khademolqorani, S.; Banitaba, S. N.; Gupta, A.; Poursharifi, N.; Ghaffari, A. A.; Jadhav, V. V.; Arifeen, W. U.; Singh, M.; Borah, M.; Chamanehpour, E.; Mishra, Y. K. Application scopes of miniaturized MXene-functionalized electrospun nanofibers-based electrochemical energy devices. *Small* **2024**, *20*, No. 2309572.
(195) Lee, D.; Jung, J.; Lee, G. H.; Li, M. X.; Lee, W. I.; Um, M. K.; Choi, S. W. Structural energy storage system using electrospun carbon nanofibers with carbon nanotubes. *Polym. Compos.* **2024**, *45* (3), 2127−2139.
(196) Üstün, B.; Aydin, H.; Koç, S. N.; Uluslu, A.; Kurtan, Ü. Electrospun polyethylenimine (PEI)-derived nitrogen enriched carbon nanofiber for supercapacitors with artificial neural network modeling. *J. Energy Storage* **2023**, *73*, No. 108970.
(197) Wei, D.; Wang, J.; Yin, J.; Xu, L. High-performance lithium-ion supercapacitors based on electrodes with nanostructures derived from zeolite imidazole frameworks in electrospun nanofibers. *J. Alloys Compd.* **2023**, *969*, No. 172364.
(198) Nie, G.; Zhao, X.; Jiang, J.; Luan, Y.; Shi, J.; Liu, J.; Kou, Z.; Wang, J.; Long, Y.-Z. Flexible supercapacitor of high areal performance with vanadium/cobalt oxides on carbon nanofibers as a binder-free membrane electrode. *Chem. Eng. J.* **2020**, *402*, No. 126294.
(199) Abdel-Salam, A. I.; Attia, S. Y.; Mohamed, S. G.; El-Hosiny, F. I.; Sadek, M. A.; Rashad, M. M. Designing a hierarchical structure of nickel-cobalt-sulfide decorated on electrospun N-doped carbon nanofiber as an efficient electrode material for hybrid supercapacitors. *Int. J. Hydrogen Energy* **2023**, *48* (14), 5463−5477.
(200) Lu, C.; Chen, X. Electrospun polyaniline nanofiber networks toward high-performance flexible supercapacitors. *Adv. Mater. Technol.* **2019**, *4* (11), No. 1900564.
(201) Martínez-Pérez, R. V.; Manríquez, J.; Aldeco-Pérez, E.; Baldenegro-Pérez, L. A.; España-Sánchez, B. L.; Avila-Niño, J. Development of an all-electrospun high-performance textile supercapacitor for wearable device applications. *J. Appl. Polym. Sci.* **2023**, *140* (44), No. e54612.
(202) Pathak, I.; Acharya, D.; Chhetri, K.; Lohani, P. C.; Subedi, S.; Muthurasu, A.; Kim, T.; Ko, T. H.; Dahal, B.; Kim, H. Y. $Ti_3C_2T_x$ MXene embedded metal-organic framework-based porous electrospun carbon nanofibers as a freestanding electrode for supercapacitors. *J. Mater. Chem. A* **2023**, *11* (10), 5001−5014.
(203) Mu, H.; Zhang, Z.; Wang, W.; Lian, C.; Wang, G.; Liu, H. Integrated construction of stretchable supercapacitor with outstanding deformation stability and flame retardancy. *Nano Energy* **2024**, *126*, No. 109635.
(204) Cárdenas-Martínez, J.; España-Sánchez, B. L.; Esparza, R.; Ávila-Niño, J. A. Flexible and transparent supercapacitors using

https://doi.org/10.1021/acsnano.4c13106
ACS Nano 2024, 18, 31737−31772

electrospun PEDOT: PSS electrodes. *Synth. Met.* **2020**, *267*, No. 116436.
(205) Veeramuthu, L.; Cho, C.-J.; Liang, F.-C.; Venkatesan, M.; Kumar G, R.; Hsu, H.-Y.; Chung, R.-J.; Lee, C.-H.; Lee, W.-Y.; Kuo, C.-C. Human skin-inspired electrospun patterned robust strain-insensitive pressure sensors and wearable flexible light-emitting diodes. *ACS Appl. Mater. Interfaces* **2022**, *14* (26), 30160−30173.
(206) An, J. E.; Kim, K. H.; Park, S. J.; Seo, S. E.; Kim, J.; Ha, S.; Bae, J.; Kwon, O. S. Wearable cortisol aptasensor for simple and rapid real-time monitoring. *ACS Sens.* **2022**, 7 (1), 99−108.
(207) Liu, Z. J.; Tian, B.; Liu, X.; Zhang, X. F.; Li, Y.; Zhang, Z. K.; Liu, J. J.; Lin, Q. J.; Jiang, Z. D. Multifunctional nanofiber mat for high temperature flexible sensors based on electrospinning. *J. Alloys Compd.* **2023**, *941*, No. 168959.
(208) Kwon, S.; Hwang, Y. H.; Nam, M.; Chae, H.; Lee, H. S.; Jeon, Y.; Lee, S.; Kim, C. Y.; Choi, S.; Jeong, E. G.; Choi, K. C. Recent progress of fiber shaped lighting devices for smart display applications—a fibertronic perspective. *Adv. Mater.* **2020**, *32* (5), No. 1903488.
(209) Haque, M. A.; Haque, M. A.; Kondawar, S. B. Facile fabrication of novel europium doped strontium yttrate (SrY_2O_4:Eu^{3+}) electrospun nanofibers for flexible display applications. *Mater. Today Commun.* **2022**, *33*, No. 104950.
(210) Hong, G.; Gan, X.; Leonhardt, C.; Zhang, Z.; Seibert, J.; Busch, J. M.; Bräse, S. A brief history of OLEDs—emitter development and industry milestones. *Adv. Mater.* **2021**, *33* (9), No. 2005630.
(211) Liu, W.; Zhang, C.; Alessandri, R.; Diroll, B. T.; Li, Y.; Liang, H.; Fan, X.; Wang, K.; Cho, H.; Liu, Y.; Dai, Y.; Su, Q.; Li, N.; Li, S.; Wai, S.; Li, Q.; Shao, S.; Wang, L.; Xu, J.; Zhang, X.; Talapin, D. V.; de Pablo, J. J.; Wang, S. High-efficiency stretchable light-emitting polymers from thermally activated delayed fluorescence. *Nat. Mater.* **2023**, *22* (6), 737−745.
(212) Chen, X.; Lin, X.; Zhou, L.; Sun, X.; Li, R.; Chen, M.; Yang, Y.; Hou, W.; Wu, L.; Cao, W.; Zhang, X.; Yan, X.; Chen, S. Blue light-emitting diodes based on colloidal quantum dots with reduced surface-bulk coupling. *Nat. Commun.* **2023**, *14* (1), 284.
(213) Xue, W.; Xu, M.; Yu, M.-N.; Sun, H.-M.; Lin, J.-Y.; Jiang, R.-C.; Xie, L.-H.; Shi, N.-E.; Huang, W. Electrospun supramolecular hybrid microfibers from conjugated polymers: Color transformation and conductivity evolution. *Chin. J. Polym. Sci.* **2021**, *39* (7), 824−830.
(214) Dayananda, B. S.; Sarojini, B. K.; Wong, Q. A.; Quah, C. K.; Srijana, P. J. J-aggregation-induced photoluminescence in electrospun pullulan/ 2-(2-fluorophenyl)-3-hydroxy-4H-chromen-4-one composite mat for photonic applications. *Opt. Mater.* **2023**, *143*, No. 114303.
(215) Choi, J.; Park, C. H.; Kwack, J. H.; Lee, D. J.; Kim, J. G.; Choi, J.; Bae, B. H.; Park, S. J.; Kim, E.; Park, Y. W.; Ju, B.-K. Ag fiber/IZO composite electrodes: Improved chemical and thermal stability and uniform light emission in flexible organic light-emitting diodes. *Sci. Rep.* **2019**, *9* (1), 738.
(216) He, B.; He, G.; Fu, C.; Jiang, S.; Fortunato, E.; Martins, R.; Wang, S. Electrospun coaxial nanowire-based FETs with annular heterogeneous interface gain for intelligent functional electronics. *Adv. Funct. Mater.* **2024**, *34* (25), No. 2316375.
(217) Li, L.-K.; Li, J.; Wen, S.-K.; Lei, Y.-X.; Zhu, W.-Q.; Zhang, J.-H. Aligned indium oxide nanofiber to achieve high mobility and high stability field-effect transistor. *IEEE Trans. Electron Devices* **2023**, *70* (5), 2606−2611.
(218) Park, K. W.; Cho, W. J. High-performance IGZO nanowire-based field-effect transistors with random-network channels by electrospun PVP nanofiber template transfer. *Polymers* **2022**, *14* (3), No. 651.
(219) Fan, L.; Yang, X.; Sun, H. A novel flexible sensor for double-parameter decoupling measurement of temperature and pressure with high sensitivity and wide range. *J. Mater. Chem. C* **2023**, *11* (30), 10163−10177.
(220) Cai, J.; Du, M.; Li, Z. Flexible temperature sensors constructed with fiber materials. *Adv. Mater. Technol.* **2022**, 7 (7), No. 2101182.
(221) Li, J.; Su, J.; Weng, M.; Xu, W.; Huang, J.; Fan, T.; Liu, Y.; Min, Y. Applications of flexible polyimide: barrier material, sensor material, and functional material. *Soft Sci.* **2023**, *3*, No. 2.
(222) Lim, S.; Suk, J. W. Flexible temperature sensors based on two-dimensional materials for wearable devices. *J. Phys. D: Appl. Phys.* **2023**, *56* (6), No. 063001.
(223) Lee, J.-H.; Chen, H.; Kim, E.; Zhang, H.; Wu, K.; Zhang, H.; Shen, X.; Zheng, Q.; Yang, J.; Jeon, S.; Kim, J.-K. Flexible temperature sensors made of aligned electrospun carbon nanofiber films with outstanding sensitivity and selectivity towards temperature. *Mater. Horiz.* **2021**, *8* (5), 1488−1498.
(224) Wei, C.; Zhou, H.; Wang, Z.; Zheng, B.; Zheng, H.; Jin, X.; Ma, A.; Chen, W.; Liu, H. Transient flexible multimodal sensors based on degradable fibrous nanocomposite mats for monitoring strain, temperature, and humidity. *ACS Appl. Polym. Mater.* **2024**, *6* (7), 4014−4024.
(225) Luo, Y.; Zhao, L.; Luo, G.; Dong, L.; Xia, Y.; Li, M.; Li, Z.; Wang, K.; Maeda, R.; Jiang, Z. Highly sensitive piezoresistive and thermally responsive fibrous networks from the in situ growth of PEDOT on MWCNT-decorated electrospun PU fibers for pressure and temperature sensing. *Microsyst. Nanoeng.* **2023**, *9* (1), 113.
(226) Li, W.-D.; Ke, K.; Jia, J.; Pu, J.-H.; Zhao, X.; Bao, R.-Y.; Liu, Z.-Y.; Bai, L.; Zhang, K.; Yang, M.-B.; Yang, W. Recent advances in multiresponsive flexible sensors towards E-skin: a delicate design for versatile sensing. *Small* **2022**, *18*, No. 2103734.
(227) Jung, M.-H.; Kwak, M.; Ahn, J.; Song, J.-Y.; Kang, H.; Jung, H.-T. Highly sensitive and selective acetylene CuO/ZnO heterostructure sensors through electrospinning at lean O_2 concentration for transformer diagnosis. *ACS Sens.* **2024**, *9* (1), 217−227.
(228) Al-Qahtani, S. D.; Al-Senani, G. M. Development of toxic gas sensor from anthocyanin-embedded polycaprolactone-co-polylactic acid nanofibrous mat. *Int. J. Biol. Macromol.* **2024**, *267*, No. 131649.
(229) Srivastava, S.; Pandey, N. K.; Verma, V.; Singh, P.; Verma, A.; Yadav, N. Fabrication of highly sensitive yceo chemo-resistive gas sensor for selective detection of CO_2. *ECS Sens. Plus* **2024**, *3* (1), No. 014401.
(230) Xin, Q.; Gao, H.; An, K.; Ding, X.; Zhang, Y.; Zhao, K. High-performance electrospun polystyrene-based nanofiber membrane for efficient SO_2 capture. *Sep. Purif. Technol.* **2024**, *330*, No. 125411.
(231) Zhang, L.; Tian, J.; Wang, Y.; Wang, T.; Wei, M.; Li, F.; Li, D.; Yang, Y.; Yu, H.; Dong, X. Polyoxometalates electron acceptor-intercalated In_2O_3@SnO_2 nanofibers for chemiresistive ethanol gas sensors. *Sens. Actuators B-Chem.* **2024**, *410*, No. 135728.
(232) Yang, B.; Thi Hanh To, D.; Sobolak, D.; Mendoza, E. R.; Myung, N. V. High performance methyl salicylate gas sensor based on noble metal (Au, Pt) decorated WO_3 nanofibers. *Sens. Actuators B-Chem.* **2024**, *413*, No. 135741.
(233) Khomarloo, N.; Mohsenzadeh, E.; Gidik, H.; Bagherzadeh, R.; Latifi, M. Overall perspective of electrospun semiconductor metal oxides as high-performance gas sensor materials for NO_x detection. *RSC Adv.* **2024**, *14* (11), 7806−7824.
(234) Sun, N.; Tian, Q.; Bian, W.; Wang, X.; Dou, H.; Li, C.; Zhang, Y.; Gong, C.; You, X.; Du, X.; Yin, P.; Zhao, X.; Yang, Y.; Liu, X.; Jing, Q.; Liu, B. Highly sensitive and lower detection-limit NO_2 gas sensor based on Rh-doped ZnO nanofibers prepared by electrospinning. *Appl. Surf. Sci.* **2023**, *614*, No. 156213.
(235) Ruksana, S.; Kumar, A.; Lakshmy, S.; Kishore, K. R.; Sharma, C. S.; Kumar, M.; Chakraborty, B. Highly efficient CuO-anchored SnO_2 nanofiber for low-concentration H_2S gas sensors. *ACS Appl. Eng. Mater.* **2024**, *2* (2), 431−442.
(236) Dong, H.; Li, X.; Liu, Y.; Cheng, W.; Li, X.; Lu, D.; Shao, C.; Liu, Y. Ultra-flexible, breathable, and robust PAN/MWCNTs/PANI nanofiber networks for high-performance wearable gas sensor application. *ACS Sens.* **2024**, *9* (6), 3085−3095.
(237) Huo, Y.; Zhang, D.; Yang, Y.; Pan, Z.; Yu, H.; Wang, T.; Dong, X. Design and synthesis of parallel bicomponent heterojunction

https://doi.org/10.1021/acsnano.4c13106
ACS Nano 2024, 18, 31737−31772

nanofibers as flexible room-temperature sensors for Ppb-level NO_2 detection. *ACS Appl. Nano Mater.* **2024**, *7* (5), 4989−4997.
(238) Lang, K.; Liu, T.; Padilla, D. J.; Nelson, M.; Landorf, C. W.; Patel, R. J.; Ballentine, M. L.; Kennedy, A. J.; Shih, W.-S.; Scotch, A.; Zhu, J. Nanofibers enabled advanced gas sensors: A review. *Adv. Sens. Energy Mater.* **2024**, *3* (2), No. 100093.
(239) Fan, S. X.; Tang, W. Synthesis, characterization and mechanism of electrospun carbon nanofibers decorated with ZnO nanoparticles for flexible ammonia gas sensors at room temperature. *Sens. Actuators B: Chem.* **2022**, *362*, No. 131789.
(240) Zhang, X.; Hao, X.; Zhai, Z.; Wang, J.; Li, H.; Sun, Y.; Qin, Y.; Niu, B.; Li, C. Flexible H_2S sensors: Fabricated by growing NO_2-UiO-66 on electrospun nanofibers for detecting ultralow concentration H_2S. *Appl. Surf. Sci.* **2022**, *573*, No. 151446.
(241) Zhai, Z.; Zhang, X.; Wang, J.; Li, H.; Sun, Y.; Hao, X.; Qin, Y.; Niu, B.; Li, C. Washable and flexible gas sensor based on UiO-66-NH_2 nanofibers membrane for highly detecting SO_2. *Chem. Eng. J.* **2022**, *428*, No. 131720.
(242) Maeng, B.; Kim, S.; An, H.; Jung, D. A tough and stretchable colorimetric sensor based on a curcumin-loaded polyurethane electrospun fiber mat for hazardous ammonia gas detection. *Sens. Actuators B. Chem.* **2023**, *394*, No. 134420.
(243) Wang, J.; Zhang, D.; Gao, Y.; Chen, F.; Wang, T.; Xia, H.; Sui, X.; Wang, Z. Fast-response hydrogen sulfide gas sensor based on electrospinning Co_3O_4 nanofibers-modified CuO nanoflowers: Experimental and DFT calculation. *Sens. Actuator B-Chem.* **2023**, *396*, No. 134579.
(244) Zhang, J.-H.; Sun, X.; Wang, H.; Li, J.; Guo, X.; Li, S.; Wang, Y.; Cheng, W.; Qiu, H.; Shi, Y.; et al. From 1D to 2D to 3D: Electrospun microstructures towards wearable sensing. *Chemosensors* **2023**, *11* (5), No. 295.
(245) Chen, J.; Rong, F.; Xie, Y. Fabrication, microstructures and sensor applications of highly ordered electrospun nanofibers: A review. *Materials* **2023**, *16* (9), No. 3310.
(246) Jeon, J.; Park, J.-W. Stretchable electrodes for interconnects in soft electronics. *Nano Lett.* **2024**, *24*, No. 9553.
(247) Zhou, W.; Yao, S.; Wang, H.; Du, Q.; Ma, Y.; Zhu, Y. Gas-permeable, ultrathin, stretchable epidermal electronics with porous electrodes. *ACS Nano* **2020**, *14* (5), 5798−5805.
(248) Horne, J.; McLoughlin, L.; Bridgers, B.; Wujcik, E. K. Recent developments in nanofiber-based sensors for disease detection, immunosensing, and monitoring. *Sens. Actuators Rep.* **2020**, *2* (1), No. 100005.
(249) García Núñez, C.; Manjakkal, L.; Dahiya, R. Energy autonomous electronic skin. *npj Flex. Electron.* **2019**, *3* (1), No. 1.
(250) Lei, P.; Bao, Y.; Zhang, W.; Gao, L.; Zhu, X.; Xu, J.; Ma, J. Synergy of ZnO nanowire arrays and electrospun membrane gradient wrinkles in piezoresistive materials for wide-sensing range and high-sensitivity flexible pressure sensor. *Adv. Fiber Mater.* **2024**, *6* (2), 414−429.
(251) Gajula, P.; Yoon, J. U.; Woo, I.; Oh, S.-J.; Bae, J. W. Triboelectric touch sensor array system for energy generation and self-powered human-machine interfaces based on chemically functionalized, electrospun rGO/Nylon-12 and micro-patterned Ecoflex/MoS_2 films. *Nano Energy* **2024**, *121*, No. 109278.
(252) Wang, T.; Shang, X.; Wang, H.; Wang, J.; Zhang, C. Porous nanofibers and micro-pyramid structures array for high-performance flexible pressure sensors. *Compos. Part A* **2024**, *181*, No. 108163.
(253) Saygılı, T.; Kahraman, H. T.; Aydın, G.; Avcı, A.; Pehlivan, E. Production of PLA-based AgNPs-containing nanofibers by electrospinning method and antibacterial application. *Polym. Bull.* **2024**, *81*, 5459−5456.
(254) Zaszczynska, A.; Kolbuk, D.; Gradys, A.; Sajkiewicz, P. Development of poly(methyl methacrylate)/nano-hydroxyapatite (PMMA/nHA) nanofibers for tissue engineering regeneration using an electrospinning technique. *Polymers* **2024**, *16* (4), No. 531.
(255) Aghdam, R. M.; Najarian, S.; Shakhesi, S.; Khanlari, S.; Shaabani, K.; Sharifi, S. Investigating the effect of PGA on physical and mechanical properties of electrospun PCL/PGA blend nanofibers. *J. Appl. Polym. Sci.* **2012**, *124* (1), 123−131.
(256) Luo, C.; Hu, H.; Zhang, T.; Wen, S.; Wang, R.; An, Y.; Chi, S. S.; Wang, J.; Wang, C.; Chang, J.; et al. Roll-to-roll fabrication of zero-volume-expansion lithium-composite anodes to realize high-energy-density flexible and stable lithium-metal batteries. *Adv. Mater.* **2022**, *34* (38), No. 2205677.
(257) Lv, F.; Wang, Z.; Shi, L.; Zhu, J.; Edström, K.; Mindemark, J.; Yuan, S. Challenges and development of composite solid-state electrolytes for high-performance lithium ion batteries. *J. Power Sources* **2019**, *441*, No. 227175.
(258) Veeramuthu, L.; Venkatesan, M.; Liang, F.-C.; Benas, J.-S.; Cho, C.-J.; Chen, C.-W.; Zhou, Y.; Lee, R.-H.; Kuo, C.-C. Conjugated copolymers through electrospinning synthetic strategies and their versatile applications in sensing environmental toxicants, ph, temperature, and humidity. *Polymers* **2020**, *12* (3), 587.
(259) Ercan, E.; Lin, Y.-C.; Hsieh, H.-C.; Hsu, L.-C.; Ho, J.-C.; Chen, W.-C. One-dimensional micro-scale patterned conjugated polymer structures in bilayer architecture and light emitting diode application. *Org. Electron.* **2020**, *87*, No. 105965.
(260) Kim, E.; Choi, J.; Ju, B. K. P-211: Late-News Poster: Extremely smooth electrospun Ag fiber electrodes embedded in PVB flexible substrate for organic light-emitting diodes. *Dig. Tech. Pap. - Soc. Inf. Disp. Int. Symp.* **2019**, *50*, 1961−1962.
(261) Choi, J.; Shim, Y. S.; Park, C. H.; Hwang, H.; Kwack, J. H.; Lee, D. J.; Park, Y. W.; Ju, B. K. Junction-free electrospun Ag fiber electrodes for flexible organic light-emitting diodes. *Small* **2018**, *14* (7), No. 1702567.

https://doi.org/10.1021/acsnano.4c13106
ACS Nano 2024, 18, 31737−31772